UNIVERSITÄT BAYREUTH

Quantifying water use by temperate deciduous forests in South Korea: roles of species diversity, canopy structure, and complex terrain

Dissertation

zur Erlangung des Doktorwürde (Dr. rer. nat.)

der Fakultät für Biologie, Chemie und Geowissenschaften

der Universität Bayreuth

von

Eunyoung Jung

aus Deajeon, Süd-Korea

Bayreuth, Juni 2013

Abstract

About seventy percent of South Korea is covered with forests, most of which are found in the mountain regions since mountains receive more rainfall and are difficult terrains not suitable for agriculture. Because mountains are important water sources for cities and human population downstream, performing water balance for forest catchments has become a research priority. The ongoing shift from coniferous to species-rich deciduous forests due to a changing government policy and the anticipated changes in future climate, associated with increasing amount of rainfall and temperature will also impact forest water use, calling for an urgent need to understand how forests, in their current status, use water. The knowledge is vital for predicting water requirements for the future forest. The warm-deciduous temperate forests found in South Korea, however, have a high diversity of tree species, have multi-layered canopies and are mostly located on rugged mountainous terrains, which make it difficult to quantify forest water use, a basic requirement for catchment water budgeting. The main objectives of this study were to: (1) identify the roles of species diversity in tree and forest water use, (2) examine the impact of canopy structure on forest transpiration, and (3) evaluate the influence of terrain on forest water use.

Site-specific studies were carried out in three different natural deciduous forests, namely, Gyebang (GB), Gwangneung (GN) and Haean (HA) forest sites, representing the general structure of S. Korean forests. GB site is known for its high species diversity, GN site is an old forest growth at climax, with clearly defined understory and overstory canopy layers while the HA site was located with in a catchment, with strong elevation changes within short horizontal distances, rising from 400 to 1,000 m a.s.l., and in different aspects. Four locations with varying elevations and aspects were chosen in the HA site. Tree water use (TWU) and canopy transpiration (E_C) were estimated from sap flux density measured with thermal dissipation probes. Understory transpiration (E_U) was measured using stem heat balance while ecosystem evapotranspiration (E_{eco}) was determined using eddy covariance technique. Air temperatures (T_a), precipitation, solar radiation, vapor pressure deficit (VPD), wind speed were measured from weather stations and soil water content was measured from frequency domain reflectometry (FDR) sensors at the respective study sites. Vegetation surveys, including diameter at breast height (DBH), tree density, species composition, sapwood area (A_S), and leaf area index were performed in all the sites. Canopy conductance (G_C) and stomatal sensitivity to VPD were assessed based on transpiration and microclimate measured at each site.

A functional allometric relationship was established between A_S and DBH, and also between TWU and DBH for all the study sites; first for single species and then combining all the species either in a single site or in all the sites. Irrespective of tree species, A_S and maximum TWU were significantly correlated with DBH in a power function for A_S (R^2 = 0.77, P <0.0001) and both in power (R^2 = 0.63, P <0.0001) and sigmoid functions (R^2 = 0.66, P <0.0001) for TWU, for the co-occurring species as well as across the sites,

suggesting that DBH can be a good predictor of stand A_S and maximum TWU, based on the established allometric functions.

Early bud break and development of the understory compared to the overstory canopy resulted in an earlier onset of forest transpiration, with E_U contributing 22% and 14% between April and May to the total forest transpiration. This high contribution was favored by high radiation and VPD in the understory, since the overstory was still undeveloped and open. Despite diminishing VPD and light conditions in the understory between June and August, the understory continued to transpire a substantial amount of water, contributing 10% of the total transpiration. The seasonal patterns of both E_O and E_U were synchronized to canopy development, while VPD and radiation determined daily trends. E_O and E_U accounted for 80% of E_{eco} in spring but only 60% during the monsoon period due to lowered radiation input, VPD, and plant area index (PAI). Thus, E_{eco} is largely influenced by transpiration rate and its seasonal variation and also canopy structure.

Early saturation of E_C at relatively low VPD and also a rapid decrease in G_C with increasing VPD were observed in the forest stand located at the highest elevation studied (950 m) in the HA site, compared to the GN and the other forest stands in HA. These differences in transpiration rates and stomatal response can be explained by greater stomatal sensitivity to VPD of 0.83 found at the 950 m site compared to 0.63–0.66 in the other study sites. However, the main controlling factor of the change in stomatal sensitivity at the 950 m stand is uncertain. Although maximum daily E_C were correlated with A_S of the forest stands at different sites ($R^2 = 0.78$, $P < 0.01$), annual E_C declined with increasing elevation, i.e., 176 >175 >110 >90 mm $year^{-1}$ at 340 >450 >650 >950 m, respectively. Decline in total E_C was due to the decline in annual T_a, daytime VPD, and length of growing season at higher elevations. The GB site, which was located at 960 m elevation, however, did not display a same response pattern as those observed at the 950 m site. It is likely because these sites were under different environmental conditions, i.e., GB site is exposed to higher T_a and higher humidity, and is sheltered (lower wind speeds). These observations emphasize the complexity associated with estimation of transpiration in rugged terrains, since general principles do not always apply and the spatial patterns of forest transpiration are complex.

Complexity arising from multiple tree species composition when estimating forest water use can be reduced by applying functional allometric relationship linking tree size and water use. Forest canopy structure and physical location should be taken into account since they influence the way forests use water resources by altering microclimate and plant physiology. Based on our findings, estimation of forest water use on rugged terrains require repeated measurements at relatively small spatial scales since the driving factors change rapidly over very narrow vertical distances.

Zusammenfassung

In Südkorea ist ca. 70% der Fläche von Wald bedeckt, welcher sich hauptsächlich über gebirgige und durch hohe Niederschläge gekennzeichnete, landwirtschaftlich nicht nutzbare Gebiete erstreckt. Diese Gebirgsregionen stellen eine wichtige Wasserressource für die städtische Bevölkerung dar, sodass die Wasserbilanzierung von bewaldeten Einzugsgebieten zu einem primären Forschungsgegenstand geworden ist.

Die gegenwärtige Verlagerung von Nadelwäldern hin zu artenreichen Laubwäldern als Folge einer sich verändernden Strategie der südkoreanischen Regierung, zur Anpassung an die sich verändernden klimatischen Bedingungen, wie steigende Niederschläge und Temperaturen, führt zu einem veränderten Wasserverbrauch der Waldbestände. Daher sollte der Status des gegenwärtigen Wasserverbrauchs der Bestände umgehend untersucht werden, um Vorhersagen über den zukünftigen Verbrauch treffen zu können. Die im warm-gemäßigten Klima in Südkorea verbreiteten Wälder sind durch eine hohe Artendiversität und einen vielschichtigen Aufbau in ihrer Struktur gekennzeichnet. Durch ihre Lage im schroffen, zerklüfteten Gelände, gestaltet sich die quantitative Erfassung des Wasserverbrauchs dieser Wälder umso schwieriger. Seine Erfassung ist jedoch für eine Wasserbilanzierung in den Waldbeständen eine Voraussetzung. Das übergeordnete Ziel dieser Studie ist (i) zu identifizieren, welche Rolle die Artendiversität in Bezug auf den Wasserverbrauch sowohl einzelner Baumindividuen als auch des gesamten Waldbestandes spielt, (ii) den Einfluss der Kronendachstruktur auf die Transpiration des Waldbestandes zu untersuchen und (iii) den Einfluss des Geländes auf den Wasserverbrauch des Waldes zu evaluieren.

Für die Untersuchungen dieser Studie wurden drei, für Südkorea repräsentative, natürliche Laubwälder in Gyebang (GB), Gwangneung (GN) und Haean (HA) ausgesucht. Das GB-Waldgebiet zeichnet sich besonders durch eine hohe Artenvielfalt aus. Das GN-Waldgebiet besteht aus einer alten Klimax-Waldgesellschaft und lässt sich strukturell in eine Unterholzschicht und eine Baumschicht gliedern. Haean (HA) zeichnet sich hingegen durch einen starken Höhengradient (400 m bis 1000 m ü. NN) über kurze Distanzen und durch eine Exposition in alle Himmelrichtungen aus, sodass in HA insgesamt vier Standorte mit unterschiedlichen Höhenlagen und Expositionen für die Untersuchungen ausgewählt wurden. Der Wasserverbrauch von Baumindividuen (TWU) und die Kronendachtranspiration (E_C) wurden mittels der Saftflussmethode, welche die Saftflussdichte misst, untersucht. Die Unterholztranspiration (E_U) wurde mit der „stem heat balance“ Methode (SHB) gemessen. Am Standort GN wurde zur Erfassung der Ökosystemevapotranspiration (E_{eco}) die Eddy-Kovarianz-Methode benutzt. Die Installation von Wetterstationen diente der Erfassung von Lufttemperatur (T_a), Niederschlag, Solarstrahlung, Wasserdampfsättigungsdefizit (VPD) und der Windgeschwindigkeit. Zusätzlich wurde FDR-Sonden installiert, um den Bodenwassergehalt zu messen. Zur Untersuchung der Vegetation wurde der Stammdurchmesser in Brusthöhe (DBH), die Bestandesdichte, die Splintholzfläche (A_S), der

Blattflächenindex und die Artenzusammensetzung an allen Standorten erfasst. Basierend auf der Transpiration und dem Mikroklima wurde die Kronendachleitfähigkeit (G_C) und die stomatäre Empfindlichkeit bezüglich des VPD untersucht.

Nicht nur die Berücksichtigung einzelner Arten, sondern auch die Einbeziehung aller Arten an einem Standort sowie aller Standorte ergab eine funktionale allometrische Beziehung, sowohl zwischen As und DBH, als auch zwischen TWU und DBH. Unabhängig von der jeweiligen Baumart zeigten die Analysen einen signifikanten Zusammenhang zwischen As und BHD, ausgedrückt in einer Potenzfunktion (P <0.0001). Auch der maximale TWU korrelierte signifikant mit dem DBH im Sinne von Potenz- und sigmoidalen Funktionen (P <0.0001), sowohl für einzelne Arten als auch standortübergreifend. Aufgrund dieser Ergebnisse ist der DBH unter Berücksichtigung der eingeführten allometrischen Funktionen ein gute Schätzgröße für die Bestandessplintholzfläche As und dem maximalen Wasserverbrauch (TWU).

Der im Vergleich zur Baumschicht frühe Blattaustrieb im Unterholz führte zu einem erhöhten Anteil der Unterholztranspiration von 22% im April und 17% im Mai an der Gesamttranspiration des Waldbestandes. Dieser hohe Anteil wurde durch die hohe Einstrahlung und das hohe Wasserdampfsättigungsdefizit (VPD) im Unterholz aufgrund der lichten Baumschicht begünstigt. Allerdings trug das Unterholz auch von Juni bis August mit einem beträchtlichen Anteil von 10% zur Gesamttranspiration bei, obwohl die solare Einstrahlung und das VPD durch die entwickelte Baumschicht geringer waren. Der saisonale Verlauf von E_O und E_U verlief synchron zur Entwicklung des Kronendaches, während hingegen der Tagesgang durch das Mikroklima, die solare Einstrahlung und das VPD gesteuert wurde. Im Frühling trugen E_O und E_U mit einem Anteil von 80% zur gesamten E_{eco} bei. Während der Monsunperiode verringerte sich dieser Anteil jedoch aufgrund einer geringeren Einstrahlung, einem geringerem VPD und einem minimierten Pflanzenflächenindex (PAI) auf 60%. Die Eeco wird daher stark durch den saisonalen Verlauf der Transpirationsrate als auch durch die Kronendachstruktur beeinflusst.

Im Vergleich zu GN, GB, und den niedrigeren Standorten im HA-Einzugsgebiet konnte eine frühe Sättigung von Ec bei relativ geringem VPD und auch eine relativ starke Abnahme von G_C bei steigendem VPD am höchsten Standort in 950 m ü.NN in HA beobachtet werden. Die unterschiedlichen Transpirationsraten und die stomatäre Reaktion können durch eine größere stomatäre Empfindlichkeit in Bezug auf ein VPD von 0.82 erklärt werden. Im Vergleich dazu wiesen die anderen Standorte nur ein VPD zwischen 0.63−0.66 auf. Dennoch sind die verursachenden Faktoren für eine Veränderung der stomatären Empfindlichkeit in größeren Höhenlagen mit gewisser Unsicherheit behaftet. Obwohl die maximale tägliche E_C mit A_S (R^2=0.78, P <0.01) der Waldbestände an verschiedenen Standorten korrelierte, konnte eine Abnahme der jährlichen Ec, mit 176 > 175 > 110 > 90 mm Jahr $^{-1}$, bezüglich der Höhenlage, 340 > 450 > 650 > 950 m ü.NN beobachtet werden. Eine Abnahme der gesamten E_C läßt sich auf die Abnahme der Jahresdurchschnittstemperatur, des tageszeitlichen VPD und der Länge der Vegetationsperiode in größeren Höhenlagen zurückführen. Die Ergebnisse des Standortes GB, welcher sich in ähnlicher Höhenlage auf 960

m befand, zeigten jedoch im Vergleich zum HA-Standort in 950 m ü.NN unterschiedliche Reaktionsmuster, welche auf die geschützte Lage mit höheren Temperaturen, höherer Luftfeuchtigkeit und geringeren Windgeschwindigkeiten zurückzuführen sind. Diese Beobachtungen unterstreichen die Schwierigkeiten bei der Schätzung der Bestandestranspiration im zerklüfteten, steilem Gelände, da aufgrund der komplexen räumlichen Muster der Waldbestandtranspiration nicht immer allgemeingültige Prinzipien abzuleiten sind.

Durch die multiple Zusammensetzung der Baumarten in einem Bestand gestaltet sich die Schätzung des Wasserverbrauchs als schwierig, dennoch können diese Schwierigkeiten durch die Anwendung funktionaler allometrischer Beziehungen zwischen dem Baumumfang und dem Wasserverbrauch reduziert werden. Insbesondere sollte die Kronendachsstruktur und die geografische Lage ausreichend berücksichtigt werden, da diese Faktoren den Wasserverbrauch der Waldbestände durch die Veränderung des Mikroklimas und der Pflanzenphysiologie beeinflussen. In Anbetracht der Ergebnisse sollte die Schätzung des Wasserverbrauchs der Bestände anhand wiederholter Messungen auf relativ kleinräumiger Skala erfolgen, da sich die treibenden Faktoren schnell und auf relativ kurzer Distanz ändern können.

Acknowledgements

First of all, I would like to thank PD Dr. Dennis Otieno, Department of Plant Ecology, University of Bayreuth, for his guidance on how to be a scientist during my Ph. D. He is not only the best teacher in my whole life but also the best friend who I was able to discuss with about anything. I am very honored to be the first Ph. D. graduate under him in Germany. I also thank Prof. Dr. John Tenhunen, Department of Plant Ecology, University of Bayreuth, for giving me a lot of opportunities to learn and to see more in the world. I admire his enthusiasm on the research, positive attitude in life, and wise leadership. I would like to thank Dr. Hyojung Kwon, Oregon State University, for her encouragement and thoughtful comments on analyzing the data, writing the manuscripts, and also having a meaningful life. I learned a lot from her through uncountable meetings and discussions while she stayed in Bayreuth.

I am grateful to Margarete Wartinger for her excellent support on preparation for the field work in Korea and Africa. I believe that I could not accomplish all the field work without her help in solving unexpected technical problems. I also thank Fiederike Rothe, Bärbel Heindl-Tenhunen, and Sandra Thomas for their tremendous cares for me to have a pleasant stay in Bayreuth.

I thank all my colleagues of the TERRECO and KiLi projects, who gave me inspiration for the possible future research and enjoyable life in Bayreuth, Haean, and Nkweseko. Special thanks to Steve Linder for taking care of me in every possible ways, to Bora Lee for just being there for me, to Bumsuk Seo for stimulating me to study our subject in more depth, Saem Lee for listening to me attentively all the time, Marianne for her help on German summary, Emily for English corrections, Thomas for German corrections, and Sina for encouraging me and teaching me promising spirit of her.

I would like to thank all my friends who I spent unforgettable time together in Bayreuth: Family Gärditz, Family Jeoung, Family Mader, Family Otto, Family Park Hoseon, Frank, Heera, Yangmin, and Yoolim.

Finally, I would like to express my special thanks to my husband Jae-Woo and my parents for their endless support, trust, patience, and love.

Table of contents

List of figures

Figure 2.4 Estimated canopy transpiration (E_C, mm d^{-1}) and transpiration of measured species, *Quercus mongolica* (Q.m.), *Tilia amurensis* (T.a.), *Ulmus davidiana* (U.d.), *Cornus controversa* (C.c.), and *Acer mono* (A.m.).

Figure 2.5 Relationship between sapwood area (A_S, cm^2) determined from increment core extracted from more than five samples per species and their respective DBH (n = 35, R^2 = 0.81, P <0.001). The regression equation for *Quercus mongolica* was $A_S = 0.2067DBH^{2.1}$ (n = 9, R^2 = 0.94), for *Tilia amurensis* was $A_S = 0.1846DBH^{2.0}$ (n = 10, R^2 = 0.85), for *Ulmus davidiana* was $A_S = 0.1745DBH^{2.1}$ (n = 3, R^2 = 0.98), for *Cornus controversa* was $A_S = 0.0757DBH^{2.2}$ (n = 3, R^2 = 0.98), for *Acer mono* was $A_S = 0.0215DBH^{2.4}$ (n = 3, R^2 = 0.98), and for all the studied species was $A_S = 0.053DBH^{2.4}$ (n = 35, R^2 = 0.81).

Figure 2.6 Relationship between DBH and (a) mean sap flux density (F_d, kg m^{-2} h^{-1}) (n = 21, R^2 = 0.21, P = 0.036), (b) mean tree water use (TWU, kg d^{-1}) (n = 21, R^2 = 0.87, P <0.001), and (c) canopy conductance (G_C, mm s^{-1}) significant (n = 17, R^2 = 0.63, P >0.001), of all the measured trees.

Figure 2.7 (a) Relation between vapor pressure deficit (VPD, kPa) and canopy transpiration (E_C, mm d^{-1}) (n = 28, R^2 = 0.78, P >0.0001), (b) between E_C and photosynthetically active radiation (PAR, mol m^{-2} d^{-1}) (n = 28, R^2 = 0.91, P >0.0001), and (c) between canopy conductance (G_C, mm s^{-1}) under non-limiting light condition and VPD (n = 22, R^2 = 0.69, P <0.0001).

Figure 3.1 Relationships (a) between stem diameter at breast height (DBH) and sapwood area (A_S) in power function ($A_S = 1.664DBH^{1.483}$, n = 14, R^2 = 0.90, P >0.001) and b between DBH and tree water use (TWU) in three-parameter sigmoidal function ($TWU = 97.07/(1 + e^{-[(DBH-49.85)/14.22]})$, n = 11, R^2 = 0.97, P <0.001) for canopy tree species of *Quercus serrata* (Q.s.) and *Carpinus laxiflora* (C.l.) from the years 2007 and 2008.

Figure 3.2 Seasonal patterns of (a) plant area index (PAI), (b) daily mean air temperature (T_a), (c) daily mean vapor pressure deficit (VPD), (d) daily sum photosynthetically active radiation (PAR), and (e) daily rainfall and soil water content (θ) in 2008. The shaded area indicates the period of *Changma*. Numbers of 40, 4, and 2 indicate 40, 4, and 2 m heights, respectively.

Figure 3.3 Seasonal patterns of (a) daily transpiration from the overstory (E_O, closed circles), the understory (E_U, open circles), and (b) ecosystem evapotranspiration (E_{eco}). Solid lines were five days running mean of daily E_O, E_U, and E_{eco}.

Figure 3.4 Relationship between monthly cumulative rainfall and the ratio of monthly averaged stand transpiration (=E_O + E_U) to monthly averaged ecosystem evapotranspiration (E_{eco}). The relationship was significant (R^2 = 0.71, P >0.01, $y = -0.131\ln(x) + 1.3247$).

Figure 3.5 Relationships between transpiration and photosynthetic active radiation (PAR) and between transpiration and vapor pressure deficit (VPD). Numbers of 40, 4, and 2 indicate 40, 4, and 2 m heights, respectively. Note that PAR_2 was multiplied by a factor 10 for the convenience of plotting with PAR_{40} except for April. Closed and open circles indicate overstory and understory, respectively. All the regressions are in polynomial functions.

Figure 3.6 Relationships between daytime canopy conductance (G_C) and daytime vapor pressure deficit (VPD) for the overstory (closed) and the understory (opened) before *Changma* (June 1–June 16) (triangles) and after *Changma* (August 1–August 30) (circles).

Figure 4.1 Relationship between stem diameter at breast height (DBH, cm) and sapwood area (A_S, cm^2) for *Quercus* species (open symbols) and for the rest of the studied species (close symbols) from all study

sites. Black solid line is the regression for *Quercus* spp.: $A_S = 0.7642 \times DBH^{1.8057}$ (n = 31, $R^2 = 0.89$, $P < 0.0001$), gray solid line is the regression for the rest of the species: $A_S = 0.8838 \times DBH^{1.8905}$ (n = 13, $R^2 = 0.98$, $P < 0.0001$), and broken line is a regression of all species: $A_S = 0.5974 \times DBH^{1.9374}$ (n = 44, $R^2 = 0.84$, $P < 0.0001$). Letters of Q, As, Bd, Tm indicate *Quercus* spp., *Alnus sibirica*, *Betula davurica*, *Tilia mandshurica*, respectively.

Figure 4.2 Seasonal patterns of meteorological variables at each study site. (a) Daily sum solar radiation (R_S, MJ m^{-2} d^{-1}), (b) mean air temperature (T_A, °C), (c) mean vapor pressure deficit (D, kPa), and (d) rainfall (mm d^{-1}) at 450, 650 and 950 m elevation. (e) Relative soil water content (θ) measured at 30 cm deep in the soil at each site where sap flow measurements were conducted.

Figure 4.3 Relationship (a) between diameter at breast height (DBH, cm) and maximum sap flow density of the sample trees (max F_{dt}, g m^{-2} s^{-1}), and (b) between DBH and maximum tree water use (max TWU, kg d^{-1}) for the sample trees from all study sites. Sigmoide function for the relation of DBH to TWU was $TWU = \frac{72.6}{1+\exp\left(-\frac{(DBH-23.1)}{4.39}\right)}$ (n = 44, $R^2 = 0.62$, $P < 0.0001$). Max F_{dt} and TWU was selected for the days with R_S >20 MJ m^{-2} d^{-1} and VPD >0.5 kPa. Letters of Q, As, Bd, Tm indicate *Quercus* spp., *Alnus sibirica*, *Betula davurica*, *Tilia mandshurica*, respectively. Bars indicate standard deviation from different days.

Figure 4.4 Diurnal patterns of (a) radiation (R_S, MJ m^{-2} $30min^{-1}$), (b) vapor pressure deficit (VPD, kPa), and (c) canopy transpiration (E_C, mm $30min^{-1}$) at each site from 23 to 25 June.

Figure 4.5 Seasonal patterns of daily canopy transpiration (E_C, mm d^{-1}) at each study site in 2010. Closed circles are measured and open circles are simulated values using Jarvis-Stewart model. The shaded area indicates the period of the monsoon in Korea, 2010.

Figure 4.6 Relationship between vapor pressure deficit (VPD, kPa) and daily canopy transpiration (E_C, mm d^{-1}) at each site from June to September 2010. Fitted functions were (a) $E_C = 1.70VPD(1-e^{(-2.21VPD)})$ for 450N, (b) $E_C = 1.30VPD(1-e^{(-2.28VPD)})$ for 650N, (c) $E_C = 1.48VPD(1-e^{(-1.58VPD)})$ for 650S, (d) $E_C = 1.48VPD(1-e^{(-5.71VPD)})$ for 950N. All the estimated parameters of each regression were statistically significant ($P < 0.0001$).

Figure 4.7 Relationships between canopy conductance (G_C, mm s^{-1}) and vapor pressure deficit (VPD, kPa) under saturating global radiation (R_S >400 W m^{-2}) at each study site. All the estimated parameters of each regression were statistically significant ($P < 0.0001$).

Figure 4.8 The response of canopy conductance to vapor pressure deficit ($-\Delta G_C/\Delta \ln VPD$, see Eq. 10) plotted against the reference conductance (G_{Cref}) for all studied trees at each site, i.e., *Quercus* spp. (Q), *Alnus sibirica* (As), *Betula davurica* (Bd), and *Tilia mandshurica* (Tm). The universal ratio of 0.6 suggested by Oren et al. (1999) is indicated by a broken line.

Figure 4.9 Stable carbon isotope (^{13}C) compositions in the leaves of *Quercus mongolica* distributed along an elevation gradient in the Haean catchment. Error bars indicate standard deviation from the means of individual trees along this gradient.

List of tables

Table 4.4 Annually averaged microclimates (solar radiation (R_S), air temperature (T_a), mean daytime vapor pressure deficit (VPD), annual rainfall and wind speed) and soil water content (θ) during growing season of the study sites in Haean catchment, South Korea in 2010. ± are standard deviation (SD).

Table 4.5 Maximum leaf area index (LAI), length of the growing season, total canopy transpiration (E_C, mm) during the growing season and mean ring width for *Quercus mongolica* at each study site. ± are standard deviation (SD).

Table 4.6 Canopy conductance (G_C, mm s^{-1}) on clear days in June, its respective vapor pressure deficit (VPD, kPa) for daytime (from 8:00h to 18:00h) and G_{Cref} (G_C at VPD = 1 kPa) at each site. ± are standard deviation (SD).

List of abbreviations and Symbols

Abbreviation/Symbol	Definition	Unit
AIC	Akaike's information criterion	-
A_S	sapwood area	[m^2]
BA	basal area	[m^2]
c_p	specific heat at constant pressure	[J kg^{-1} K^{-1}]
DBH	diameter at breast height	[cm]
E_C	canopy transpiration	[mm h^{-1}, mm d^{-1}]
E_{eco}	ecosystem evapotranspiration	[mm h^{-1}, mm d^{-1}]
E_{max}	maximum stand transpiration	[mm h^{-1}, mm d^{-1}]
E_O	overstory transpiration	[mm h^{-1}, mm d^{-1}]
E_U	understory transpiration	[mm h^{-1}, mm d^{-1}]
F_d	sap flux density	[g m^{-2} s^{-1}]
G_A	aerodynamic conductance	[m s^{-1}]
g_b	boundary layer conductance	[m s^{-1}]
G_C	canopy conductance	[mm s^{-1}]
G_{Cref}	canopy conductance at VPD = 1 kPa	[mm s^{-1}]
g_t	turbulent conductance	[m s^{-1}]
G_V	gas conductance of water vapor	[m^3 kPa kg^{-1} K^{-1}]
KoFlux	Korean Flux group	-
LAI	leaf area index	[-]
LAI_{max}	maximum leaf area index	[-]
LAI_U	understory leaf area index	[-]
MLT	modified lookup table	-
PAI	plant area index	[-]
PAR	photosynthetic active radiation	[mol m^{-2} s^{-1}]
PPFD	photosynthetic photon flux density	[mol m^{-2} s^{-1}]

RMSE	Root-mean-square-error	[-]
R_N	net radiation	[W m^{-2}]
R_S	solar radiation	[W m^{-2}]
SHB	stem heat balance	-
SLA	specific leaf area	[cm^2 g^{-1}]
SWAT	Soil and Water Assessment Tool	-
T_a	air temperature	[°C]
TDP	thermal dissipation probes	-
T_k	air temperature in kelvin	[K]
U	wind speed above the vegetation layer	[m s^{-1}]
VPD	vapor pressure deficit	[kPa]
WUE	water use efficiency	-
z	canopy height	[m]
z_0	roughness length	[m]
α	attenuation coefficient for wind speed inside the canopy	[-]
Δ	change of saturation water vapor pressure with temperature	[Pa K^{-1}]
γ	psychometric constant	[Pa K^{-1}]
θ	soil water content	[%]
κ	von Karman constant	[-]
λ	latent heat of vaporization of water	[J kg^{-1}]
ρ	density of dry air	[kg m^{-3}]
ρ_w	density of water	[kg m^{-3}]

Chapter 1

Detailed summary

1.1 General introduction and literature review

1.1.1 Temperate deciduous forests: distribution and structure

Temperate deciduous forests are widely distributed across the globe, covering an area of approximately 7.8 million km^2 worldwide (Allaby 2006). They occur in Eastern North America, western and central Europe, eastern Asia, Near East, and in parts of South America such as Patagonia and Chile. These forests occur in relatively warm-temperate moist climates, with an average temperature of the coldest month ranging between −18 and −3°C and the warmest month ranging between 18 and 30°C (Röhrig 1991a; Allaby 2006). The mean annual precipitation ranges from 750 to 1,500 mm, and is allocated evenly throughout the season for most of the regions except for eastern Asia, which experiences severe rain storms during summer (Röhrig 1991a; Allaby 2006).

Compared to the forests in Europe and North America, the temperate deciduous forests of eastern Asia are two or three times higher in plant species diversity (Latham and Ricklefs 1993; Qian and Ricklefs 1999). Historically, this substantial difference in plant diversity appears to result from greater physiographic heterogeneity in Asia, which allowed for allopatric speciation in response to climate and sea level fluctuations after temperate forest zones became disjunct in the late Tertiary (Qian and Ricklefs 2000). Moreover, repeated glaciation during the Pleistocene was more extreme in Europe and North America than in eastern Asia (Qian and Ricklefs 2000). In eastern North America, more uniform climate and simpler geography have not fostered evolutionary conditions among the same families as in eastern Asia (Qian and Ricklefs 2000). In the case of Europe, even lower diversity is found in forest vegetation due to the restrictions on refugia for migrating species that were imposed by the Alps barrier and the location of the Mediterranean Sea during Pleistocene glaciations (Ellenberg 1978), resulting in large numbers of extinctions.

Generally, the temperate deciduous forests of eastern Asia can be classified into two main groups, namely cool- and warm-temperate deciduous forests (Kira 1991). The cool-temperate deciduous forests mainly inhabit western Japan, while the warm-temperate deciduous forests occur in other parts of Japan, China and Korean Peninsula (Nakashizuka and Iida 1995). Characteristically, the cool-temperate deciduous forests are dominated by *Fagus crenata*, which accounts for more than 80% of the total forest basal area (Nakashizuka 1987). Warm-temperate deciduous forests, on the other hand, are species-rich, for example,

the dominant genus *Quercus* occur as 66 different species (Röhrig 1991b). This high species diversity likely resulted from the warm and humid summer conditions associated with high radiation and moisture inputs from the monsoon (Röhrig 1991a). Dominant genera include *Quercus, Carpinus, Ulmus*, and *Tilia* (Velichko and Spasskaya 2002). Thus, the warm-temperate deciduous forests of Korea and other parts of Asia represent an important ecosystem type with multi-layered physiognomy (Kim 2002), where both the overstory and understory are well developed and display diverse species compositions. As a result, large differences are expected in terms of water use between the cool-and warm-temperate deciduous forests.

1.1.2 Forests in South Korea

1.1.2.1 History of forests in South Korea

South Korea is a mountainous country, with 70% of its land covered by mountains with elevations of up to 2,000 m a.s.l. separated by deep and narrow valleys. Two thirds of the land area is, therefore, difficult terrain that is not suitable for agriculture and is, instead, under forest cover. Most streams originate from the high elevation forests, and supply most of the water requirements for the population downslope. During the colonial period of 1910 to 1945 and the Korean War of 1950 to 1953, forests were excessively devastated, which led to frequent floods and landslides. In order to rehabilitate forests, the government initiated a nation-wide, large-scale reforestation program from 1973, with a goal of restoring 1 million ha of forests within a short period by planting fast growing tree species, mostly conifers (*Pinus koraiensis*, *Abies holophylla* and *Larix leptolepis*) and restricting the burning of forests to create land for cultivation. Through this action, about 730 thousand ha of degraded land was restored through an extensive plantation of about 10 billion trees on an area of over 350 thousand ha (Lee et al. 1997; Korea Forest Service 2009).

1.1.2.2 Current status of forests in South Korea

In the recent past, forest coverage in South Korea has been declining at an alarming rate of 40 thousand ha per year (Korea Forest Service 2006), due to conversion into agricultural land, urbanization and expansion of the manufacturing industry (Youn et al. 2009). The proportional coverage of coniferous and deciduous forests has changed as well. Coniferous forests have declined from 55% to 42% (600 thousand ha), while the area covered with deciduous forests has increased from 17% to 40% (540 thousand ha), between 1972 and 2008 (Korea Forest Service 2009). Although total forest area has declined, the growing stock of trees has increased 11 times during the last 40 years (i.e., growing stock was 70 million m^3 in 1972 and increased to 800 million m^3 in 2010), as a result of natural re-growth and improved forest management practices (Korea Forest Service 2011). A substantial proportion of the forests is at early and mid succession stages.

According to the Korea Forest Service report of 2009, forests under 10 years and over 51 years of age cover 7% and 2% of the total forest area, respectively. Most (close to 70%) of the forest area is occupied by trees aged between 20 and 40 years. Oaks occupy 75% of the area under natural deciduous forests, with *Q. mongolica* being one of the dominant species growing from 100 m to 1,800 m a.s.l., but mostly abundant at around 700 m a.s.l. (Chung and Lee 1965).

1.1.2.3 The future of forests in South Korea

The climate of South Korea has experienced a gradual warming during the 20th century (Oh et al. 2004; National Institute of Environmental Research 2011). In the last century alone, the average air temperature increased by about 1.5°C, which is twice as high compared to the global warming projections. This has been attributed to rapid industrialization (Oh et al. 2004; Kwon 2005). This temperature increase is contributing to the current shifts in plant species distribution ranges. For example, bamboos (*Phyllostachys*) have shifted from 35°N to 36°N in the continental region and 38°N in the eastern coastal region during the last 200 years (Gong 2001; Oh et al. 2004). Also, the tree line of Korean fir (*Abies koreana*), which grows only at high elevations, has been continuously moving upwards and the species is now threatened with high mortality rate of 20–50% in its natural range (Lim et al. 2008).

Based on the high-resolution climate simulations for 2021 to 2050, under the B2 scenario (IPCC 2000), warming in the range of 1–4 °C is expected in the northern part of S. Korea during the cold season (Im et al. 2008). Precipitation will also be regionally variable, with increased summer rains in the north, but a decline in the southern regions (Im et al. 2008). Based on these climate projections, deciduous and mixed forests could increase by 60% and 10%, respectively, while coniferous forest cover could decrease by 10% by the year 2080 (Shin et al. 2012). The projected changes in climate and forest structure stimulate interests in assessing the ongoing changes and how they will influence forest water budget in the short- and long-term since most of the country's water requirement is met by water from forested mountains. Already, hydrological simulations with the SWAT (Soil and Water Assessment Tool) model, using climate scenarios of ca. 4°C and 20–35% precipitation increase, respectively, show that an evapotranspiration (E_{eco}) increase of 15–20% is expected between 2000 and 2080 (Park et al. 2011). Most forests are located in mountains and they are perceived as water reservoirs for agricultural lands and populations downstream. Historically, rulers of the ancient Korean kingdoms gave a high priority to forest protection since they considered the water regulation function of forests as a fundamental service for agriculture (Youn et al. 2009), a concept that is widespread among South Koreans to date. Forest soils perform as reservoirs for water from precipitation and losing water by runoff and E_{eco}. Any vegetation changes strongly influence E_{eco}, which necessarily affects runoff, because E_{eco} is one of the large components of the forest hydrologic budget. For example, conifer forests produce less runoff than deciduous forests due to their higher rates and longer season for E_{eco} (Swank

and Douglass 1974). Understanding how forest catchments store rain water and also the regulation of water release from forests, either as river discharge or through E_{eco} is, therefore, critical for the management of natural water resources (Chapin et al. 2011).

1.1.3 Regulation of water use by forest ecosystems

In most forest ecosystems, canopy transpiration is determined by the prevailing microclimate, soil moisture status and the plant characteristics (Körner 1994; Schulze et al. 2005). A gradient in vapor pressure between the intercellular spaces and the surrounding air outside the leaf surface determines the rate of water transfer from the leaf into the atmosphere and consequently, transpiration rate: as long as the stomata remain open. Under favorable soil moisture conditions, light intensity controls stomatal opening and stomatal conductance increases with higher light intensities (Schulze et al. 2005). On a daily basis, during ample soil moisture availability, therefore, canopy transpiration increases exponentially with increasing vapor pressure deficit (VPD), as long as the prevailing photosynthetic photon flux density (PPFD) is high enough to allow for full stomatal opening (Granier and Bréda 1996; Oren and Pataki 2001; Ewers et al. 2002). At higher VPD increases in transpiration are, however, regulated by the stomata such that the species-maximum capacity for hydraulic conductivity is not surpassed and cavitation does not occur. For example, saturation of daily stand transpiration for European beech forest stands occurred at mean daily VPD of 2.5–3.0 kPa, while for a spruce stand, transpiration saturated at VPD of 2.0–2.5 kPa (Köstner 2001). Similarly, more pronounced stomatal closure in response to increasing VPD (>2.5 kPa) in European beech (*F. sylvatica*) than in sessile oak (*Q. petraea*) has been reported, revealing larger sensitivity of beech to VPD changes (Aranda et al. 2000). Stomatal closure occurs to prevent the development of dangerously low water potentials, which can cause cavitation, and to protect the conducting vessels (Jones and Sutherland 1991).

During a fully developed canopy stage in deciduous forests, soil water availability regulates the potential transpiration rates, while PPFD and VPD control diurnal patterns of transpiration water loss (Körner 1994). When soil moisture is limited, leaf water potential declines. Under such conditions, stomatal closure will occur in order to control transpiration water loss (Cochard et al. 1996). In European and North American temperate forests, several studies found that the critical value of relative extractable water from the soil was about 0.4, which is calculated as the ratio of extractable water (available soil water – minimum soil water) and maximum extractable water (soil water content at field capacity – minimum soil water), at which soil water content begins to limit maximum transpiration (Black 1979; Granier 1987; Granier et al. 1999; Wilson and Baldocchi 2000).

While environmental drivers control forest stand transpiration in a relatively short period of time, forest structure, i.e., number and size of the trees, age and species composition, regulates stand transpiration over

longer time scales. Transpiration from monocultural forest stands is likely to be dependent on the total sapwood area (A_S) of the stand or leaf area index (LAI) (Ewers et al. 2002; Wullschleger et al. 2001). For example, Zimmermann et al. (2000) found that canopy transpiration was correlated with stand A_S which was determined by stand density and tree A_S in pine forest monoculture stands, with diverse ages ranging from 28 to 383 years of age. Köstner (2001) showed an increasing pattern of the maximum stand transpiration with LAI for five European beech forests, regardless of the stand age. In mixed forest stands, however, differences in species composition may modify rates of transpiration, since species differ in water-resource acquisition, xylem anatomy, and phenology. For example, tree species with deep rooting systems like *Q. alba* show higher rates of transpiration as the soil dries, compared to shallow rooted ones such as *Acer rubrum* (Oren and Pataki 2001; Bovard et al. 2005). Oren et al. (1999) showed that the stomatal conductance of ring-porous species was less sensitive to variations in light and VPD than diffuse-porous species. This then resulted in lower mean canopy conductance and lower maximum canopy transpiration for the forest stands composed of a high proportion of ring-porous species than diffuse-porous species (Oren and Pataki 2001). The timing of leaf flushing and senescence also vary among deciduous species (Vitasse et al. 2009), which can have an impact on annual canopy transpiration, since it determines the period of active leaf transpiration.

Complexity in terrain, such as along mountain slopes and valleys or exposition increases the complexity in patterns of tree transpiration and the quantities of water used by forest stands. At higher elevations transpiration rates are likely to decrease because of lower air temperatures (T_a), higher humidity (higher rainfall frequencies and amounts) and lower VPD (Kubota et al. 2005; Körner et al. 2007; Kumagai et al. 2008; McDowell et al. 2008; Matyssek et al. 2009). Soil characteristics also change with elevation, with relatively shallow soils found at higher elevations compared to down slope due to increased runoff and erosion at higher elevations and deposition at lower elevations (Hirobe et al. 1998; Tateno et al. 2004; Tromp-van Meerveld and McDonnell 2006). South-facing aspects receive higher solar radiation, which results in warmer and drier conditions on south than north-facing aspects (Van de Water et al. 2002). Spatial variability in microclimate and soil properties at different elevations in complex terrains are, therefore, likely to generate heterogeneous transpiration rates defined by the complex interactions of stand structure, edaphic and the prevailing microclimatic conditions above the forest stands.

1.1.4 Estimation of water use by forests in South Korea

Using different approaches, a number of studies have attempted to ascertain water budgets for isolated forests in S. Korea. Kim and Woo (1988) and Lee et al. (1989) reported that direct interception water loss by the forest canopy in the planted coniferous forests was 15–20% higher compared to natural deciduous

forests by measuring throughfall and stemflow under the canopy. In comparison, E_{eco} was higher in coniferous forests than deciduous forests growing together at similar elevations, based on the calculations using the Thornthwaite method (Kim 1987). Since 2001, the Korean Flux group (KoFlux) has been assessing E_{eco} in different forest types using the eddy covariance technique in an attempt to obtain an overall water budget for the S. Korean forests (Kim et al. 2006; Kang et al. 2009; Kang et al. 2012). Kang et al. (2009) showed a characteristic seasonality, with mid-season depressions in E_{eco} that are associated with the reduced amount of available energy during the monsoon season. The application of the eddy covariance technique in the estimation of forest water use in S. Korea is, however, challenging and questions are raised regarding data accuracy, since most of the forests are located in mountainous landscapes that are highly heterogeneous and complex. One of the main assumptions of the eddy technique is a flat and homogeneous fetch for footprint measurement sites (Baldocchi et al. 1988), which is not met in most of these forest stands.

Forest transpiration can be measured by sap flow techniques at relatively high temporal scales (Wullschleger et al. 1998). Since they apply at single tree level, the techniques are not limited by terrain complexity and tree species diversity (Wilson et al. 2001; Kumagai et al. 2008). Forest stand transpiration can be determined by summing up the values of transpiration by every single tree in the stand multiplied by its respective A_S. A reasonable scaling process from tree to stand level requires accurate estimates of water use from a limited number of representative trees within the stand (Kumagai et al. 2008). The sap flow measurements are, therefore, suitable for estimation of water use by forest stands, the analysis of species effects on forest water use and for partitioning E_{eco} into transpiration and evaporation (Wilson et al. 2001; Ford et al. 2007). In S. Korea, sap flow measurements have been used to estimate tree transpiration of major species such as *Quercus mongolica* and *Larix leptolepis* (Han and Kim 1993; Han and Kim 1996), but not to estimate forest stand transpiration so far. Compared to Europe and North America where significant research in the temperate forests has been conducted, knowledge on the structure and function of the temperate forests in Asia is still lagging behind, both at regional and local scales. Thus, more studies are needed in order to fill the gaps in knowledge, which will allow for a more informed and sustainable forest management.

1.1.5 Statement of research challenges

Natural regeneration of forests in South Korea has favored the expansion of the species-rich deciduous forests over conifers, which were massively planted in the previous restoration programs. This shift in forest composition is likely to change the hydrology of most S. Korean forests in a way that is not yet well understood. Climate projections for S. Korea (Im et al. 2008) also show future changes in rainfall patterns and amounts and increases in T_a, which are likely to significantly impact water use by forests. These forests

are at different succession stages (forest age) and are likely to respond differently to their physical environment. Forest composition may also change during the succession stages, with certain species becoming dominant. Such changes are also likely to influence the way forests use water. Most forests in S. Korea occur in rugged mountainous terrain subject to rapidly changing microclimatic and edaphic conditions, factors that have a strong influence on water availability to plants and how they use it. The complex interactions among the dynamic processes involving forest water use, species composition, forest age and the physical environment make it difficult to quantify the amount of water used by these forests, a basic requirement for catchment water budgeting. Finding solutions to such complexities calls for more focused, site-specific studies to unravel the mechanisms that are involved in the regulation of water use by these temperate deciduous forests.

This study was carried out in three different deciduous forests, each with isolated unique characteristics and together they represent the general structure of forests in S. Korea. The roles of each of these characteristics on forest water use could, therefore, be assessed in isolation, thereby reducing the complexity arising from multiple factor interactions. This allowed us to isolate the impacts of tree species composition, forest canopy structure and the nature of the terrain on which forests grow on forest water use. The hypotheses were: 1. In a mixed forest, species composition directly influences the way individual trees use water resources, and 2. Forest canopy structure and its physical location influence total forest water use.

1.1.6 Objectives of the research

Objective 1: Identify the role of species diversity in tree and forest transpiration

In mixed forest stands, species diversity may complicate the estimation of total forest stand water use due to the variations in tree structure and function among species, which may influence water use by individual trees (O'Grady et al. 2009). Recent studies demonstrate that tree size, rather than species, may be the main determinant of stand transpiration (Wullschleger et al. 2001; Meinzer et al. 2005; Zeppel and Eamus 2008). For example, significant correlation occurred between tree diameter at breast height (DBH) and daily sap flux of individual trees among 20 different rainforest tree species (Meinzer et al. 2005). Two different species, co-occurring in an open temperate woodland in Australia did not differ in the relationship between DBH and daily total water use (Zeppel and Eamus 2008). Tree allometry relating tree water use to DBH has not been performed for the species growing in Asian temperate forests that include more diverse tree species, compared to the European and North American temperate forests.

The specific objectives of this study were to:

- estimate water use in individual trees in a deciduous forest stand composed of diverse species
- compare the differences in values of tree water use among different species
- identify simple and easily measurable structural traits that universally defining tree water use

The following hypothesis guided the formulation of this study:

- Tree transpiration is less influenced by species than by tree size (stem diameter)

Objective 2: Examine the impact of canopy structures on forest transpiration

Warm temperate deciduous forests of East Asia including S. Korea are multi-layered and both the overstory and the understory are well developed with a diverse species composition (Kim 2002). The composition of understory vegetation is partly determined by the overstory canopy structure since it modifies the understory environments such as wind speeds, T_a, light availability, soil water contents, and soil nutrients (Canham et al. 1994; Babier et al. 2008). For example, in temperate deciduous forests, light availability for the understory species is high in early spring before canopy closure, but decreases in early summer as the overstory trees develop their leaves. Similarly, large differences in wind speeds, T_a and VPD occur with increasing canopy development over the growing season. These environmental conditions of the understory influence understory transpiration (Wullschleger et al. 2001) as well as total forest water use. Wullschleger et al. (2001) observed seasonality in transpiration of overstory (E_O) and understory layers (E_U), which was dependent on the dynamics of canopy cover. Studies examining the relationships between canopy structure and E_O and E_U are rarely likely due to limitation in appropriate methodologies. In this study, we applied two different sap flow methods; one for the canopy trees, with larger than 5 cm stem diameter (thermal dissipation probes, TDP) and the other for the understory trees, with diameters ranging from 9 to 12.5 mm (stem heat balance, SHB) in order to quantify E_O and E_U, separately. Quantification of E_O and E_U allows evaluation of their contribution to E_{eco}, which has been successfully measured in South Korean forests using eddy covariance method (Kim et al. 2006; Kang et al. 2009; Kang et al. 2012). However, contributions of E_O and E_U to E_{eco} have not been carried out for any forests in South Korea so far, although they are the dominant components of E_{eco} in the temperate deciduous forests (Baldocchi and Vogel 1996; Wullschleger et al. 1998). Partitioning E_{eco} provides better understanding of the seasonal changes of E_{eco}, which is necessary for planning forest water management (Hatton et al. 2003; Zeppel et al. 2006).

The specific objectives of this study were to:

- quantify E_O and E_U over the growing season
- identify controlling factors on the total amount and rates of E_O and E_U
- determine the relative contribution of E_O and E_U to E_{eco} throughout the growing season

The hypothesis for this study was:

- Canopy structure (canopy layering) has a significant influence on total forest ecosystem water use (E_{eco})

Objective 3: Evaluate the effect of the terrain on forest water use

Most forests in S. Korea are located in mountainous regions, with complex terrain. The location of forest stands on such a terrain (elevations and aspect) is likely to influence water access and requirement by trees, since soil properties and microclimate change along a mountain slope (Lauscher 1976; Körner 2007). For example, decreasing T_a, increasing precipitation (humidity), and hence decreasing VPD with increasing elevation are observed in the temperate zone (Körner 2007). Soil water availability is most favorable at stands located at intermediate altitudes since stands at higher altitudes often receive large amounts of precipitation, but the soils here are shallow, while forest stands at lower elevations have deep soils but receive small amounts of precipitation (Tromp-van Meerveld and McDonnell 2006). These spatial gradients in abiotic variables along a mountain slope can lead to physiological and morphological variations in trees. Canopy duration (Dittermar and Elling 2006; Vitasse et al. 2009) and sapwood area, for example, tend to decrease with increasing elevation due to reduced length of the growing season and growth rate at cooler temperatures at high elevations (Hoch and Körner 2005; Miyajima and Takahashi 2007). These variations due to elevation and aspect are likely to have an impact on annual forest water budget (Matyssek et al. 2009), potentially lowering transpiration at higher elevations (Matyssek et al. 2009). Few studies have examined spatial patterns of microclimate and soil moisture along mountain slopes and how they influence forest transpiration in mountain terrains (Kubota et al. 2005; Kumagai et al. 2008; McDowell et al. 2008; Matyssek et al. 2009), but they present contradicting outcomes. McDowell et al. (2008) reported decreasing daily canopy transpiration with increasing elevation at different types of conifer forests in the Rocky Mountain, but Matyssek et al. (2009) observed a non-significant trend in daily canopy transpiration with changing elevations in mixed forest stands in the Bavarian Alps. The fact that most forests in S. Korea occur in a mountainous terrain demands that we understand how elevation and aspect influence forest canopy transpiration, in order to design models which allow for a quantification of water use by these forests.

The specific objectives of this study were to:

- quantify canopy transpiration at different elevations and aspects
- examine how soil characteristics and microclimatic environments change along an elevation gradient
- analyze the impact of shifting soil and microclimate conditions on tree growth and forest canopy transpiration of a complex mountaineous terrain

The guiding hypothesis for this study was:

- Canopy transpiration declines with increasing elevation because T_a, soil water availability, VPD and tree growth decrease at higher elevations

1.2 General materials and methods

1.2.1 Description of study sites

Guided by the above objectives, we designed a study that was implemented in three deciduous forests, with unique characteristics representing forests in S. Korea. The three sites were located in Mt. Geybang, Gwangneung arboretum, and Haean basin, which are situated in the northern part of South Korea (Figure 1.1 and Table 1.1). To clarify different water use strategies of different tree species in a mixed forest site with high species diversity (chapter 2), we selected Gyebang forest as study site (site GB). This place is known for its high species diversity (Lee et al. 2006). The dominant tree species were *Tilia amurensis*, *Ulmus davidiana*, *Quercus mongolica*, *Acer mono*, *A. pseudo-sieboldianum*, *Maackia amurensis*, and *Cornus controversa*, comprising 31, 14, 12, 8, 5, 4, and 4%, respectively, of the total tree basal area (Table 1.2). The average DBH of the trees with larger than 5 cm DBH was 13.3 cm and stand age was about 50 years old.

The warm-temperate deciduous forests comprise well-developed understory and overstory canopy layers. To examine how such a forest structure affects forest water use (chapter 3), we chose Gwangneung forest site (site GN), which is a climax forest (about 200 years old), with clearly defined the understory canopy layer at 2 m and overstory layer at 20 m heights. The overstory was dominated by *Q. serrata* and *Carpinus laxiflora*, accounting for 71 and 22% of the total basal area (for the trees with larger than 5 cm DBH), respectively (Table 1.2). The understory was co-dominated by *Euonymus oxyphyllus*, *Celtis jessoensis*, *Sorbus alnifolia*, and *Styrax obassia*. Maximum leaf area index (LAI) of the overstory was 3; the maximum LAI of the understory was 1.

To address the terrain complexity question (chapter 4), we chose a site in the Haean catchment (site HA). That study site appeared to be very suitable as the same genus, *Quercus*, spreads from an elevation of 400 to 1000 m above sea level and also in all aspects. Measurements were conducted at three locations with varying elevations (450, 650, and 950 m a.s.l.) to address the question of elevation, and in two aspects of north and south to address azimuth differences. Names of the study sites were derived from their elevations and aspects: 450N, 650N, 650S, and 950N sites. 450N, 650N, and 650S sites were about 30 year-old forests with maximum tree height of 10 m. The 950N site was about 10 years younger and its trees were about 5 m shorter compared to the other sites considered in this study.

The average annual T_a were 12.4, 10.4, and 8.7°C, while the average annual precipitation were 1457, 1462, 1617 mm for GB, GN, and HA, respectively (13 years average) (Figure 1.2). At all sites, 60 to 70% of annual precipitation occurs during the summer monsoon, normally in July and frequent typhoons in August. The basic rock layer is granitic gneiss at the GB, GN, and HA-950N sites and granite at the HA-450N, 650N, and 650S sites. All forest sites were located on sloping terrain with slopes ranging between 15° to 23°.

Figure 1.1 Satellite images of (a) South Korea, (b) Gyebangsan (GB), (c) Gwangneung (GN), and (d) Haean (HA), and pictures of the study sites (e) GB, (f) GN, (g) 450N, (h) 650N, (i) 650S, (j) 950N. Satellite images were downloaded from Google earth on 16 May 2012 and pictures were taken in March 2009, March 2008, June 2010, March 2010, May 2010, May 2010, respectively.

Table 1.1 Locations, sizes, geological traits and soil characteristics of the study sites in Gyebangsan (GB), Gwangneung (GN) and Haean (HA). Data for GB and GN were compiled from Lim et al. (2003) and Lee et al. (2006), and data for HA were from the measurements conducted by S. Arnhold (unpublished) and author in 2010.

	GB	GN	HA			
			450N	650N	650S	950N
Coordinates	128°26’45.7’’E 37°44’41.30’’N	127°9’11.62’’E 37°45’25.37’’N	128°7’50.09’’E 38°17’18.64’’N	128°8’26.07’’E 38°18’56.83’’N	128°8’27.13’’E 38°18’57.07’’N	128°6’0.86’’E 38°14’43.37’’N
Region	Hongcheon-county, Kangwon-province	Pocheon-city, Kyeongi-province	Yanggu-county, Kangwon-province			
Elevation [m a.s.l.]	960	340	450	650	650	950
Plot area [m^2]	2000	900	625	625	625	625
Inclination [°]	15	15	20	23	15	21
Exposition	SE	S	N	N	S	N
Bedrock	Granitic gneiss	Granitic gneiss and schist	Granite	Granite	Granite	Granitic gneiss
Soil texture	Loam	Loam or sandy-loam	Loam	Sandy-loam	Sandy-loam	Sandy for surface, and loam for sub-surface layer
Soil depth [cm]	Not measured	38−66	8−100	18−68	19−65	22−100

Table 1.2 Stand structure of the six natural deciduous forest sites in Gyebangsan (GB), Gwangneung (GN), and Haean (HA). LAI, BA, A_S and DBH indicate leaf area index, basal area, sapwood area and diameter at breast height (DBH). Trees with diameter at breast height (DBH) ≥5 cm and trees with 2 cm ≤ DBH <5 cm are selected for the overstory (O/S) and the understory (U/S), respectively. Stand density and DBH-based data are interpolated from the inventory conducted in 2008 for GB and GN, and in 2010 for HA.

		GB	GN	HA			
				450N	650N	650S	950N
Stand age [yrs]		ca. 50	ca. 200	ca. 30	ca. 30	ca. 30	ca. 20
LAI		Not measured	4.3	4.9	5.3	6.3	5.7
Tree density [trees ha^{-1}]	O/S	1,025	63	1,252	1,640	2,523	4,350
	U/S	1,730	1,035	5,165	960	3,969	15,050
BA [m^2 ha^{-1}]	O/S	24.0	38.5	21.8	17.5	20.5	22.4
	U/S	Not measured	0.9	2.3	0.8	2.5	1.0
Stand A_S [m^2 ha^{-1}]	O/S	5.7	16.5	12.5	13	15.5	10.5
Average DBH [cm]	O/S	13.3	25.7	10.8	10.8	9.4	6.2
Max DBH [cm]	O/S	40.7	64.0	28.4	33.5	23.5	9.9
Max tree height [m]		15	20	10	12	10	5
Species composition (BA cover [%])	O/S	*Tilia amurensis* (31) *Ulmus davidiana* (14) *Quercus mongolica* (12) *Acer mono* (8) *Acer pseudo-sieboldianum* (5) Maackia amurensis (4) *Cornus controversa* (4)	*Quercus serrata* (71) *Carpinus laxiflora* (22) *Carpinus cordata* (5)	*Quercus mongolica* (24) *Alnus sibirica* (18) *Quercus aliena* (15) *Quercus serrata* (15) *Ulmus laciniata* (10) *Quercus dentate* (8) *Tilia mandshurica* (6)	*Qurcus dentate* (65) *Betula davurica* (19) *Quercus mongolica* (14)	*Quercus mongolica* (50) *Tilia mandshurica* (25) *Quercus dentate* (14) *Fraxinus rhynchophylla* (4) *Quercus serrata* (4)	*Quercus mongolica* (72) *Fraxinus rhynchophylla* (13) *Euonymus hamiltonianus* (9)
	U/S	Not measured	*Euonymus oxyphyllus* *Celtis jessoensis* *Sorbus alnifolia* *Styrax obassia*	*Euonymus alatus* *Rhododendron yedoense* *Rhododendron schlippenbachii*	*Qurcus dentate* *Stephanandra incisa*	*Quercus mongolica* *Acer pseudo-sieboldianum* *Euonymus alatus*	*Acer pseudo-sieboldianum* *Staphylea bumalda*

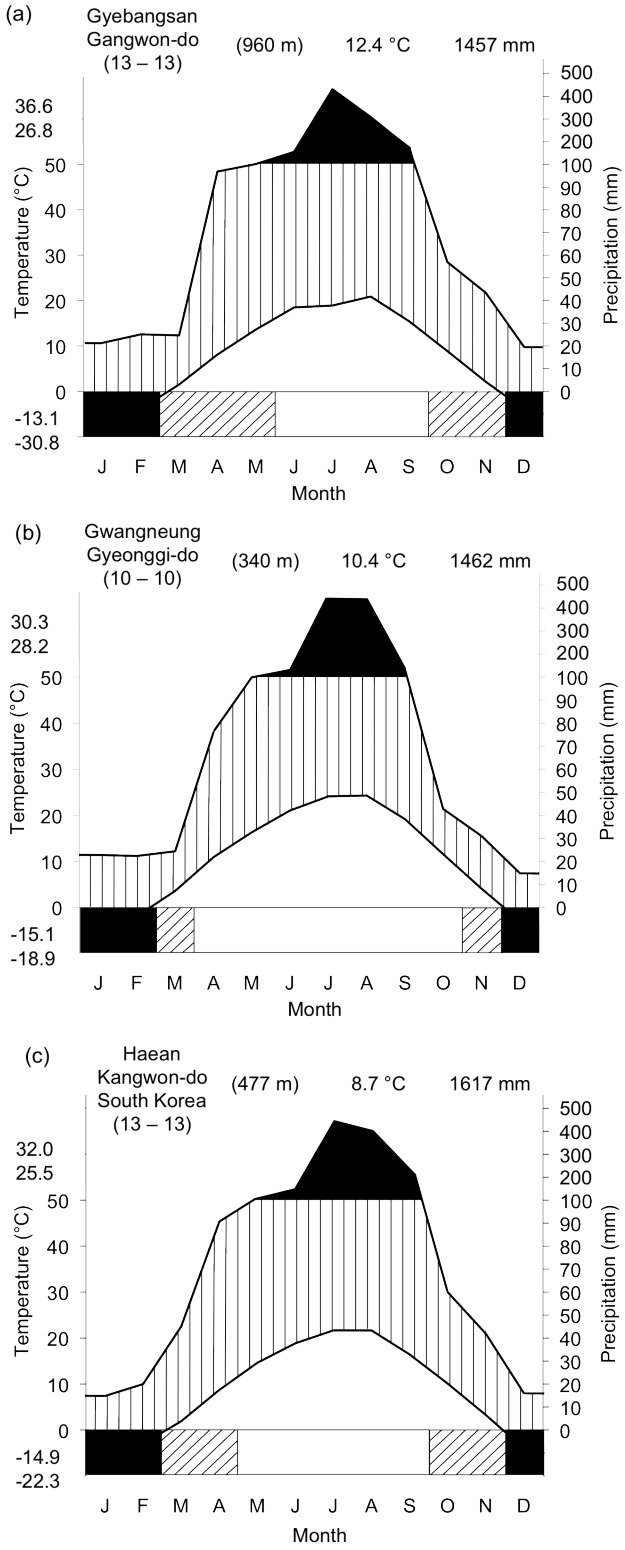

Figure 1.2 Climatic charts following Walter and Lieth (1967) for Gyebangsan (GB), Gwangneung (GN), and Haean (HA) forest sites.

1.2.2 Methods

1.2.2.1 Sap flow measurements

Sap flow techniques were used to measure transpiration of individual trees. For trees with stem diameter larger than 5 cm, thermal dissipation probes (TDP; Granier 1987) were applied (Figure 1.3a). The TDP is generally accepted as a reliable method for estimating tree transpiration and has been widely used in previous studies to estimate forest water use in various ecosystems (Barbour et al. 2005; Granier and Bréda 1996; Matyssek et al. 2009; Oren and Pataki 2001; Wullschleger et al. 2001; Zeppel et al. 2006). For the understory trees with stem/branch diameters ranging from 9 to 13 mm, stem heat balance (SHB) technique (Sakuratani 1981; 1984 and improved by Weibel and de Vos 1994) was employed (Figure 1.3b). The SHB method has been successfully employed to estimate transpiration of whole saplings (Lei et al. 2010; Weibel and de Vos 1994) and branches of large trees (Otieno et al. 2007). The TDP was applied in all the study sites, while the SHB was used only in the GN site. Sample trees were selected according to species and tree size distribution in the study plots. Characteristics of the sample trees for sap flow measurements such as tree species, DBH, tree height, and sapwood area, are summarized in Table 2.1 (chapter 2), Table 3.1 (chapter 3), and Table 4.2 (chapter 4).

Sap flow measurements were carried out in June and July 2008 and repeated over the same period in 2009 at the GB site (chapter 2), April to September in 2008 at the GN site (chapter 3), and from May to October in 2010 at the HA sites (chapter 4).

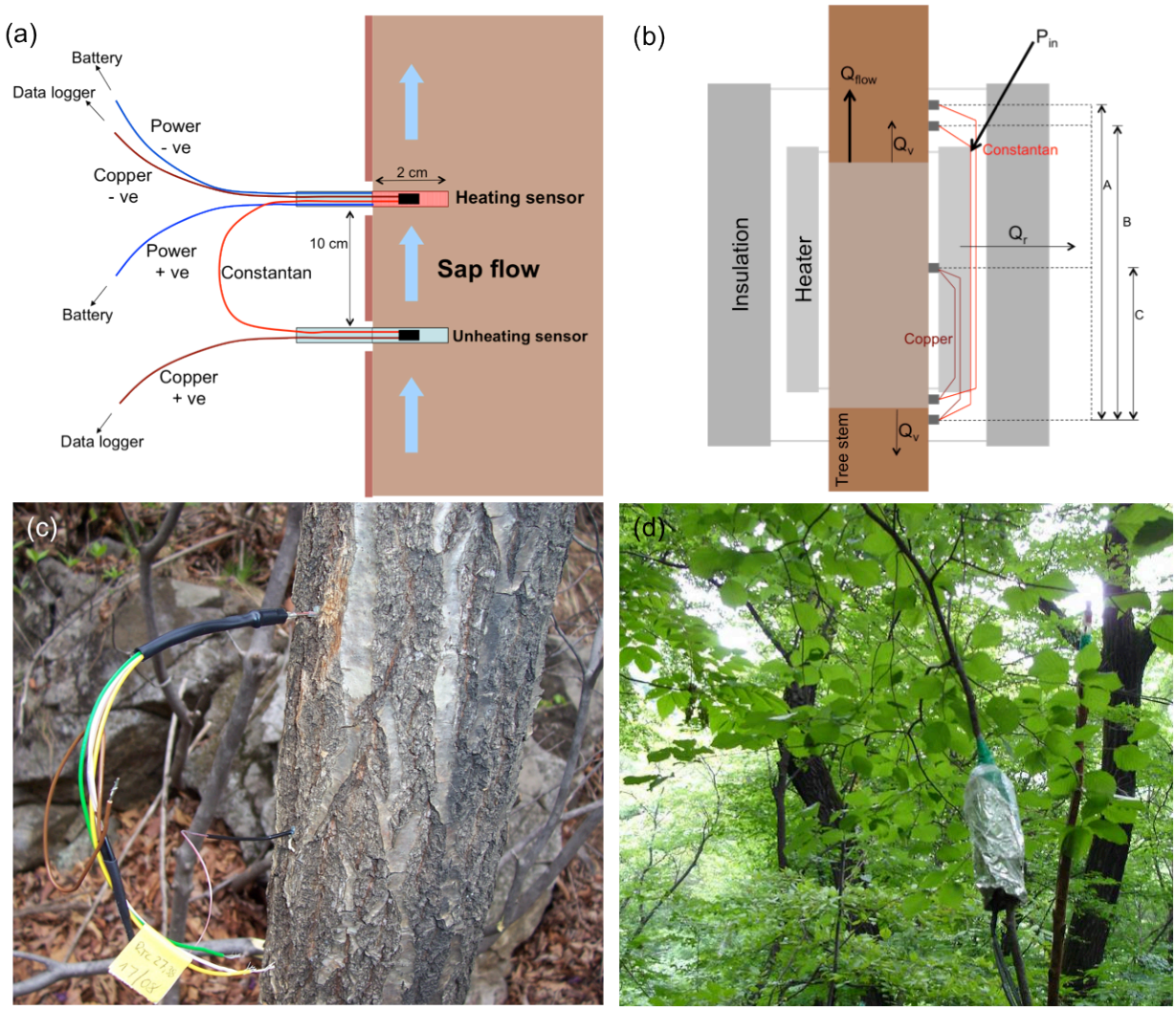

Figure 1.3 Sap flow methods: (a) A schematic representation of thermal dissipation probe (TDP, Granier 1987) installed on to a tree. The upper probe was heated with a constant current power supply while the lower one (reference) was not heated. (b) A schematic representation of stem heat balance (SHB, Sakuratani 1981; 1984), showing arrangement of the thermocouples around the tree stem. A, B and C represent the respective temperature differences recorded at the logger. Q_{flow}, Q_v, Q_r and P_{in} represent convective heat loss by the sap flow, vertical heat conduction, radial heat conduction and heating power, respectively. (c) Installation of TDP in the trees with DBH >5 cm and (d) installation of SHB in the understory trees with stem/branch diameters 9−13 mm.

A modified Jarvis-Stewart model as defined by Whitley et al. (2008) was used to estimate canopy transpiration (E_C) for the period when data gaps occurred due to power failure. Whitley et al. (2008; 2009) expressed E in the same way as G_C described by Jarvis (1976) and Stewart (1988).

$$E_C = E_{C\max} \cdot f_1(R_S) \cdot f_2(VPD) \cdot f_3(\theta) \cdot f_4(LAI) \qquad (1)$$

The functions of solar radiation (R_S), vapor pressure deficit (VPD), soil water content (θ), and leaf area index (LAI) are a set of scaling terms reducing a maximum E_C (E_{Cmax}) in response to changes in each one of the variables. Daily E_C was determined by the functions using the optimal estimates of parameters. A function describing a radiation response was,

$$f_1(R_S) = \left(\frac{R_S}{1000}\right) \cdot \left(\frac{1000 + k_1}{R_S + k_1}\right) \qquad (2)$$

where, k_1 is an empirical coefficient describing the curvature of the relationship. A function response of E_C to VPD was,

$$f_2(VPD) = k_2 \cdot VPD \cdot \exp(-k_3 \cdot VPD) \qquad (3)$$

where, k_2 and k_3 are the parameters describing the rate of changes in VPD. A function describing soil moisture response was expressed as three-phase relationships,

$$f_3(\theta) = \begin{cases} 0, & \theta < \theta_w \\ \dfrac{\theta - \theta_w}{\theta_c - \theta_w}, & \theta_w < \theta < \theta_c \\ 1, & \theta > \theta_c \end{cases} \qquad (4)$$

where, θ_w is the wilting point and θ_c is the field capacity. A function of LAI response to E_C was,

$$f_4(LAI) = \frac{LAI}{LAI_{\max}} \qquad (5)$$

where, LAI_{max} is maximum LAI. Model parameterization was performed using measured data on daily basis via nonlinear least squares analysis using R (R development Core Team, 2009). To avoid errors of division by zero and conditions of wet canopy, daytime data between 8 and 18h was used for the calculations, and the data of the rainy days was excluded. Root-mean-square-error (RMSE) and an agreement index developed by Willmott (1981) were used to evaluate the agreement between the predicted E_C and the observed E_C (see Table 4.3 in chapter 4). The best estimations of parameters (k_1, k_2, and k_3) are shown in Table 4.3 as well. Total gap-filled periods of each site were 27, 54, 68, and 8 days for 450N, 650N, 650S, and 950N, respectively. Predicted E_C was only used to calculate annual E_C of each site, but it was not used for calculations of canopy conductance as well as for analyses of the relationship between E_C and controlling factors.

1.2.2.2 Canopy conductance

Biological regulation of transpiration occurs at the stomata and is measured by stomatal conductance. Canopy conductance (G_C) was estimated from estimated stand transpiration derived from sap flow measurements and microclimate (T_a and VPD) according to the Penman−Monteith equation (Granier et al. 1996; Köstner 1992; Oren et al. 1998),

$$G_C = (\rho_w \cdot G_v \cdot T_k) \cdot \frac{E_C}{VPD} \quad (6)$$

where, ρ_w is density of water, G_v is gas conductance of water vapor, T_k is air temperature in kelvin, and E_C is canopy transpiration. This simplification of the Penman−Monteith equation is based on the assumption that tree canopies are well coupled to the atmosphere, when leaves are exposed to sufficiently high wind speeds, which results in larger aerodynamic conductance (G_A) than G_C. Thus, VPD can be used as an approximation of the total driving force for transpiration. The assumption of strong coupling was tested in all the study sites by comparing G_A and G_C. The results were in agreement with the assumption, i.e., G_C is close to 1% of G_A, for GB and HA sites, but not for GN, particularly the understory layer. Therefore, this simplified equation was used for the studies in GB (chapter 2) and HA (chapter 4), whereas a separate equation arranged from the Penman−Monteith equation was used for GN site (chapter 3) (Monteith 1965; Herbst et al. 2008).

$$G_C = \frac{\lambda \cdot E \cdot \gamma \cdot G_A}{\Delta \cdot R_N + \rho \cdot c_p \cdot VPD \cdot G_A - \lambda \cdot E \cdot (\Delta + \gamma)} \quad (7)$$

where, λ is the latent heat of vaporization of water, γ is the psychometric constant, Δ is the change of satuaration water vapor pressure with temperature, R_N is net radiation, ρ is the density of dry air, and c_p is the specific heat of air at constant pressure. Using this equation, canopy conductance for the overstory and the understory were calculated separately. G_A of the overstory and the understory were also estimated using the boundary layer conductance (g_b) and the turbulent conductance (g_t) according to Köstner et al. (1992), Mangnani et al. (1998), and Tateishi et al. (2010) as,

$$G_A^{-1} = g_b^{-1} + g_t^{-1} \quad (8)$$

$$g_b = b \cdot \sqrt{\frac{U \cdot [1 - \exp(-\alpha/2)]}{d_m \cdot \alpha}} \quad (9)$$

$$g_t = \frac{\kappa^2 \cdot U}{LAI \cdot \{\ln[(z-d)/z_0]\}^2} \quad (10)$$

where, b is the proportionality coefficient, U is the wind speed above the vegetation layers, α is the attenuation coefficient for wind speed inside the canopy, d_m is the characteristic dimension calculated as the square root of a leaf area, κ is the von Karman constant, LAI is the leaf area index of the canopy, z is the canopy height, d is the zero-plane displacement, and z_0 is the roughness length. To calculate G_C based on these two models, data from the measurements between 11h and 17h (daytime) were used.

To assess stomatal sensitivity to VPD, a modified Lohammar's function was applied as,

$$G_C(VPD) = G_{Cref} - m \cdot \ln(VPD) \quad (11)$$

where, G_{Cref} is the canopy conductance at VPD = 1 kPa and $-m$ is the sensitivity of G_C response to VPD (Oren et al. 1999). This analysis only took into account VPD larger than 0.6 kPa to keep the errors in G_C estimates under 10% (Ewers and Oren 2000). G_{Cref} was also used to compare the capacity of water use response to VPD among different tree species or forest stands (Oren et al. 1999).

1.2.2.3 Biometric measurements

To examine seasonal changes of the forest cover and quantify the maximum leaf area of the forests, we measured plant area index (PAI) and maximum leaf area index (LAI) at GN and HA sites. PAI was measured every month during the vegetative period using a plant canopy analyzer (LAI-2000, LI-COR Inc., Lincoln, USA) under diffuse light conditions at fixed 6−12 sampling points. The maximum LAI for the forest sites in HA was estimated from leaf litter collected with 1 m high, 0.5 m × 0.5 m litter traps randomly placed at five points above the forest floor. The litter was transferred to the laboratory, sorted according to species, dried for 48 hours at 75°C and weighed. Specific leaf area (SLA) was determined from the ratio of single leaf area and dry mass for each species. Total leaf area of each species from each site was computed from total leaf dry weight over the season multiplied by SLA and divided by the area of the litter trap. The maximum understory LAI (LAI_U) for GN site was measured by collecting leaf samples of all the understory trees in three plots with 2 m × 2 m size in early July when LAI_U was at the peak. The total area of the leaf samples was measured using a leaf area meter (LI-3100, LI-COR Inc.).

We performed vegetation surveys of all tree stems larger than 5 cm in DBH in a 40 m × 50 m plot at the GB site, in a 30 m × 30 m plot at the GN, and in 25 m × 25 m plots at the HA sites. Based on the survey, mean DBH, basal area (BA), tree density, and species composition were determined for each plot (see Table 1.2). To calculate sapwood area (A_S) of the sample trees, we measured bark and sapwood depths from the extracted cores taken from the stems at sap flow sensor height at the end of the measurements using an increment corer. Sapwood was identified by dying the core samples using bromocresol green (Sigma Chemicals, Germany) (Burrows 1980). A_S was calculated from the measured DBH and depths of bark and sapwood. Based on the calculated A_S and measured DBH, an allometric function was established (Vertessy et al. 1995, Meinzer et al. 2005) as,

$$A_S = \alpha DBH^{\beta} \quad (12)$$

where, α is a constant and β is the allometric scaling exponent. Allometric relationships were made for each one of the studied species as well as for all the species together. Since the differences in the estimations of stand A_S (total A_S of all trees in the plot) from separate regressions and from a combined species regression

were less than 10% at all sites, we chose the general regression for further analyses related to A_S. For example, the values of stand A_S determined by the general regression were used for the estimations of canopy transpiration of each site.

1.2.2.4 Micrometeorological measurements

Air temperature (T_a), precipitation, net radiation (R_N) or solar radiation (R_S), photosynthetic active radiation (PAR), relative humidity or water vapor density, and wind speed (U) were measured with a 20 m tower in GB, with a 40 m tower in GN, and at 2 m above the ground in the open space next to the forest sites in HA. Microclimates below the canopy of T_a, PAR, and humidity were measured at 5 m in GB, at 4 m (but at 2 m for PAR) in GN, and at 2 m in HA sites. VPD was derived from air temperature and relative humidity (Murray 1967). In the GN site, U in the understory at a height of 4 m was additionally measured. Soil water content (θ) and temperature were measured at 30 cm depth in all the sites. Data were read every 30 seconds, averaged, and stored every 30 minutes using data loggers. Soil water retention was determined from measured θ and soil characteristics (i.e., soil texture and bulk density).

1.2.2.5 Eddy covariance flux measurements

At the GN site, evapotranspiration (E_{eco}) was measured with an eddy covariance system installed on a 40 m high tower in GN site for the same period as sap flow measurements (chapter 3). Data quality was controlled using the standardized KoFlux protocol including planar fit rotation, Webb-Pearman-Leuning correction, spike detection, and gap filling (Hong et al. 2009). Data gaps were filled using a modified lookup table following the method proposed by FLUXNET (Reichstein et al. 2005) and modified by Kang et al. (2012).

1.2.2.6 Water use efficiency

From each site, five sun- and five shade-leaves each from five *Q. mongolica* canopy trees were collected on 24 June 2010, during mid season. The samples were oven-dried at 75°C for 48 hours and then ball-milled before subjected to $^{13}C/^{12}C$ isotopic ratio analysis at BayCEER – Laboratory of Isotope Biogeochemistry, Germany. Analyses were conducted with an elemental analyzer NA 1108 (CE Instruments, Milan, Italy) coupled to an isotope ratio mass spectrometer delta S (Finnigan MAT, Bremen, Germany) via an open split interface ConFlo III (Finnigan MAT, Brement, Germany) as described by Bidartondo et al. (2004). Standard CO_2 gas was calibrated with respect to international standard (CO_2 in Pee Dee Belemnite) by use of the reference substance NBS 16 to 20 for carbon isotopic ratio provided by the international Atomic Energy

Agency IAEA, Vienna, Austria. The $^{13}C/^{12}C$ isotopic ratios, denoted as delta values were calculated according to the equation

$$\delta^{13}C = \left[\frac{R_{sample}}{R_{std}} - 1 \right] \times 1000 \qquad (13)$$

where $\delta^{13}C$ is the isotope ratio of carbon in delta units relative to the PDB standard. R_{sample} and R_{std} are the $^{13}C/^{12}C$ of the samples and the PDB standard, respectively. $\delta^{13}C$ was used as an index of seasonally integrated water use efficiency (WUE) (Tieszman and Archer 1990).

1.3 General results and discussions

1.3.1 Tree and forest water use in diverse species composition

An allometric equation was used to find a general relationship between DBH and A_S for different species co-occurring in each study site. A significant relationship, $A_S = \alpha DBH^{\beta}$, linking A_S to DBH, was established (see Figure 2.5 in chapter 2, Figure 3.1 in chapter 3, and Figure 4.2 in chapter 4). These regression models were applied to calculate A_S for all the trees in each study plot. To examine the applicability of this general relationship across the sites, we combined the data of 13 deciduous tree species growing in different study sites. We found that all the species, regardless of their location, significantly ($R^2 = 0.77$, $P < 0.0001$) fitted into a single power curve (Figure 1.4a). This indicates that the general regression model established in this study can be applicable to similar forests in S. Korea, outside our study sites located in other places.

To reduce complexity in estimation of transpiration in mixed deciduous forests, a similar analysis relating TWU and DBH was performed. Maximum daily TWU was significantly related to DBH in a power function for the species co-occurring at each study site ($P < 0.001$ for all sites). To check if this relationship is applicable across the studied sites, the 12 tree species measured in the three different study sites were combined in the analysis. A significant ($R^2 = 0.77$, $P < 0.0001$) single power function was established for the combined data (Figure 1.4b), although there was a tendency of higher TWU for the trees growing in the HA site, which can be explained by greater values of maximum F_d, compared to the others growing in GB and GN sites (Figure 1.5). This result was consistent with the previous studies conducted in temperate forest in North America (Wullschleger et al. 2001), tropical rain forest (Meinzer et al. 2005), and open woodland in Australia (Zeppel and Eamus 2008). Our findings support the hypothesis that different tree species growing together in common locations have converging function in water use determined by tree sizes (Kallarakal et al. 2013). As long as soil water is not limiting, transient changes in tree transpiration are due to the prevailing microclimate, while the potential maximum transpiration is determined by the xylem transport capacity (Oren and Pataki 2001). This implies that the same power scaling parameters, determining A_S and

TWU of single trees by the DBH sizes, can be applied to different tree species growing in deciduous forests in S. Korea as long as trees are exposed to similar environments. Thus, our findings can be applied to estimate maximum daily TWU and stand transpiration using a simple empirical allometry model and DBH of the target sites, irrespective of the species. The power regressions and the statistics of these analyses are shown in Table 1.3 and 1.4.

To identify the most suitable function explaining the relationship between TWU and DBH, the same data set was fitted to the three-parameter sigmoid function (Meinzer et al. 2005) (Figure 1.4b). We found similar goodness of fit between a sigmoid and power function (see AIC values in Table 1.4). Meinzer et al. (2005) found superior fitting from a sigmoid function than power function for angiosperm trees, which was supported by the evidences that transpiration and photosynthesis are limited as trees grow above a threshold size (McDowell et al. 2002, Niinemets 2002). Based on our study, however, both power and sigmoid functions can be used for the estimation of TWU from DBH.

Unlike A_S and TWU, there was no significant relationship between maximum F_d and DBH (Figure 1.5). This is consistent with the study conducted by Phillips et al. (1999). Meinzer et al. (2001), however, obtained a negative correlation, while Oren et al. (1998) found positive correlation between maximum F_d and DBH suggesting that DBH can be a good predictor of F_d among species from diverse locations. Several studies have also considered wood density as an alternative predictor not only for F_d but also for hydraulic conductivity and stomatal conductance (Bucci et al. 2004; O'Grady et al. 2009; Kallarackal et al. 2013). This is an alternative approach that we recommend in future studies, since wood density combines both the tree age and growth conditions.

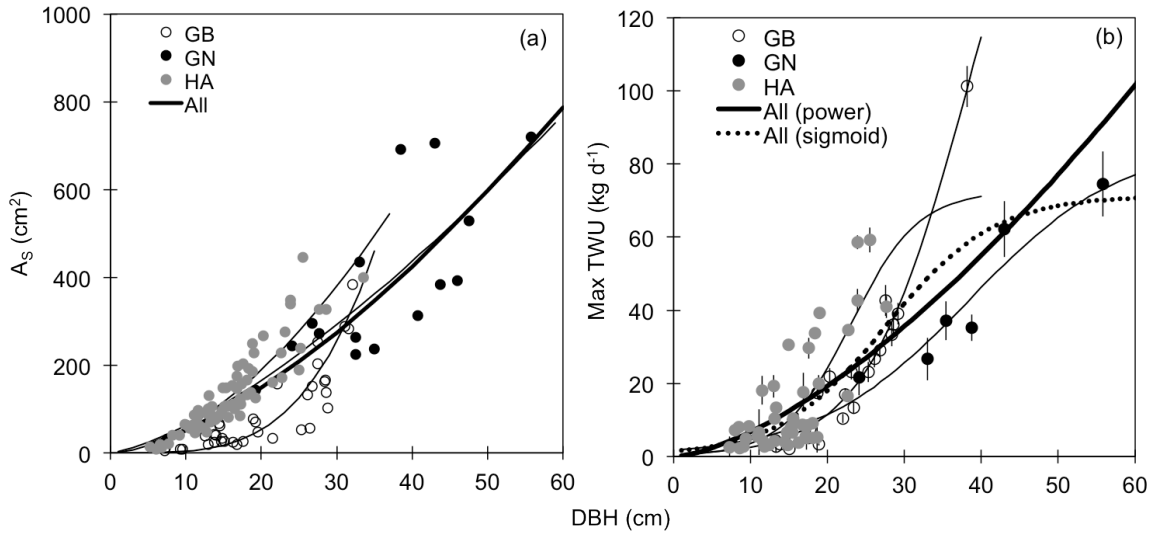

Figure 1.4 Relationships (a) between sapwood area (A_S) and stem diameter at breast height (DBH), and (b) between maximum tree water use (TWU) and DBH for all the species from all study sites, Gyebangsan (GB), Gwangneung (GN), and Haean (HA). The regression equations and statistics are indicated in Table 1.3 and Table 1.4.

Table 1.3 Allometric power regressions between cross-sectional sapwood area (A_S, cm^2) and stem diameter at breast height (DBH, cm) for the tree species growing at Gyebangsan (GB), Gwangneung (GN), and Haean (HA) sites. R^2, n, *P* and d denote the goodness of fit, number of samples, *P*-value, and range of stem diameters, respectively. Regressions are shown in Figure 1.4a.

Study site	Equation	R^2	n	*P*	d [cm]
GB	$A_S = 0.0005DBH^{3.8624}$	0.80	35	<0.0001	7.2–32.1
GN	$A_S = 2.4944DBH^{1.4001}$	0.73	17	<0.0001	7.5–62.3
HA	$A_S = 1.1062DBH^{1.7165}$	0.82	71	<0.0001	5.2–33.5
GB+GN+HA	$A_S = 1.5514DBH^{1.5216}$	0.77	123	<0.0001	5.2–62.3

Table 1.4 Allometric equations between maximum tree water use (TWU, kg d^{-1}) and stem diameter at breast height (DBH, cm) for the tree species from Gyebangsan (GB), Gwangneung (GN), and Haean (HA). R^2, n, *P*, and AIC denote the goodness of fit, number of samples, *P*-value, and Akaike's information criterion (AIC), respectively. Regressions are shown in Figure 1.4b.

Study site	Equation	R^2	n	*P*	AIC
GB	$TWU = 0.0004DBH^{3.3787}$	0.96	21	<0.0001	6.0
	$TWU = 194.89/(1+e^{-(DBH-37.72)/6.396})$	0.96	21	<0.0001	6.1
GN	$TWU = 0.1018DBH^{1.6482}$	0.89	6	0.005	7.2
	$TWU = 93.90/(1+e^{-(DBH-40.38)/10.59})$	0.91	6	< 0.01	7.4
HA	$TWU = 0.0076DBH^{2.6833}$	0.61	44	<0.0001	7.4
	$TWU = 72.60/(1+e^{-(DBH-23.06)/4.388})$	0.63	44	<0.0001	7.4
GB+GN+HA	$TWU = 0.2063DBH^{1.5143}$	0.63	71	<0.0001	7.8
	$TWU = 71.56/(1+e^{-(DBH-27.63)/7.029})$	0.66	71	<0.0001	7.8

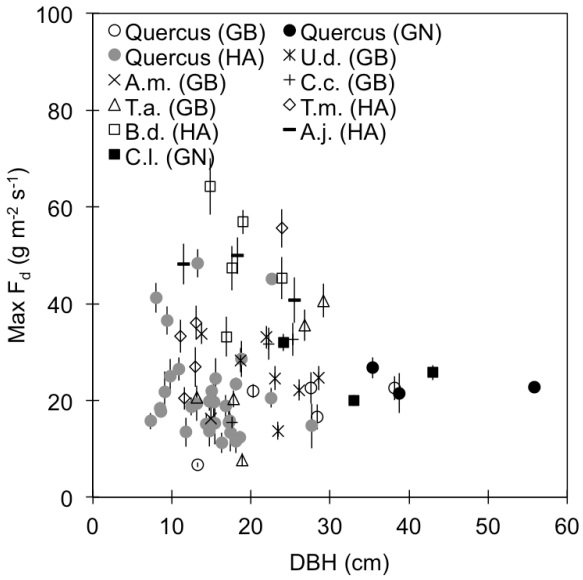

Figure 1.5 Maximum sap flux density (F_d) in relation to stem diameter at breast height (DBH) for *Quercus* species (*Q. mongolica*, *Q. serrata*, *Q. aliena*, *Q. dentata*), *Ulmus davidiana* (U.d.), *Acer mono* (A.m.), *Cornus controversa* (C.c.), *Tilia amurensis* (T.a.), *Tilia mandshurica* (T.m.), *Betula davurica* (B.d.), *Alnus sibirica* (A.s.), and *Carpinus laxiflora* (C.l.) from all the study sites.

1.3.2 Impact of the forest structure on forest water use

We observed well-structured understory and overstory canopy layers in all the studied forest stands. In all these cases, the overstory and understory layers exhibited different growth patterns during the season. The understory emerged and attained its maximum leaf area almost one month earlier than the overstory. Similar patterns were reported for similar forests in Japan (Nasahara et al. 2008). Temporal differences in canopy development between the two layers differentially alter the microclimate, especially in the understory. Before bud break in the overstory canopy mean T_a in the understory (at 4 m height) was 1°C lower than T_a over the canopy (at 40 m height), but the difference increased to 5°C at overstory canopy maturity. Similar changes in VPD in the understory also accompany overstory canopy development. The difference in VPD between the air above the overstory and in the understory increased from 0.1 to 1.0 kPa at full canopy development. There was also a strong reduction in PAR in the understory as the overstory canopy matured. These changes had a strong influence on the seasonal patterns of E_U. Due to early development of the understory and favorable microclimatic conditions, E_U significantly contributed to the total forest transpiration (22%) in April, which resulted in relatively high amount of forest transpiration earlier in the season. Despite diminishing VPD and light conditions, the understory continued to transpire a substantial amount of water, contributing 10% of the total transpiration between June and August, a time when maximum water loss from the ecosystem occurred. Thus, E_U is an important component of water use in warm-temperate deciduous forest and, therefore, should be considered into forest hydrology modeling.

In several studies conducted in European and North American temperate deciduous forests, E_U was not considered seperately, but as a combination with soil evaporation for the analysis of forest water balance (Granier et al. 1999; Unsworth et al. 2004). They considered the radiation reaching the understory as the main driver of understory evapotranspiration, based on previous studies demonstrating poor coupling of the understory vegetation to the atmosphere (Berbigier et al. 1991; Kelliher et al. 1993). In our study, however, E_U was primarily controlled by VPD in the understory throughout the season (Figure 3.5 in chapter 3). Therefore, both VPD and radiation in the understory should be taken into account in forests with a well-developed understory layer in order to have proper estimation of E_U.

Seasonal pattern of E_O was synchronized to overstory canopy development (Figure 3.3 in chapter 3, Figure 4.5 in chapter 4), while daily fluctuations were due to microclimatic changes. The maximum E_O occurred in late June associated with full canopy development and high radiation input, since soil moisture was never limiting in these forests. These high transpiration rates were, however, depressed between July and August as a result of the monsoon, which is an annual phenomenon unique in East Asia. A second transpiration peak occured in September after the monsoon, which was smaller and short-lived, compared to the peak rates attained in June. This was likely as a result of reduced overstory canopy leaf area during the monsoon and typhoons. This defoliation due to storms has been reported in similar forests elsewhere (Ito et

al. 2005). This seasonal pattern occurred in all our study sites. In April and May, the stand transpiration (E_O + E_U) accounted for more than 80% of E_{eco}. The contributions of stand transpiration to E_{eco}, however, declined to less than 60% in July and August because of the monsoon. Thus, E_{eco} is significantly influenced by transpiration rate and its seasonal variation and, therefore, by canopy structure and canopy layering as well (Baldocchi et al. 2002). The S. Korean warm-temperate deciduous forests are unique with respect to a well-developed understory, which switches on transpiration earlier in the season and continues to contribute a significant amount of water lost from the forest ecosystem, and the monsoon period, which significantly lowers radiation input, VPD, and canopy area at a time when maximum transpiration rates are expected. Despite its uniqueness, warm-temperate deciduous forests have rarely been studied so far. Our results of seasonal pattern and contributions of E_O and E_U to E_{eco} can improve understanding and estimation of the total water use by these forests and, hence, enhance the accuracy of forest hydrology or biophysical models, which are mostly developed for European and North Amerian forests, by adjusting them to the local conditions in Korean forests.

1.3.3 Forest water use in complex terrain

Air temperature (T_a) and the amount of rainfall increased at higher elevations, changes that occured at short vertical distances. Both T_a and rainfall influenced VPD, which also declined at higher elevations. Kubota et al. (2005) reported a similar trend of VPD in the mountainous terrains of Japan, which host similar forest types. As opposed to the moisture dynamics model prescribed for complex terrains by Tromp-van Meerveld and McDonnell (2006), upon which this study was designed, there were no gradients in soil moisture along the hill slope. This is likely because of high rainfall amounts received in S. Korea. The length of the growing season also decreased with increasing elevation (4 days shorter per 100 m), which is comparable to mountain terrains of Europe and North America (Richardson et al. 2006; Vitasse et al. 2009). This translates into about 3–5 days 100 m^{-1} of elevation increase. Temperature changes with elevation gradient influenced tree productivity and growth (Vitasse et al. 2009), as we observed increasing annual tree ring width with increasing mean annual T_a of the respective sites.

Diurnal patterns of canopy transpiration (E_C) were similar at all studied sites, except for the higher site at 950 m in HA (950N site). Although the GB site is located at 960 m elevation, since it is positioned about 120 km down to south from the HA site and in the valley of the mountain ranges, the site is exposed to higher T_a, higher humidity, and lower wind speeds compared to the 950N site. In all the sites studied, except for the 950N, E_C increased during the morning, attaining peak rates at around noon, and gradually decreased in the evening in response to declining radiation and VPD. Similar trends are reported elsewhere (Köstner et al. 1992; Granier et al. 1996; Ewers et al. 2002; Matyssek et al. 2009). The trees at the 950N, however, showed a bimodal daily course of E_C with a strong midday depression on sunny days, although daytime

VPD was lower than the other sites. In most cases, midday depression in transpiration due to decreased stomatal conductance is observed when trees are under water-stress or excessive light (Tenhunen et al. 1984; Muraoka and Koizumi 2005). This was not the case at the 950N site. The observed midday depression in E_C is likely due to greater stomatal sensitivity to VPD found at the 950N site (0.83), compared to the GN, GB and the other sites in HA having values of 0.63–0.66, which are comparable to the universal value of 0.6 (Oren et al. 1999). A significant (P <0.0001) difference in response of G_C to VPD, i.e., steeper slope of G_C against VPD, was observed at the 950N site (see Figure 4.7 in chapter 4). This means that G_C is greater at relatively low VPD, but rapidly decreases as VPD increases when the trees have higher stomatal sensitivity to VPD. Related to this, a peak E_C at the 950N was observed at the VPD <1 kPa, whereas a maximum E_C occurred at the VPD of 1.5−2.0 kPa at the GN and the other HA sites (see Figure 3.5 in chapter 3 and Figure 4.6 in chapter 4). This high stomatal sensitivity can also be attributed to high WUE observed at the 950N site, compared to sites at different elevations in the HA sites. Similar patterns of decreasing WUE with increasing elevations have been reported by other studies (Cordell et al. 1998; Körner et al. 1988; Körner et al. 1991; Sparks and Ehleringer 1997). The exact reason why the forest located at higher elevation showed higher stomatal sensitivity could not be established with the scope of this study, however, one explanation could be the strong wind speeds which the site was exposed to (Campbell-Clause 1998). Since whole dynamics of microclimate and and stomatal responses along an elevation gradient are relatively complex, we conclude that it is not only elevation, which determines forest water use, but also other geographical features of forests.

To investigate what stand characteristics determine maximum daily E_C across the sites, we analyzed the relationships between maximum E_C and stand A_S, LAI, and elevation for all study sites. Maximum E_C was significantly (R^2 = 0.52, P <0.1) correlated with stand A_S, but not with LAI nor elevation (Figure 1.6). This was consistent with the result reported by Zimmermann et al. (2000) for pine forests. The goodness of fit for the relationship between maximum E_C and stand A_S increased to 0.78 (P <0.01), when the 950N site was excluded. This indicates that potential water use by forests is mostly determined by total conducting sapwood area as long as the forests experience a similar microclimate.

Unlike maximum E_C, total E_C showed a significant (R^2 = 0.87, P <0.001) gradient along the elevation. Total E_C during the growing season increased with decreasing elevation, i.e., 176 >175 >115 >110 >90 mm $year^{-1}$ at GN (340 m) > 450N >650N >650S >950N, respectively (Figure 1.7). The GB site was excluded in this analysis, because GB was not measured throughout the growing season. The increasing patterns of the cumulative E_C and total E_C of the GN and 450N sites were similar, although E_C at the GN site started and stopped about 20 days earlier than at the HA sites. This result of increasing E_C with decreasing elevation was consistent with the previous findings of McDowell et al. (2008), who reported similar trend for the coniferous forests in Rocky Mountains. Increasing total E_C with decreasing elevation was related to the changes in lengths of the growing season, VPD, and T_a along the elevations. We observed significant linear

relationships between elevation and annual mean T_a, annual daytime mean VPD, and growing season length (Figure 1.8), although the range of elevation gradient was relatively narrow in our study (340−950 m). Körner (2003; 2007) also reported that the elevation determined growing season length and mean T_a, which contributed to the reduction in annual E_C at higher elevations, especially in humid, temperate forests where soil moisture is not limiting. All these results support our hypothesis that the differences in forest water use along the elevation can be attributed not only to the microclimates but also to the length of the growing period and stomatal sensitivity to VPD. These controlling factors of E_C related to the elevations should be considered when estimating forest water use or water budget in larger scales such as catchment or landscape for the mountainous regions such as S. Korea.

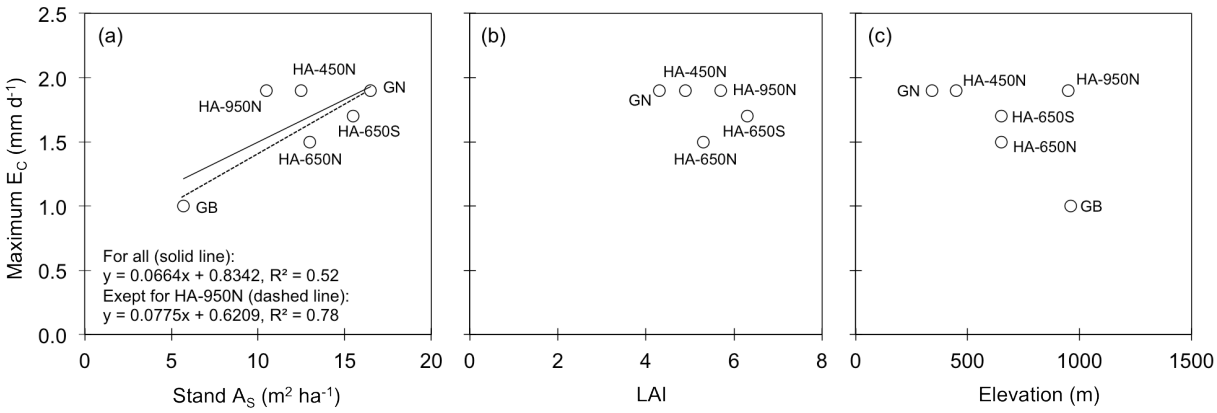

Figure 1.6 Relation of maximum daily canopy transpiration (E_C) to (a) stand sapwood area (A_S), (b) leaf area index (LAI), and (c) elevation of each study site.

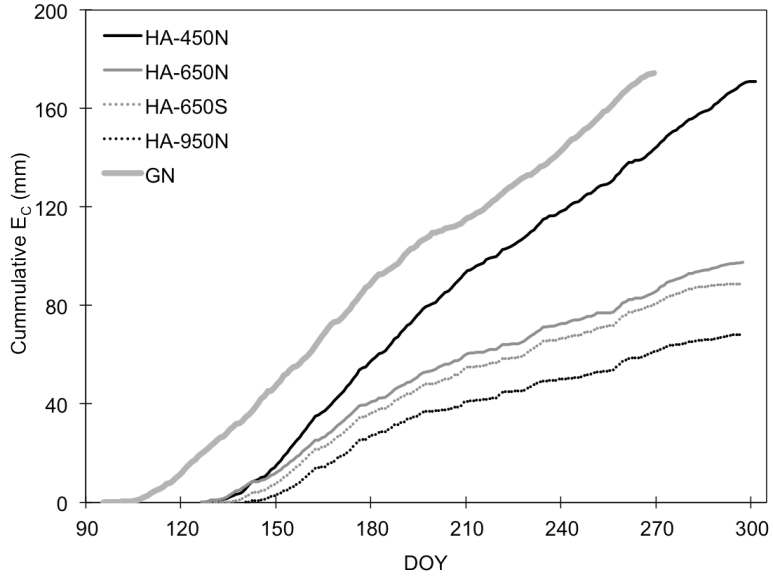

Figure 1.7 Cumulative canopy transpiration (E_C) from Gwangneung (GN) and Haean (HA) sites.

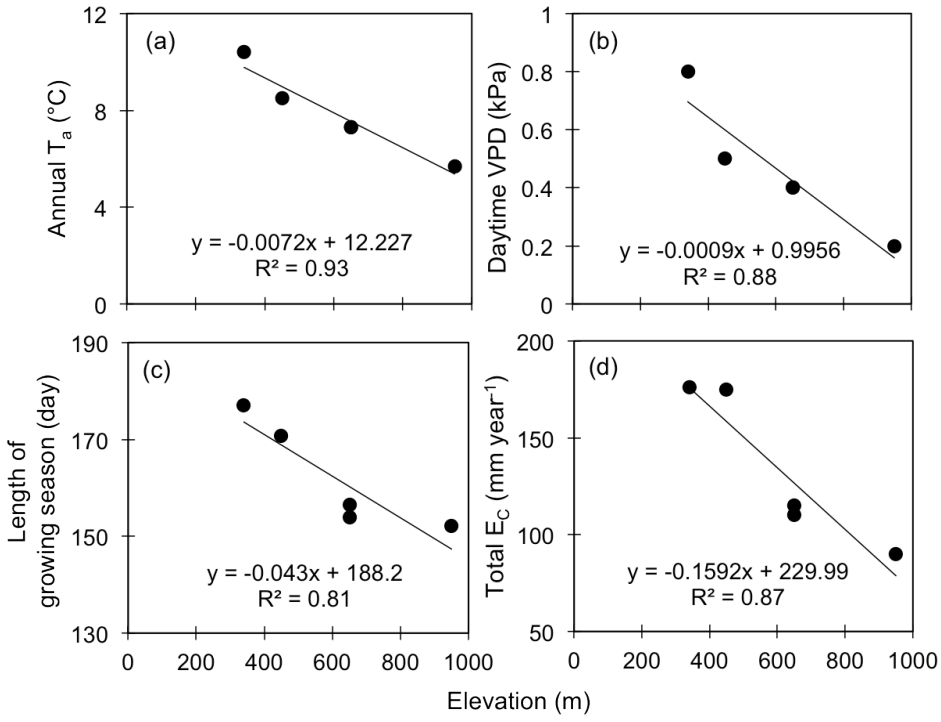

Figure 1.8 Relationships between elevation and (a) annual mean T_a (b) annual daytime mean VPD, (c) length of growing season, and (d) total canopy transpiration (E_C) for the Gwangneug (GN) and Haean (HA) sites.

1.4 General conclusions

This study investigated the challenges imposed by multiple tree species, multiple canopy layering and complex terrain when attempting to determine water use by warm-temperate forest species in S. Korea. Our main findings and suggestions are summarized below:

- DBH was correlated with A_S (in a power function) and maximum TWU (both in power and sigmoid functions) not only for the tree species co-occurring in a single forest stand but also growing in differently aged and structured deciduous forests.
- This functional relationship between DBH and TWU provides a relatively simple but accurate approach for the prediction of water use by trees and forest stands in mixed deciduous forests, thus reducing the complexity arising from multiple tree species.
- Temporal differences in the overstory and understory developments, with earlier bud break and leaf expansion of the understory trees, altered the microclimate in the understory and hence the rate of E_U before and after the overstory canopy maturity.
- The seasonal pattern of both E_O and E_U are regulated by canopy development and microclimate, primarily VPD and PAR, which determine their daily trend.
- E_U significantly contributed to total forest transpiration during the whole growing season, with the highest contributions in April and May, which resulted in relatively high total transpiration early in the season.
- Since E_{eco} is strongly influenced by E_O and E_U, both the overstory and understory should be considered when estimating E_{eco} for forests consisting of a well-developed understory layer.
- High stomatal sensitivity to VPD of the forest located at higher elevation resulted in early saturation and midday depression of E_C at relatively low daytime VPD and possibly high WUE, although the main driver of the shift in stomatal sensitivity is still unclear.
- Total E_C during the growing season decreased with increasing elevation, corresponding to the decrease in T_a, daytime VPD, and length of growing season at the higher elevation. These variables should be carefully taken into account for the estimation of forest water use in mountainous regions in complex terrains.

Our study addressed the challenges involved in estimating water use by the warm-temperate deciduous forests in S. Korea, comprised of diverse tree species, multi-layered canopy, and rugged mountainous terrains. We observed that the complexity arising from multiple tree species can be solved using a functional relationship between DBH and TWU. We also found that for forests with a multi-layered canopy, both E_O and E_U should be taken into consideration when estimating E_{eco}. Finally, in complex terrains, elevation alone

does not determine forest water use, but works in tandem with microclimate and plant growth characteristics, factors that need to be determined at relatively small spatial scales since they change rapidly.

1.5 List of manuscripts and specification of contributions

This dissertation includes three manuscripts. The first manuscript is published in *Plant Ecology* and the second manuscript is published in *Journal of Plant Research*. The third manuscript is submitted to *Plant and Soil* and is currently 'under review'. Specific contributions by the co-authors of each manuscript are listed below.

Manuscript 1 (Chapter 2)

Authors	EY Jung, D Otieno, B Lee, JH Lim, SK Kang, MWT Schmidt, J Tenhunen
Title	Up-scaling to stand transpiration of an Asian temperate mixed-deciduous forest from single tree sap flow measurements
Status	Published in *Plant Ecology* (2011) 212:383-395
Contributions	EY Jung: concepts, field work, discussion and presentation of results, manuscript preparation, corresponding author D Otieno: concepts, field work, discussion of results, manuscript editing B Lee: field work JH Lim: field work, logistics in Korea SK Kang: logistics in Korea MWT Schmidt: discussion of results J Tenhunen: concepts, manuscript editing

Manuscript 2 (Chapter 3)

Authors	EY Jung, D Otieno, H Kwon, B Lee, JH Lim, J Kim, J Tenhunen
Title	Water use by a warm-temperate deciduous forest under the influence of the Asian monsoon: contributions of the overstory and understory to forest water use
Status	Published in the *Journal of Plant Research* (2013) DOU 10.1007/s10265-013-0563-5
Contributions	EY Jung: concepts, field work, presentation and discussion of results, manuscript preparation, corresponding author D Otieno: concepts, field work, discussion of results, manuscript editing H Kwon: field work, discussion of results, manuscript editing B Lee: field work

JH Lim: field work, logistics in Korea

J Kim: logistics in Korea

J Tenhunen: concepts, manuscript editing

Manuscript 3 (Chapter 4)

Authors EY Jung, D Otieno, H Kwon, S Berger, M Hauer, J Tenhunen

Title Influence of elevation on canopy transpiration of temperate deciduous forests in a complex mountainous terrain of South Korea

Status Submitted to *Plant and Soil*; current status 'in revision'

Contributions EY Jung: concepts, field work, presentation and discussion of results, manuscript preparation, corresponding author

D Otieno: concepts, field work, discussion of results, manuscript editing

H Kwon: discussion of results, manuscript editing

S Berger and M Hauer: field work

J Tenhunen: concepts, logistics in Korea

1.6 References

Allaby M (2006) Biomes of the Earth: Temperate Forests. New York, NY: Chelsea House

Aranda I, Gil L, Pardos JA (2000) Water relations and gas exchange in *Fagus sylvatica* L. and *Quercus petraea* (Mattuschka) Liebl. In a mixed stand at their southern limit of distribution in Europe. Trees 14:344–352

Baldocchi DD, Hicks BB, Meyers TP (1988) Measuring biosphere-atmosphere exchanges of biologically related gases with micrometeorological methods. Ecology 69:1331–1340

Baldocchi DD, Vogel C (1996) A comparative study of water vapor, energy and CO_2 flux densities above and below a temperate broadleaf and a boreal pine forest. Tree Physiol 16:5–16

Baldocchi DD, Wilson KB, Gu L (2002) How the environment, canopy structure and canopy physical functioning influence carbon, water and energy fluxes of a temperate broad-leaved deciduous forest–an assessment with the biophysical model CANOAK. Tree Physiol 22:1065–1077

Barbier S, Gosselin F, Balandier P (2008) Influence of tree species on understory vegetation diversity and mechanisms involved – A critical review for temperate and boreal forests. For Ecol Manage 254:1–15

Barbour MM, Hunt JE, Walcroft AS, Rogers GND, McSeveny TM, Whitehead D (2005) Components of ecosystem evaporation in a temperate coniferous rainforest, with canopy transpiration scaled using sapwood density. New Phytol 165:549–558

Berbigier P, Diawara A, Loustau D (1991) A microclimatic study of the effect of drought on evapotranspiration in a maritime pine stand and its understory. Ann Sci For 48:157–177

Bidartondo MI, Burghardt B, Gebauer G, Bruns TD, Read DJ (2004) Changing partners in the dark: isotopic and molecular evidence of ectomycorrhizal liaisons between forest orchids and trees. Proc R Soc Lond B 271:1799−1806

Black TA (1979) Evapotranspiration from Douglas fir stands exposed to soil water deficits. Water Resour Res 15:164–170

Bovard BD, Curtis PS, Vogel CS, Su H-B, Schimid HP (2005) Environmental controls on sap flow in a northern hardwood forest. Tree Physiol 25:31–38

Bucci SJ, Goldstein G, Meinzer FC, Scholz FG, Franco AC, Bustamante M (2004) Functional convergence in hydraulic architecture and water relations of tropical savanna trees: from leaf to whole plant. Tree Physiol 24:891−899

Burrows LE (1980) Differentiating sapwood, hearwood and pathological wood in live mountain beech. New Zealand Forest Service, Forest Research Institute, Protection Forestry Report 172

Campbell-Clause M (1998) Stomatal response of grapevines to wind. Aust J Exp Agric 38:77−82

Canham DC, Finzi AC, Pacala SW, Burbank DH (1994) Causes and consequences of resource heterogeneity in forests: interspecific variation in light transmission by canopy trees. Can J For Res 24:337−349

Chapin FS, Matson PA, Vitousek PM (2011) Principles of Terrestrial Ecosystem Ecology. Second edition. Springer, New York

Chung TH, Lee WC (1965) A study of the Korean woody plant zone and favorable region for the growth and proper species. Thesis Collection of Sungkyunkwan University 10:329−435

Cochard H, Bréda N, Granier A (1996) Whole tree hydraulic conductance and water loss regulation in *Quercus* during drought: evidence for stomatal control of embolism? Ann Sci For 53:197−206

Cordell S, Goldstein G, Mueller-Dombois D, Webb D, Vitousek PM (1998) Physiological and morphological variation in *Metrosideros polymorpha*, a dominant Hawaiian tree species, along an altitudinal gradient: the role of phenotypic plasticity. Oecologia 113:188-196

Dittmar C, Elling W (2006) Phenological phases of common beech (*Fagus sylvatica* L.) and their dependence on region and altitude in Southern Germany. Eur J For Res 125:181−188

Ehleringer JR (1993) Carbon and water relations in desert plants: an isotopic perspective. In Ehleringer JR, Hall AE, Farquhar GD (Eds.), Stable isotopes and plant carbon-water relations, Academic Press, San Diego, California, USA

Ellenberg H (1978) Zur Populationsökologie des Rehes (*Capreolus capreolus* L., Cervidae) in Mitteleuropa. Spixiana 2, München

Ewers BE, Oren R (2000) Analyses of assumptions and errors in the calculation of stomatal conductance from sap flux measurements. Tree Physiol 20:579−589

Ewers BE, Mackay DS, Gowers ST, Ahl DE, Burrows SN, Samanta SS (2002) Tree species effects on stand transpiration in northern Wisconsin. Water Resources Res 38:1103

Ford GR, Hubbard RM, Koeppel BD, Vose JM (2007) A comparison of sap flux-based evapotranspiration estimates with catchment-scale water balance. Agric For Meteorol 145:176−185

Gong WS (2001) Temporal and spatial changes in the distribution of *Phyllostachys* habitation (in Korean). Kor Geograph Soc 36:444−457

Granier A (1987) Evaluation of transpiration in a Douglas-fir stand by means of sap flow measurements. Tree Physiol 3:309−320

Granier A, Bréda N (1996) Modelling canopy conductance and stand transpiration of an oak forest from sap flow measurements. Ann Sci For 53:537−546

Granier A, Huc R, Barigah ST (1996) Transpiration of natural rain forest and its dependence on climatic factors. Agric For Meteorol 78:19−29

Granier A, Bréda N, Biron P, Villette S (1999) A lumped water balance model to evaluate duration and intensity of drough constraints in forest stands. Ecol Mod 116:269−283

Han SS, Kim SH (1993) Ecophysiological interpretations on the water relations parameters of trees (VII) − Measurement of water flow by the heat pulse method in a *Larix leptolepis* stand. J Kor For Soc 82: 152–165

Han SS, Kim SH (1996) Ecophysiological interpretations on the water relations parameters of trees (IX) − Measurement of the transpiration rate by the heat pulse method in a *Quercus mongolica* stand. J Kor For Soc 85: 288–299

Hatton TJ, Ruprecht J, George RJ (2003) Preclearing hydrology of the Western Australia wheatbelt: Target for the future. Plant Soil 257:341–356

Herbst M, Rosier PTW, Morecroft MD, Gowing DJ (2008) Comparative measurements of transpiration and canopy conductance in two mixed deciduous woodlands differing in structure and species composition. Tree Physiol 28:959−970

Hirobe H, Naoko T, Iwatsubo G (1998) Spatial variability of soil nitrogen transformation patterns along a forest slope in a *Cryptomeria japonica* D. Don plantation. Eur J Soil Biol 34:123−131

Hoch G, Körner C (2005) Growth, demography and carbon relations of *Polylepis* trees at the world's highest tree line. Funct Ecol 19:941−951

Hong J, Kwon H, Lim JH, Byun YH, Lee J, Kim J (2009) Standardization of KoFlux eddy-covariance data processing. Kor J Agric For Meteorol 2:12−26

Hubick KT, Farquhar GD, Shorter R (1986) Correlation between water-use efficiency and carbon isotope discrimination in diverse peanut (*Arachis*) germplasm. Australian J Plant Physiol 13:803−816

Im E-S, Ahn J-B, Kwon W-T, Giorgi F (2008) Multi-decadal scenario simulation over Korea using a one-way double-nested regional climate model system. Part 2: future climate projection (2021−2050). Clim Dym 30:239−254

Ito A, Saigusa N, Murayama S, Yamamoto S (2005) Modeling of gross and net carbon dioxide exchange over a cool-temperate deciduous broad-leaved forest in Japan: Analysis of seasonal and interannual change. Agric For Meteorol 134:122−134

IPCC (2000) Special report on emissions scenarios. A Special report of working group III of the intergovernmental panel on climate change (Nakicenovic N and lead authors). Cambridge University Press, Cambridge

Jarvis PG (1976) The interpretation of the variations in leaf water potential and stomatal conductance found in canopies in the field. Phil Trans Roy Soc Lond B 273:593−610

Jones HG, Sutherland RA (1991) Stomatal control of xylem embolism. Plant Cell Environ 14: 607−612

Kallarackal J, Otieno DO, Reineking B, Jung E, Schmidt MWT, Granier A, Tenhunen JD (2013) Functional convergence in water use of trees from different geographical regions: a meta-analysis. Trees 27: 787−799

Kang M, Park S, Kwon H, Choi HT, Choi YJ, Kim J (2009) Evapotranspiration from a deciduous forest in a complex terrain and a heterogeneous farmland under monsoon climate. Asia-Pacific J Atmos Sci 45:175−191

Kang M, Kwon H, Cheon JH, Kim J (2012) On estimating wet canopy evaporation from deciduous and coniferous forests from Asian monsoon climate. J Hydrometeorl 13:950−965

Kelliher FM, Leuning R, Schulze ED (1993) Evaporation and canopy characteristic of coniferous forests and grasslands. Oecologia 95:153−163

Kim JS (1987) Forest effects on the flood discharges and the estimation of the evapotranspiration in the small watershed. Korea Forest Research Institute Reports, Vol.35

Kim JH (2002) Community ecological view of the natural deciduous forest in Korea. In: Ecology of Korea, Bumwoo, Seoul

Kim KH, Woo BM (1988) Study on rainfall interception loss from canopy in forest (I). Journal of Korean Forestry Society, Vol.77, No.3

Kim J, Lee D, Hong J, Kang S, Kim S-J, Moon S-K, Lim J-H, Son Y, Lee J, Kim S, Woo N, Kim K, Lee B, Lee B-L, Kim S (2006) HydroKorea and CarboKorea: cross-scale studies of ecohydrology and biogeochemistry in a heterogeneous and complex forest catchment of Korea. Ecol Res 21:881−889

Kira T (1991) Forest ecosystems of east and southeast Asia in a global perspective. Ecological Research 6:185−200

Korea Forest Service (2006) Statistical Yearbook of Forestry. Seoul, KFS

Korea Forest Service (2009) National Report on Sustainable Forest Management in Korea, 2009. Daejeon, KFS

Korea Forest Service (2011) 2010 Basic Statistics of Forest. Daejeon, KFS

Körner C, Farquhar GD, Roksandik Z (1988) A global survey of carbon isotope discrimination in plants from high altitude. Oecologia 74:623−632

Körner C, Farquhar GD, Wong SC (1991) Carbon isotope discrimination by plants follows latitudinal and altitudinal trends. Oecologia 88:30−40

Körner C (1994) Leaf diffusive conductances in the major vegetation types of the globe. In: Schulse E-D, Caldwell MM (eds.) Ecophysiology of Photosynthesis. Springer-Verlag, Heidelberg

Körner C (2003) Alpine Plant Life (2nd ed.), Springer-Verlag, Berlin Heidelberg New York

Körner C (2007) The use of 'altitude' in ecological research. Trends Ecol Evol 22:569–574

Köstner BMM, Schulze E-D, Kelliher FM, Hollinger DY, Byers JN, Hunt JE, McSeveny TM, Meserth R, Weir PL (1992) Transpiration and canopy conductance in a pristine broad-leaved forest of *Nothofagus*: an analysis of xylem sap flow and eddy correlation measurements. Oecologia 91:350−359

Köstner B (2001) Evaporation and transpiration from forests in Central Europe – relevance of patch-level studies for spatial scaling. Meteorol Atmos Phys 76:69−82

Kubota M, Tenhunen J, Zimmermann R, Schmid M, Adiku S, Kakubari Y (2005) Influences of environmental factors on the radial profile of sap flux density in *Fagus crenata* growing at different elevations in the Naeba Mountains, Japan. Tree Physiol 25:545−556

Kumagai T, Tateishi M, Shimizu T, Otsuki K (2008) Transpiration and canopy conductance at two slope positions in a Japanese cedar forest watershed. Agric For Meteorol 148:1444−1455

Kwon W-T (2005) Current status and perspectives of climate change sciences (in Korean with English abstract). J Kor Meteorol Soc 41:325−336

Latham RE, Ricklefs RE (1993) Global patterns of tree species richness in moist forests: energy-diversity theory does not account for variation in species richness. Oikos 67:325−333

Lauscher F (1976) Weltweite Typen der Höhennabhängigkeit des Niederschlags. Wetter Leben 28:80−90

Lee JH, Kim TH, Lee WK, Choi K, Lee CY, Joo JS (1989) A study on regulating discharges by forest. Korea Forest Research Institute Reports, Vol.38, Seoul

Lee YH, Park TS, Youn YC, Ryu TK, Lim YJ, Choi JC, Byun WH, Kim EG (1997) History of Korean Forestry Policy. Korea Forest Service, Seoul

Lee IK, Lim JH, Kim C, Kim YK (2006) Nutrient dynamics in decomposing leaf litter and litter production at the long-term ecological research site I Mt. Gyebangsan (in Korean with English abstract). J Ecol Field Biol 29:585−591

Lei H, Zhi-Shan Z, Xin-Rong L (2010) Sap flow of *Artemisia ordosica* and the influence of environmental factors in a revegetated desert area: Tengger Desert, China. Hydrol Process 24:1248−1253

Lim JH, Chun JH, Woo SY, Kim YK (2008) Increased declines of Korean fir forest caused by climate change in Mountain Halla, Korea. In: Oral Presentation At: International Conference "Adaptation of Forests and Forest Management to Changing Climate with Emphasis on Forest Health: A Review of Science, Policies, and Practices", Umeá, Sweden, FAO/IUFRO, 25–28 August 2008

Magnani F, Leonardi S, Tognetti R, Grace J, Borghetti M (1998) Modeling the surface conductance of a broad-leaf canopy: effects of partial decoupling from the atmosphere. Plant Cell Environ 21:867−879

Matyssek R, Wieser G, Patzner K, Blaschke H, Häberle K-H (2009) Transpiration of forest trees and stands at different altitude: consistencies rather than contrasts? Eur J For Res 128−579596

McDowell NG, Phillips N, Lunch C, Bond BJ, Ryan MG (2002) An investigation of hydraulic limitation and compensation in large, old Douglas-fir trees. Tree Physiol 22:763−774

McDowell NG, White S, Pockman WT (2008) Transpiration and stomatal conductance across a steep climate gradient in the southern Rocky Mountains. Ecohydrol 1:193−204

Meinzer FC, Goldstein G, Andrade JL (2001) Regulation of water flux through tropical forest canopy trees: do universal rules apply? Tree Physiol 21:19−26

Meinzer FC, Bond BJ, Warren JM, Woodruff DR (2005) Does water transport scale universally with tree size? Funct Ecol 19:558−565

Miyajima Y, Takahashi K (2007) Changes with altitude of the stand structure of temperate forests on Mount Norikura, central Japan. J For Res 12:187−192

Monteith JL (1965) Evaporation and environment. Symp Soc Exp Biol XIX:205−234

Monteith JL, Unsworth MH (1990) Principles of environmental physics. Edward Arnold, London

Muraoka H, Koizumi H (2005) Photosynthetic and structural characteristics of canopy and shrub trees in a cool-temperate deciduous broadleaved forest: Implication to the ecosystem carbon gain. Agric For Meteorol 134:39−59

Murray FW (1967) On the computation of saturation vapor pressure. J Appl Meteorol 6:203−204

Nakashizuka T (1987) Regeneration dynamics of beech forests in Japan. Vegetatio 69:169−175

Nakashizuka T, Iida S (1995) Composition, dynamics and disturbance regime of temperate deciduous forests in Monsoon Asia. Vegetatio 121:23−30

Nasahara KN, Muraoka H, Nagai S, Mikami H (2008) Vertical integration of leaf area index in Japanese deciduous broad-leaved forest. Agric For Meteorol 148:1136−1146

National Institute of Environental Research (2011) Korea Climate Change Valuation 2010, Incheon, NIER

Niinemets U (2002) Stomatal conductance alone does not explain the decline in foliar photosynthetic rates with increasing tree age and size in *Picea abies* and *Pinus sylvestris*. Tree Physiol 22:515−535

O'Grady AP, Cook PG, Eamus D, Duguid A, Wischusen JDH, Fass T, Worldege D (2009) Convergence of tree water use within an arid-zone woodland. Oecologia 160:643−655

Oh J-H, Kim T, Kim M-K, Lee S-H, Min S-K, Kwon W-T (2004) Regional climate simulation for Korea using dynamic downscaling and statistical adjustment. J Meteorol Soc Jpn 82:1629−1643

Oren R, Phillips N, Katul G, Ewers BE, Pataki DE (1998) Scaling xylem sap flux and soil water balance and calculating variance: a method for partitioning water flux in forests. Ann Sci For 55:191−216

Oren R, Phillips N, Ewers BE, Pataki DE, Megonigal JP (1999) Sap-flux-scaled transpiration responses to light, vapor pressure deficit, and leaf area reduction in a flooded *Taxodium distichum* forest. Tree Physiol 19:337−347

Oren R, Pataki DE (2001) Transpiration in response to variation in microclimate and soil moisture in southeastern deciduous forests. Oecologia 127:549−559

Otieno DO, Schmidt MWT, Kurz-Besson C, Lobo Do Vale R, Pereira JS, Tenhunen JD (2007) Regulation of transpirational water loss in *Quercus suber* trees in a Mediterranean-type ecosystem. Tree Physiol 27:1179−1187

Park J-Y, Park M-J, Ahn S-R, Park G-A, Yi J-E, Kim G-S, Sinivasan R, Kim SJ (2011) Assessment of future climate change impacts on water quantity and quality for a mountainous dam watershed using SWAT. Trans ASABE 54:1725−1737

Phillips N, Oren R, Zimmermann R, Wright SJ (1999) Temporal patterns of water flux in trees and lianas in a Panamanian moist forest. Tree 14:116−123

Qian H, Ricklefs RE (1999) A comparison of the taxonomic richness of vascular plants in China and the United States. Am Nat 154:160−181

Qian H, Ricklefs RE (2000) Large-scale processes and the Asian bias in species diversity of temperate plants. Nature 407:180−182

R Development Core Team (2009) R: A Language and Environment for Statistical Computing. Vienna, Austria: R Foundation for Statistical Computing

Reichstein M et al. (2005) On the separation of net ecosystem exchange into assimilation and ecosystem respiration: revies and improved algorithm. Glob Change Biol 11:1424−1439

Richardson AD, Bailey AS, Denny EG, Martin CW, O'Keefe J (2006) Phenology of a northern hardwood forest canopy. Glob Change Bio 12:1174−1188

Röhrig E (1991a) Climatic conditions. pp. 7−16. In: Röhrig E and Ulrich B (eds.) Temperate Deciduous Forests. Elsevier, Amsterdam

Röhrig E (1991b) Floral composition and its evolutionary development. pp. 17−33. In: Röhrig E and Ulrich B (eds.) Temperate Deciduous Forests. Elsevier, Amsterdam

Sakuratani T (1981) A heat balance method for measuring water flux in the stem of intact plants. J Agric Meteorol 37:9–17

Sakuratani T (1984) Improvement of the probe for measuring water flow rate in intact plants with the stem heat balance method. J Agric Meteorol 40:273–277

Schulze E-D, Leuning R, Kelliher FM (1995) Environmental regulation of surface conductance for evaporation from vegetation. Vegetatio 121:79−87

Schulze E-D, Beck E, Müller-Hohenstein K (2005) Plant Ecology. Springer Berlin, Heidelberg

Shin H-J, Park G-A, Park M-J, Kim S-J (2012) Projection of forest vegetation change by applying future climate change scenario MIROC3.2 A1B. Journal of the Korean Association of Geographic Information Studies 15:64−75

Sparks JP, Ehleringer JR (1997) Leaf carbon discrimination and nitrogen content for riparian trees along elevational transects. Oecologia 109:362-367

Stewart JB (1988) Modelling surface conductance of pine forest. Agric For Meteor 43:19−35

Swank WT, Douglass JE (1974) Streamflow greatly reduced by converting deciduous hardwood stands to pine. Science 185:857−859

Tateishi M, Kumagai T, Suyama Y, Hiura T (2010) Differences in transpiration characteristics of Japanese beech trees, *Fagus crenata*, in Japan. Tree Physiol 30:748−760

Tateno R, Hishi T, Takeda H (2004) Above- and belowground biomass and net primary production in a cool-temperate deciduous forest in relation to topographical changes in soil nitrogen. Forest Ecol Manag 193:297−306

Tenhunen JD, Lange OL, Gebel J, Beyschlag W, Weber JA (1984) Changes in photosynthetic capacity, carboxylation efficiency, and CO_2 compensation point associated with midday stomatal closure and midday depression of et CO_2 exchange of leaves of *Quercus suber*. Planta 162:193−203

Tieszmann LL and Archer S (1990) Isotope assessment of vegetation changes. In: Osmond CB, Pitelka LF, Hidy GM (Eds.), Plant Biology of the Basin and Range, vol. 80. Ecological Studies, pp. 144−178

Tromp-van M, McDonnell JJ (2006) On the interrelations between topography, soil depth, soil moisture, transpiration rates and species distribution at the hillslope scale. Adv Water Resour 29:293−310

Unsworth MH, Phillips N, Link T, Bond BJ, Falk M, Harmon ME, Hinckley TM, Marks D, Paw UK-T (2004) Component and controls of water flux in an old-growth Douglas-fir-western hemlock ecosystem. Ecosystems 7:468−481

Van de Water PK, Leavitt SW, Betancourt JL (2002) Leaf $\delta^{13}C$ variability with elevation, slope aspect, and precipitation in the southwest United States. Oecologia 132:332−343

Velichko AA, Spasskaya I (2002) Climatic change and the development of landscapes. In: Shahgedanova M (Eds.), The Physical Geography of Morthern Eurasia, Oxford University Press, Oxford, pp. 36−69

Vertessy RA, Benyon RG, O'sullivan SK, Gribben PR (1995) Relationships between stem diameter, sapwood area, leaf area and transpiration in a young mountain ash forest. Tree Physiol 15:559−567

Vitasse Y, Porté AJ, Kremer A, Michalet R, Delzon S (2009) Responses of canopy duration to temperature changes in four temperate tree species: relative contributions of spring and autumn leaf phenology. Oecologia 161:187−198

Walter H, Lieth H (1967) Klimadiagramm-Weltatlas. VEB Gustav Fischer Verlag, Jena

Weibel FP, de Vos JA (1994) Transpiration measurements on apple trees with an improved stem heat balance method. Plant Soil 166:203−219

Willmott CJ (1981) On the validation of models. Physical Geography 2:184−194

Wilson KB, Baldocchi DD (2000) Seasonal and interannual variability of energy fluxes over a broad-leaved temperate deciduous forest in North America. Agric For Meteorol 100:1−18

Wilson KB, Hanson PJ, Mulholland PJ, Baldocchi DD, Wullschleger SD (2001) A comparison of methods for determining forest evapotranspiration and its components: sap-flow, soil water budget, eddy covariance and catchment water balance. Agric For Meteorol 106:153−168

Whitley R, Zeppel M, Armstrong N, Macinnis-Ng C, Yunsa IAM, Eamus D (2008) A modified JS model for predicting stand-scale transpiration of an Australian native forest. Plant Soil 305:35−47

Whitley R, Medlyn B, Zeppel M, Macinnis-Ng C, Eamus D (2009) Comparing the Penman-Monteith equation and a modified Jarvis-Stewart model with an artificial neural network to estimate stand-scale transpiration and canopy conductance. J Hydrol 373:256−266

Wullschleger SD, Hanson PJ, Tschaplinski TJ (1998) Whole-plant water flux in understory red maple exposed to altered precipitation regimes. Tree Physiol 18:71−79

Wullschleger SD, Hanson PJ, Todd DE (2001) Transpiration from a multi-species deciduous forest as estimated by xylem sap flow techniques. For Ecol Manage 143:205−213

Youn Y-C (2009) Use of forest resources, traditional forest-related knowledge and livelihood of forest dependent communities: Case in South Korea. For Ecol Manage 257:2027−2034

Zeppel MJB, Yunusa IAM, Eamus D (2006) Daily, seasonal and annual patterns of transpiration from a stand of remnant vegetation dominated by a coniferous *Callitris* species and a broad-leaved *Eucalyptus* species. Physiol Plantarum 127:413–422

Zeppel M, Eamus D (2008) Coordination of leaf area, sapwood area and canopy conductance leads to species convergence of tree water use in a remnant evergreen woodland. Aust J Bot 56:97−108

Zimmermann R, Schulze ED, Wirth C, Schulze EE, McDonald KC, Vygocskaya NN, Ziegler W (2000) Canopy transpiration in a chronosequence of Central Siberian pine forests. Global Change Biol 6:25−37

Chapter 2

Up-scaling to stand transpiration of an Asian temperate mixed-deciduous forest from single tree sap flow measurements

Plant Ecology (2011) 212: 383-395

E.Y. Jung[a*], D. Otieno[a], B. Lee[a], J.H. Lim[b], S.K. Kang[c], M.W.T. Schmidt[d], J. Tenhunen[a]

[a]Department of Plant Ecology, University of Bayreuth, 95440 Bayreuth, Germany

[b]Korea Forest Research Institute, 57 Hoegiro, Dongdaemun-gu, Seoul, Republic of Korea

[c]Department of Environmental Science, Kangwon National University, 192-1 Chuncheon, Republic of Korea

[d]BIOEMCO (UPMC-Paris 6), Campus AgroParisTech, 78850 Thiverval-Grignon, France

Abstract

Species diversity in mixed forest stands is one of the factors that complicate up-scaling of transpiration from individual trees to stand level, since tree species are architecturally and functionally different. In this study, thermal dissipation probes were used to measure sap flow in five different tree species in a mixed deciduous mountain forest in South Korea. Easily measurable tree characteristics that could serve to define individual tree water use among the different species were employed to scale up transpiration from single trees to stand level. Tree water use (TWU) was derived from sap flux density (F_d) and sapwood area (A_S). Canopy transpiration (E_C) was scaled from TWU, while canopy conductance (G_C) was computed from *E* and vapor pressure deficit (VPD). SFD, TWU and G_C were correlated with tree diameter at breast height (DBH) for all the five measured species (F_d: R^2 = 0.21, *P* = 0.036; TWU: R^2 = 0.83, *P* <0.001; G_C: R^2 = 0.63, *P* <0.001). Maximum E_C during June, before the onset of the Asian monsoon rains, was estimated at 0.97 ± 0.12 mm d^{-1}. There was a good (R^2 = 0.94, *P* <0.0001) agreement between measured and estimated E_C using the relationship between TWU and DBH. Our study shows that using functional models that employ converging traits among species could help in estimating water use in mixed forest stands. Compared to A_S, DBH is a better scalar for water use of mixed forest stands since it is non-destructive and easily obtainable.

Key-words: Allometric scaling, Sap flow, Temperate deciduous forest, Thermal, Dissipation probes, Tree water use

2.1 Introduction

Understanding of water use by forest stands is critical in order to build a sustainable water resource management scheme. Previous attempts have been made to estimate transpiration in diverse tree species using sap flow measurement techniques, which can measure water use at tree level (Granier 1987; Oren et al. 1998; Hubbard et al. 2004; Dierick and Hölscher 2009). In forest monocultures, the individual tree transpiration is then up-scaled to stand level using simple allometrics (Alsheimer et al. 1998; Köstner et al. 2001). In mixed forest stands, however, species diversity may complicate the up-scaling procedure, due to variations in species structure and function that influence water use by the individual tree species (O'Grady et al. 2009). In cases where species vary in growth forms, for example, those with shorter crowns remain in the sub-canopy where light levels are reduced, the humidity is higher and more constant, with little direct sunlight. Under such conditions, they are bound to experience lower transpiration rates compared to the canopy species, which are subjected to intense radiation, higher wind speeds, and lower humidity.

In cases where the forest is a mixture of deciduous and evergreen tree species, the evergreen species may have higher daily sap flow than the deciduous and semi-deciduous species because of their higher biomass and larger sapwood area involved in water transport (Dünisch and Morais 2002). Tree species may also differ in the way they respond to their abiotic environment, particularly during mild water stress that may occur during the day, and this could also determine the patterns of water use among co-occurring species (Bovard et al. 2005). Differences in transpiration have also been reported between diffuse-porous and ring-porous tree species, regardless of their position in the canopy as a result of differences in their wood structure and function (Oren and Pataki 2001). Structural and functional differences may, therefore, limit the application of simple allometric procedures for scaling up to stand transpiration from single trees.

On the other hand, Bucci et al. (2004) demonstrated that wood density, hydraulic architecture, and plant water relations are related and that wood density is age-dependent and not species-specific characteristic. Thus tree size, rather than species, is the main determinant of stand transpiration, as demonstrated in other more recent studies (Vertessy et al. 1995; Wullschleger et al. 2001; Meinzer 2003; O'Brien et al. 2004; Meinzer et al. 2005; Zeppel and Eamus 2008). Significant correlation occurred between tree diameter and daily sap flux among 20 different rainforest species (Meinzer et al. 2005). Wullschleger et al. (2001) derived daily stand transpiration from sap fluxes of five different deciduous tree species using sapwood area, and demonstrated that tree size and not species differences had overriding influence on stand transpiration. O'Brien et al. (2004), investigating 10 tree species in a wet tropical forest reported that structural characteristics such as tree height were the main determinants of tree sap flow. They concluded that the effect of species-specific differences was small and had less influence on stand transpiration. Similar conclusions were drawn by Dierick and Hölscher (2009) and Herbst et al. (2008), showing that maximum tree water use in forest stands is strongly related to tree diameter.

Competition for resources, particularly in resource-limited environments, is likely to compel the convergence of functional traits among diverse species, particularly those that relate to efficient resource acquisition, allowing species to functionally substitute each other (Meinzer 2003; Bucci et al. 2004; O'Grady et al. 2009). This suggests that differences in species may have limited influence on forest water use. In this article, we present results of tree water use from a mixed-deciduous temperate forest stand in South Korea. We hypothesize that stand transpiration is determined by tree structural characteristics, such as tree height, stem diameter etc., and is independent of species composition. The objectives of the study were to (1) estimate water use in individual trees in a mixed, deciduous forest stand, (2) identify simple and easily measurable structural traits that universally define transpiration of single trees in a mixed temperate deciduous forest, and (3) find a general principle, based on simple functional relationships, which describes mixed stand transpiration.

2.2 Materials and methods

2.2.1 Study sites

The study was conducted at the Long-term Ecological Research site in Mt. Gyebangsan, Gangwon-do (Province) in South Korea (37°44'41.3"N, 128°26'45.7"E, 960 m. a.s.l), which is located in the northern, cool temperate forest zone. The forest was ca. 40−50 years old and was a natural re-growth after the disturbance through massive logging of Korean forests that took place during and after the Korean War. Mean annual precipitation at Nae-myun (county) weather station, the nearest long-term site (1997−2009) weather recording station located 5.2 km away from the study site was 1,453 ± 337 mm (Figure 2.1). Approximately 45% of the total annual rainfall occurred between June and July, associated with the Asian monsoon. The period between March and April was relatively dry. Mean annual temperature was around 7.8°C with maximum and minimum daily mean air temperatures of 29.3 and –22.5°C occurring in August and January, respectively. The relative humidity within the forest canopy ranged between 52 and 86% most of the year, with July to September being the most humid months. Soils at the study site were classified as brown forest soils (B3) originating from metamorphic bedrock (Kim 2003; Lee et al. 2006).

2.2.2 Vegetation

Long-term vegetation survey has been conducted by the Korea Forest Research Institute (KFRI) at this site since the last 14 years. We demarcated a study plot measuring 40 m × 50 m (0.2 ha) during 2008 and 2009 to measure tree transpiration using sap flow techniques. A total of 24 different tree species were identified at the study site. Sap flow measurements were carried out on five dominant tree species, including *Tilia*

amurensis, *Ulmus davidiana*, *Quercus mongolica, Acer mono* and *Cornus controversa*. A total of 205 trees with tree diameter at breast height DBH >5 cm were identified within the study plot. Tree density was 1,025 trees ha^{-1}, with a mean canopy height of 10 m. Mean DBH was 15.9 cm with a total basal area of 21.2 m^2 ha^{-1}. The basal area of the trees was calculated from DBH and included the bark. The selected trees for sap flux measurement covered 70% of the total basal area within the demarcated study plot.

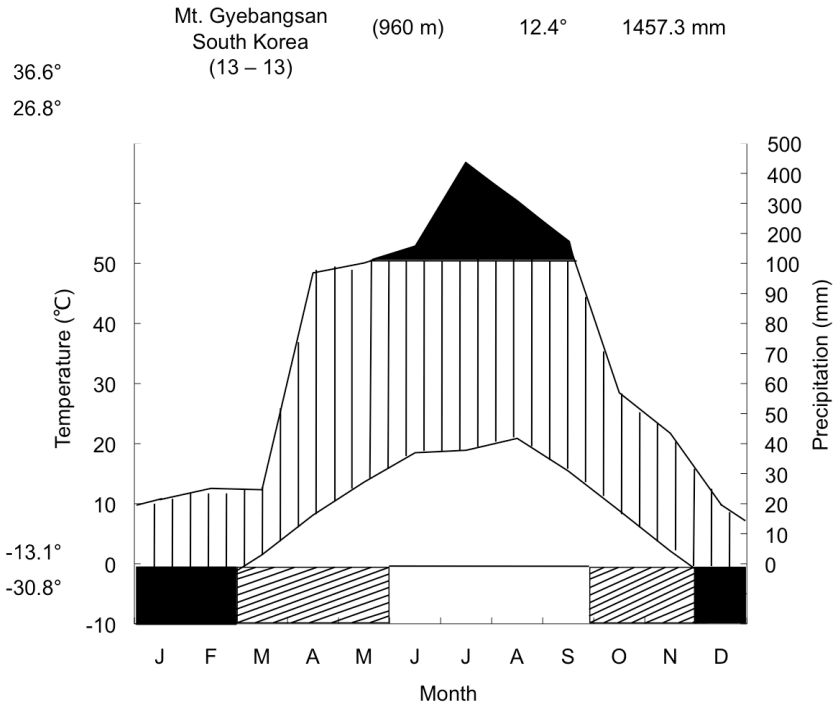

Figure 2.1 Climate diagram according to Walter and Lieth (1967) for Mt. Gyebangsan, South Korea. Data was collected at the weather station between 1997 and 2009. Lined area indicates humid period and black area is when average monthly precipitation exceeds 100 mm (from May to September). The altitude of the site was 960 m a.s.l., mean annual temperature was 12.4° and mean annual amount of precipitation was 1,457 mm.

2.2.3 Micrometeorology

Micrometeorology measurements were carried out on the site using automated instruments installed at different locations within the plot in June and July 2008 and repeated over the same period in 2009, concurrently with sap flow measurements. Measurements were conducted inside and above the canopy, the latter using a 20 m scaffolding tower constructed on the site. Weather parameters included: light intensity

(UA-002-08, Onset, USA) at 1 m (below the canopy) and at 20 m height (above the canopy), photosynthetic active radiation (PAR) (LI-190, LI-COR, USA) at 20 m, air temperature and humidity (HMP35C, Cambell Scientific Inc., USA) at 5, 10, and 20 m height below, within and above the canopy, and soil water content and temperature (5TE, Decagon Devices, USA) at −5, −15 and −30 cm. These parameters were measured continuously during the experimental period. Data were averaged and logged every 30 min, either with loggers built into the sensors (light intensity) or a central data logger (DL2e, Delta-T Devices, UK). Vapor pressure deficit (VPD) was calculated from air temperature and relative humidity. Precipitation data were obtained from an automated weather station built by the Korea meteorological administration located 5.2 km away from our study site.

2.2.4 Tree allometrics

The sample trees were selected according to species and tree size distribution in the plot (Figure 2.2). *T. amurensis* was the dominant species in the plot, occupying 31.5% of the total basal area. *U. davidiana*, *Q. mongolica*, *A. mono*, and *C. controversa* were co-dominant and occupied 13.6, 10.7, 8.1, and 4.4% of the total basal area of the plot, respectively. Thus, these dominant and co-dominant species covered almost 70% of the total basal area of the study plot. We chose five trees each from *Q. mongolica, T. amurensis*, and *U. davidiana* and three trees each from *C. controversa* and *A. mono,* respectively, for the sap flow measurements. DBH ranges of 13.2−38.2 cm were considered (Table 2.1).

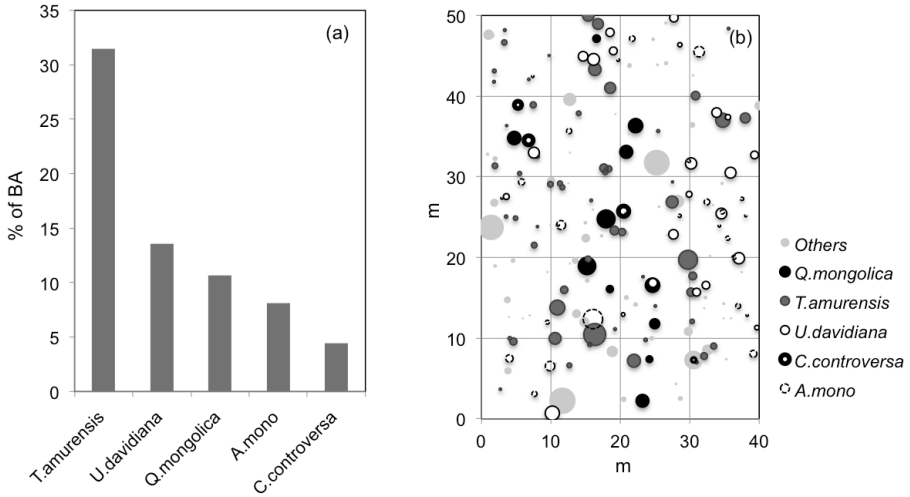

Figure 2.2 (a) Percentage of basal area of sample tree species in the study plot. The basal area (BA) for the five measured species occupied 70% of all trees in the plot. (b) Study site with specific location and relative size of trees. Total plot size was 2,000 m^2.

Table 2.1 Studied sample trees and respective diameter of breast height (DBH), tree height, sapwood depth, canopy area, mean sap flux density (F_d), and maximum F_d at Mt. Gyebangsan, June and July in 2008 and 2009.

Species	Sample trees	DBH (cm)	Tree height (m)	Sapwood depth (cm)	Canopy area (m^2)	Mean F_d ($g\ m^{-2}\ s^{-1}$)	Max F_d ($g\ m^{-2}\ s^{-1}$)
Q. mongolica	Q1[a]	27.6	14	2.9	16.0	21.9 ± 3.4	27.7
	Q2[a]	28.4	14	3.1	37.8	15.9 ± 3.9	23.8
	Q3	20.3	13	2.0	19.8	21.8 ± 3.9	30.8
	Q4	13.3	12	1.4	9.1	4.3 ± 2.6	11.7
	Q5[a]	38.2	15	4.9	46.5	24.4 ± 4.0	34.6
T. amurensis	T1	29.2	17	1.5	18.8	38.9 ± 9.3	54.5
	T2	18.9	14	0.8	9.0	7.7 ± 2.8	13.5
	T3	26.8	15	1.3	14.7	38.7 ± 8.9	53.2
	T4	13.2	12	0.6	16.8	21.4 ± 7.8	33.9
	T5	17.8	13	0.8	18.5	18.6 ± 7.7	32.7
U. davidiana	U1	23.1	15	1.6	11.2	22.9 ± 5.4	32.0
	U2	23.4	14	1.7	37.2	14.3 ± 2.4	18.3
	U3	28.6	16	2.2	22.7	23.3 ± 3.9	30.4
	U4	26.1	15	1.9	37.1	21.3 ± 4.9	30.1
	U5	18.7	15	1.3	18.5	28.9 ± 4.1	35.4
C. controversa	C1	25.3	15	1.2	62.5	34.0 ± 7.6	48.8
	C2	22.3	15	1.0	41.9	33.4 ± 7.0	49.3
	C3	17.6	15	0.7	28.8	15.7 ± 5.7	27.9
A. mono	A1	15.0	13	0.3	13.3	15.7 ± 5.7	27.0
	A2	22.0	14	0.5	38.7	30.7 ± 12.4	50.2
	A3	13.8	11	0.3	12.1	31.9 ± 13.9	57.8

DBH was sapwood depth was estimated by empirical regression models of DBH (see Figure 2.5). Projected canopy area was measured in late fall, 2008 and sap flux density (F_d) was measured during June 2008 and 2009

[a] Trees with a sapwood depth larger than 20 mm had two sensors in different depth

To estimate the sapwood area (A_S) of the sample trees, an increment borer was used to extract cores of sapwood at the sensor installation height (about 1.3 m height) on same species, but different trees from those installed with the sap flow sensors. Sapwood depth was determined visually on those cores since sapwood and heartwood were clearly distinguishable. A_S was determined from sapwood depth and tree DBH based on the equation (Vertessy et al. 1995; Meinzer et al. 2005):

$$A_S = \alpha \cdot DBH^{\beta} \quad (1)$$

where α is a constant and β is the allometric scaling exponent, and both species-specific coefficients. Coefficients of the regression models for each measured species, number of samples and R^2 are provided in the legend of Figure 2.5.

The ground-projected crown area (A_{cp}, m^2) of sample trees was measured in eight horizontal directions using a compass, crown mirror, and measuring tape. The octagonal area was calculated as the sum of eight triangles (Schmidt 2007). These results were used to compute canopy conductance (G_C, mm s^{-1}).

2.2.5 Tree sap flow

Sap flux density (F_d) was measured in the tree stems of five trees per species using the thermal dissipation method (Granier 1987) during June and July 2008 and repeated during the same period in 2009. This period was chosen as it was considered the most active period in the context of plant water use, just before the onset of the Monsoon rains. All sensor installations were made on the north-facing side of the trees to avoid exposure to the sun and minimize direct short-wave radiation (Wilson et al. 2001; Wullschleger et al. 2001). In addition, the sensors were covered with a radiation shield (Styrofoam sheets with aluminium foil) to further minimize the direct thermal load. Power for heating the sensors was provided by lead-acid batteries that were recharged with solar panels via a charge controller. Each sensor consisted of a pair of 2 mm diameter probes vertically aligned ca. 15 cm apart. Each probe included a 0.2 mm diameter copper-constantan thermocouple. The two thermocouples were joined at the constantan leads, so that the voltage measured across the copper leads provided the temperature difference between the heated upper probe and the lower reference. Heating across the entire length of the 20 mm upper probe was achieved with a constant current of 120 mA supplied to a constantan heating wire, resulting in a heating power of 200 mW (Granier 1987).

Sensors were placed in the outer 20 mm of the sapwood (annulus 1, 0−20 mm radial sapwood depth). In cases where the tree trunk was large with a sapwood radius greater than 20 mm (Table 2.1), a second sensor was implanted 20 to 40 mm into the sapwood. Sensors were spaced 10–15 cm circumferentially, away from the first sensor pair, on the same side of the stem to avoid azimuth differences. Temperature differences were measured every 5 min and a 30-min mean value was logged (DL2e with LAC-1 in single ended mode,

Delta-T Devices, England). Sap flux density (F_d, g m^{-2} s^{-1}) for each sensor was calculated from ΔT in accordance with Granier (1987), assuming zero F_d (i.e., ΔT_{max}) at night and VPD near zero:

$$F_d = 119 \cdot K^{1.231} \qquad (2)$$

where,

$$K = \frac{(\Delta T_{\max} - \Delta T)}{\Delta T} \qquad (3)$$

Tree water use (TWU, kg h^{-1}) was obtained by multiplying F_d by sapwood cross-sectional area (A_S, m^2).

$$TWU = \sum_{i=1}^{n} (F_{di} \cdot A_{Si}) \qquad (4)$$

where, F_{di} is sap flux density of the annulus *i* (g m^{-2} s^{-1}) and A_{Si} is sapwood area of the annulus *i* (m^2). This took into account the second annulus ring, in case a second sensor was installed into the tree. For example, *i* = 1 was annulus ring 0−20 mm sapwood depth, *i* = 2 was annulus ring 20−40 mm sapwood depth.

Canopy transpiration (E_C, mm per day) was computed by summing the contributions from all the trees in the study plot:

$$E_C = \sum_{j=1}^{n} TWU_j \times A_{plot}^{-1} \qquad (5)$$

where, TWU_j is tree water use of tree *j* (kg h^{-1}) and A_{plot} is plot area (m^2). TWU of the trees on which sensors were not installed was estimated from the relationship between F_d and the computed A_S of each species (Eq. 1).

2.2.6 Estimation of canopy conductance

Canopy conductance was calculated from the sap flow measurements or stand/canopy transpiration, in relation to climate variables: half hourly averaged air temperature, VPD, and canopy transpiration as described by Köstner et al. (1992):

$$G_C = (\rho_w \cdot G_v \cdot T_k) \cdot \frac{E_C}{VPD} \qquad (6)$$

where, ρ_w is density of water (998 kg m^{-3}) and G_v is gas constant of water vapor (0.462 m^3 kPa kg^{-1} K^{-1}), T_k is air temperature (*K*), and E_C is canopy transpiration (mm s^{-1}) (Schmidt 2007). To estimate G_C based on this model, data from measurements between 10 and 15 h, when half hourly rates of E_C were highest, were used. This model assumed that tree canopies were well coupled to the atmosphere, so that aerodynamic conductance (G_A) was larger than G_C (Köstner et al. 1992; Phillips and Oren 1998).

2.2.7 Statistical analyses

F_d and environmental variables were recorded as half hourly averaged values. These variables, including TWU and G_C estimated from F_d were converted into daily averages. Data are presented as mean ± standard deviation (SD). F_d, TWU, and G_C were compared between years and also among tree species using one-way ANOVA. Where differences were found among species, a post-hoc Kruskal-Wallis test was carried out. Normality of samples was established by testing the residuals obtained from the ANOVA. Measured and estimated E_C by the relationship between TWU and DBH were compared with *t*-test. Regression analysis was tested with Pearson correlation test. All statistical analyses including regression models were based on a 0.05 significance level and performed with R version 2.6.2 (R Development Core Team, 2008).

2.3 Results

2.3.1 Micrometeorological and soil moisture measurements

Daily mean air temperatures over the measurement period of June and July were about 19.3°C in 2008 and 18.3°C in 2009. Averaged daily VPD were 0.34 kPa in 2008 and 0.28 kPa in 2009, while the summed daily PAR were 32.6 mol m^{-2} d^{-1} in 2008 and 25.9 mol m^{-2} d^{-1} in 2009 respectively (Figure 2.3a). The total amount of precipitation recorded during the measurement period was 89 mm in 2008, and 178.5 mm in 2009. Mean soil water content (θ) within the 30cm soil profile was 0.24 ± 0.04 m^3 m^{-3} in 2008 and 0.21 ± 0.05 m^3 m^{-3} in 2009 (Figure 2.3a). Before the onset of our experiments 2009 was comparatively drier than 2008, as demonstrated by lower θ at the beginning of measurements. A rainstorm event on June 3, 2009 amounting to 73 mm, however, significantly raised θ (from 0.11 to 0.29 m^3 m^{-3}), and θ thereafter was comparable to 2008.

2.3.2 Transpiration rate and canopy conductance

Mean maximum F_d for the 21 trees measured was 247.5 ± 93.1 kg m^{-2} h^{-1} in 2008 and 271.5 ± 97.1 kg m^{-2} h^{-1} in 2009 (Table 2.2). There was no significant ($F = 0.88$, $P = 0.35$) difference in F_d between the two years. And also, mean maximum TWU was 21.0 ± 21.8 kg d^{-1} in 2008 and 32.9 ± 22.0 kg d^{-1} in 2009 (Table 2.2). A comparison of maximum TWU from different years showed same results ($F = 1.00$, $P = 0.33$). Mean daily F_d of *Q. mongolica*, *T. amurensis*, *U. davidiana*, *C. controversa*, and *A. mono* were 40.9 ± 17.8 kg m^{-2} h^{-1} (n = 5), 49.5 ± 26.1 kg m^{-2} h^{-1} (n = 5), 49.2 ± 8.4 kg m^{-2} h^{-1} (n = 5), 59.5 ± 24.5 kg m^{-2} h^{-1} (n = 3) and 55.4 ± 17.8 kg m^{-2} h^{-1} (n = 3). TWU and G_C averaged over the measurement period are shown in Table 2.3. The mean daily TWU ranged from 1.2 kg d^{-1} for *A. mono* with DBH of 15.0 cm to 70.1 kg d^{-1} for *Q.*

mongolica with DBH of 38.2 cm. And mean G_C amounted from 0.7 mm s^{-1} for *Q. mongolica* with DBH of 13.3 cm to 16.1 mm s^{-1} for *T. amurensis* with 29.2 cm. Mean maximum G_C of the stand was 5.6 ± 4.8 mm s^{-1}.

The averaged E_C was 0.64 ± 0.26 mm d^{-1} in 2008 and 0.70 ± 0.30 mm d^{-1} in 2009. The maximum E_C occurred around day 177 in 2009 (June 26, 0.97 mm d^{-1}, Figure 2.4), coinciding with the highest daily total PAR and VPD. There were no significant (F = 0.31, *P* = 0.73) differences in daily transpiration among *Q. mongolica*, *T. amurensis*, and *U. davidiana.* The percentage mean contribution of the three species was about 30% each, while *C. controversa* and *A. mono* each accounted for about 4% of the total transpiration. There was no significant influence of species on F_d (*P* = 0.82), TWU (*P* = 0.19) and G_C (*P* = 0.23).

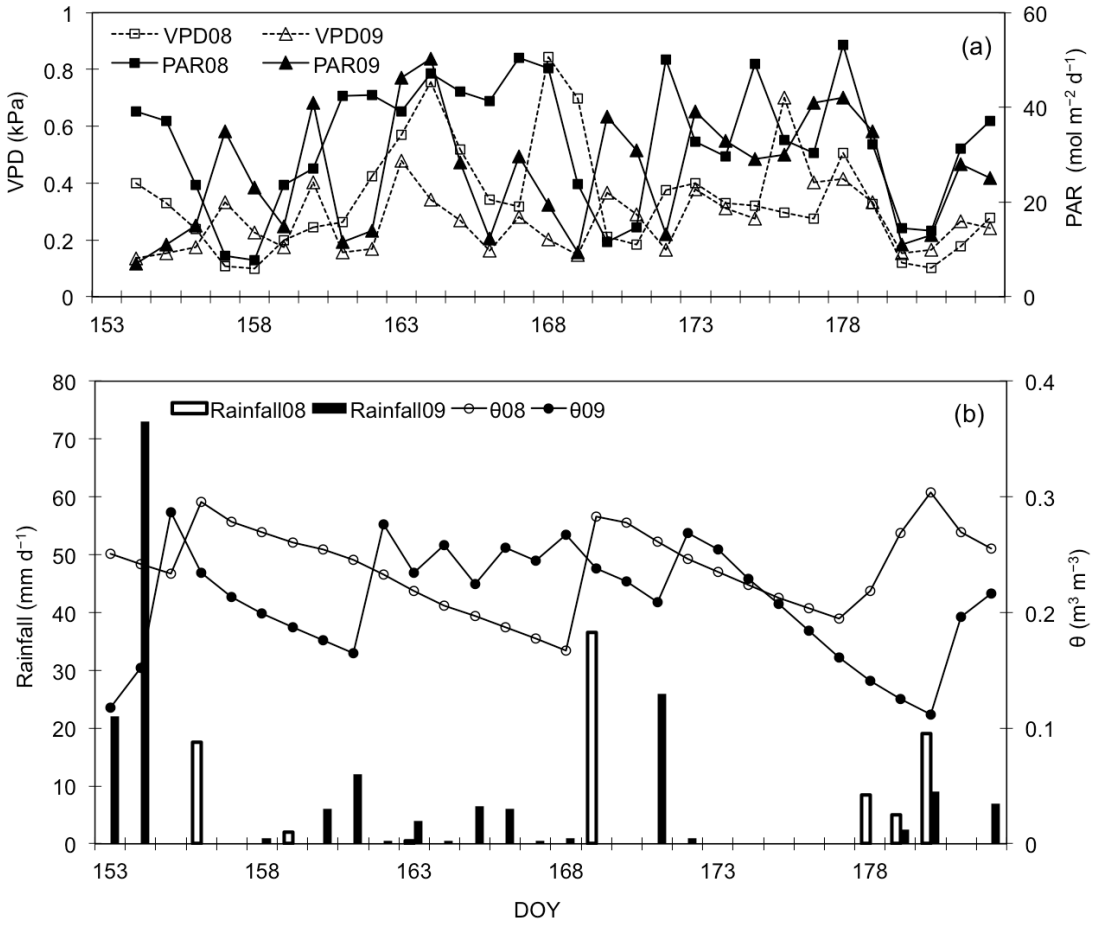

Figure 2.3 (a) Daily mean vapor pressure deficit (VPD, kPa) and daily amounts of photosynthetic active radiation (PAR, mol m^{-2} d^{-1}), (b) rainfall (mm d^{-1}) and soil water content (θ, m^3 m^{-3}) recorded at the study site during June 2008 and 2009 when sap flow measurements were conducted.

Table 2.2 Maximum sap flux density (F_d) and maximum tree water use (TWU) averaged for 21 measured trees from June 2008 and June 2009.

	June 2008	June 2009	*F-value*	*P-value*
Max F_d (kg m^{-2} h^{-1})	247.48	271.46	0.8834	0.3529
SD	93.13	97.14		
Max TWU (kg d^{-1})	21.02	32.91	0.9971	0.3264
SD	21.77	22.02		

Table 2.3 Mean tree water use (TWU, kg d^{-1}) and canopy conductance (G_C, mm s^{-1}) of individual tree species.

Species	Sample trees	Mean TWU (kg d^{-1})	Mean G_C (mm s^{-1})
Q. mongolica	Q1	27.8 ± 11.6	13.1 ± 4.3
	Q2	20.1 ± 9.1	3.4 ± 0.9
	Q3	14.2 ± 6.4	4.3 ± 1.7
	Q4	1.3 ± 0.7	0.7 ± 0.2
	Q5	70.1 ± 23.4	9.7 ± 4.1
T. amurensis	T1	20.4 ± 9.7	16.1 ± 4.3
	T2	1.9 ± 0.9	2.0 ± 0.8
	T3	17.2 ± 5.2	6.7 ± 2.2
	T4	2.6 ± 1.3	2.1 ± 0.6
	T5	3.7 ± 2.0	2.4 ± 0.6
U. davidiana	U1	13.7 ± 5.7	13.4 ± 2.9
	U2	9.2 ± 2.9	7.0 ± 1.2
	U3	22.3 ± 7.7	9.2 ± 2.9
	U4	17.3 ± 5.5	5.4 ± 2.3
	U5	9.1 ± 3.7	2.9 ± 0.8
C. controversa	C1	14.7 ± 5.4	4.2 ± 1.8
	C2	10.8 ± 4.0	2.8 ± 0.9
	C3	2.8 ± 1.3	1.5 ± 0.4
A. mono	A1	1.2 ± 0.6	2.3 ± 0.6
	A2	5.4 ± 3.1	2.6 ± 0.7
	A3	2.0 ± 1.0	1.6 ± 0.5

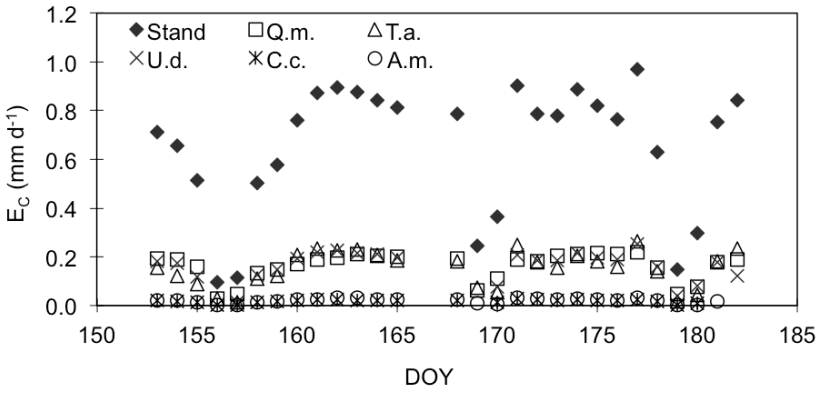

Figure 2.4 Estimated canopy transpiration (E_C, mm d^{-1}) and transpiration of measured species, *Quercus mongolica* (Q.m.), *Tilia amurensis* (T.a.), *Ulmus davidiana* (U.d.), *Cornus controversa* (C.c.), and *Acer mono* (A.m.).

2.3.3 Relationship between tree water use and tree size

Parameters derived from the allometric equation (Eq. 1) relating A_S and DBH of the five different species are shown in Figure 2.5. The converged regression model inverted from the five different species showed a strong relationship (n = 35, R^2 = 0.81, P <0.001) between A_S and DBH. This model was used to compute A_S of non-measured species to arrive at A_S for the whole study plot. *Q. mongolica* (0.15 m^2 ha^{-1}), *T. amurensis* (0.29 m^2 ha^{-1}), *U. davidiana* (0.16 m^2 ha^{-1}), *C. controversa* (0.03 m^2 ha^{-1}), and *A. mono* (0.06 m^2 ha^{-1}), accounted for 79.3% of total A_S which was 0.87 m^2 ha^{-1} (study plot = 0.2 ha).

Observed F_d, TWU and G_C were dependent on tree size, determined by DBH and A_S. F_d and TWU had a stronger dependency on DBH than on A_S. For example, a regression of F_d in individual trees against A_S did not show any relationship (n = 21, R^2 = 0.03, P >0.44), but a regression between F_d and DBH showed that DBH could explain 21% of the observed variability (n = 21, R^2 = 0.21, P = 0.036) in F_d among the studied trees (Figure 2.6a). Moreover, the relationship between mean daily TWU and DBH was stronger (n = 21, R^2 = 0.87, P <0.001) for all measured species (Figure 2.6b). SA was also significantly correlated with TWU, but less than DBH (n = 21, R^2 = 0.83, P <0.001). G_C had significant relationship with both DBH and A_S, and also like other relations G_C was correlated better with DBH (n = 17, R^2 = 0.63, P <0.001) (Figure 2.6c) than A_S (n = 17, R^2 = 0.48, P = 0.002).

E_C estimated from measured TWU was compared with E_C* estimated from modelled TWU based on the relationship of DBH and TWU (Figure 2.6b). In this study, the empirical model was TWU =

$0.0002DBH^{3.4302}$ for mean daily TWU over the measurement period (P <0.001). There was a strong agreement (n = 22, R^2 = 0.94, P <0.0001) between the measured and modeled E_C*.

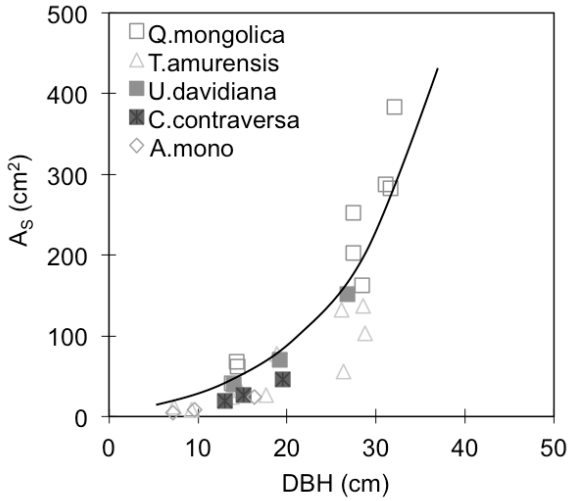

Figure 2.5 Relationship between sapwood area (A_S, cm^2) determined from increment core extracted from more than five samples per species and their respective diameter at breast height (DBH) (n = 35, R^2 = 0.81, P <0.001). The regression equation for *Quercus mongolica* was $A_S = 0.2067DBH^{2.1}$ (n = 9, R^2 = 0.94), for *Tilia amurensis* was $A_S = 0.1846DBH^{2.0}$ (n = 10, R^2 = 0.85), for *Ulmus davidiana* was $A_S = 0.1745DBH^{2.1}$ (n = 3, R^2 = 0.98), for *Cornus controversa* was $A_S = 0.0757DBH^{2.2}$ (n = 3, R^2 = 0.98), for *Acer mono* was $A_S = 0.0215DBH^{2.4}$ (n = 3, R^2 = 0.98), and for all the studied species was $A_S = 0.053DBH^{2.4}$ (n = 35, R^2 = 0.81)

2.3.4 Relationship between tree water use and climate factors

Both VPD (R^2 = 0.78 and P <0.0001) and PAR (R^2 = 0.91, P <0.0001) (Figure 2.7) could explain most of the daily fluctuations in E_C. E_C increased with increasing VPD, attaining a maximum at VPD = 0.5 kPa, but later dropped at higher VPD (Figure 2.7a). On days when VPD was high, E_C increased during morning hours with increasing PAR and reached a maximum at around midday, when PAR was >1,200 μmol m^{-2} s^{-1} (Figure 2.7b). G_C of the stand corresponding to the light conditions more than 20 mol m^{-2} d^{-1} of PAR, was plotted against VPD (Figure 2.7c). The selected data showed a log-linear relationship between G_C and VPD (R^2 = 0.69, P <0.0001). This regression model agreed with the simplified model of Lohammar *et al*. (1980):

$$G_C = b - c \cdot (\ln VPD) \qquad (7)$$

where, b is G_C at a reference VPD = 1 kPa.

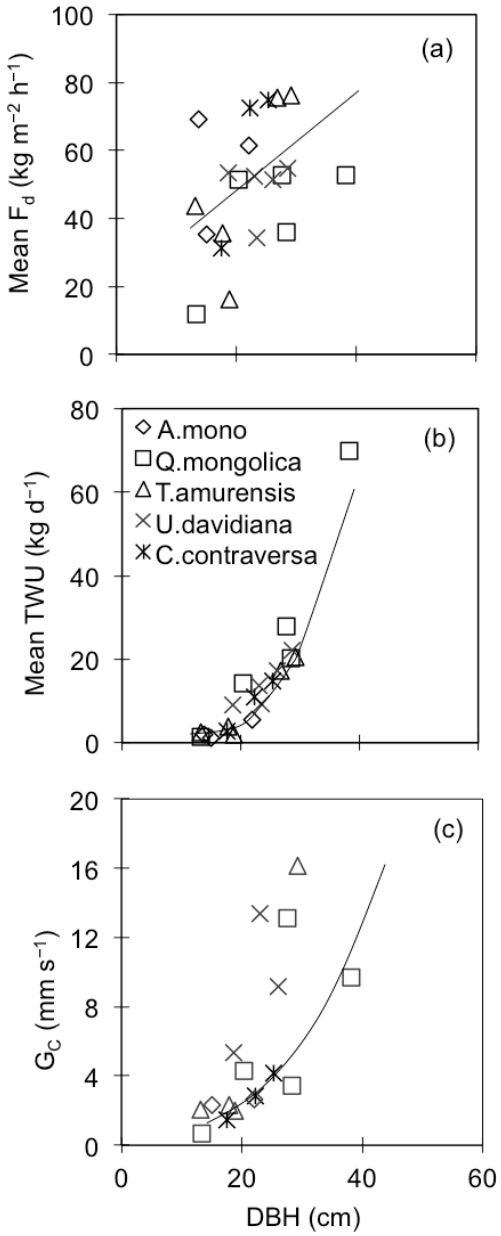

Figure 2.6 Relationship between DBH and (a) mean sap flux density (F_d, kg m^{-2} h^{-1}) (n = 21, R^2 = 0.21, *P* = 0.036), (b) mean tree water use (TWU, kg d^{-1}) (n = 21, R^2 = 0.87, *P* <0.001) and (c) canopy conductance (G_C, mm s^{-1}) significant (n = 17, R^2 = 0.63, *P* <0.001), of all the measured trees.

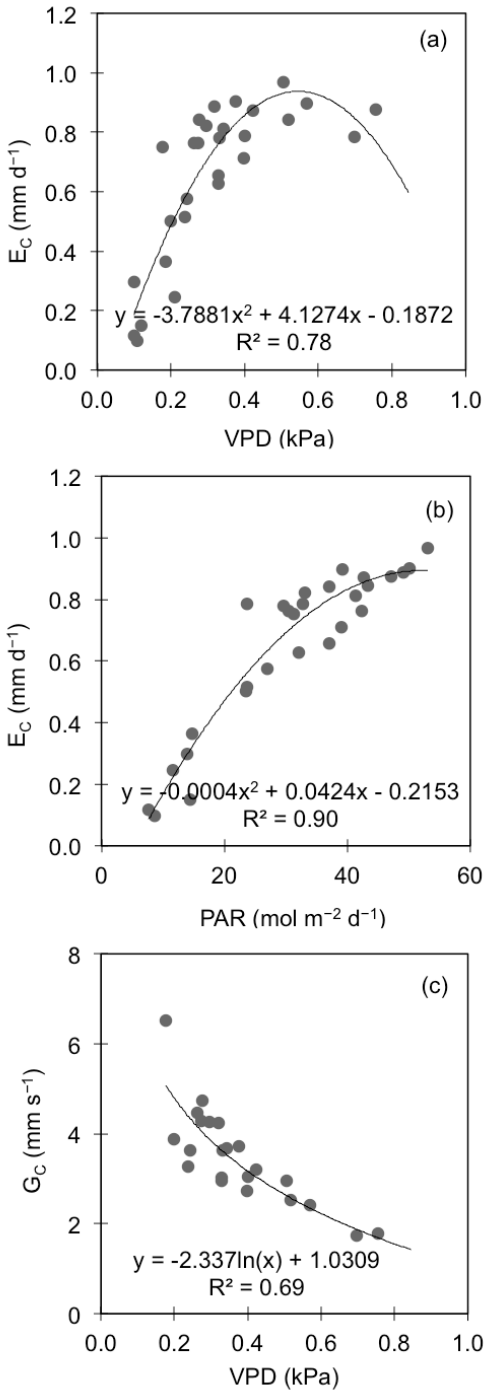

Figure 2.7 (a) Relation between vapor pressure deficit (VPD, kPa) and canopy transpiration (E_C, mm d^{-1}) (n = 28, R^2 = 0.78, *P* <0.0001), (b) between E_C and photosynthetically active radiation (PAR, mol m^{-2} d^{-1}) (n = 28, R^2 = 0.91, *P* <0.0001). (c) Canopy conductance (G_C, mm s^{-1}) under non-limiting light condition sand VPD (n = 22, R^2 = 0.69, *P* <0.0001).

2.4 Discussion

2.4.1 Tree water use and environmental factors

Five phylogenetically diverse temperate forest tree species were studied to identify any shared characteristics in their water use and whether these shared characteristics could aid in upscaling of transpiration in mixed-deciduous forest stands. We examined the relationship between tree size and the area of hydraulically active xylem and used this functional relationship to scale up tree water use from single trees to stand level, based on simple and easily measurable allometry. We provide the first estimates of tree water use in this region and report the first study in which sap flux measurements have been concurrently carried out on several species in mixed-deciduous forests of South Korea. Han and Kim (1996) measured F_d of *Q. mongolica* during a growing season in S. Korea using heat pulse methodology and reported maximum F_d values of 40 kg m^{-2} h^{-1}, occurring in May. These rates are comparable with the maximum F_d of 40.9 ± 17.8 kg m^{-2} h^{-1} observed for *Q. mongolica* in our study.

The maximum E_C was 0.97 mm d^{-1} when daily sum VPD was 24.2 kPa, daytime mean VPD was 0.67 kPa and the daily sum PAR was 53.1 mol m^{-2} d^{-1}. These rates are lower compared to those reported in other studies on temperate deciduous stands (Oren and Pataki 2001; Wullschleger et al. 2001). For example, peak stand transpiration of upland oak forest of east Tennessee, USA was 2.2 mm d^{-1} in May prior to canopy closure when the maximum daily sum VPD was 35 kPa (Wullschleger et al. 2001). Maximum daily stand transpiration of the Duke forest, North Carolina, dominated by *Quercus* and *Acer* species reached 2 mm d^{-1} when daytime mean VPD was almost 2.2 kPa (Oren and Pataki 2001). Under conditions of sufficient soil water availability, light and VPD control the canopy conductance and hence transpiration (Granier and Bréda 1996). Mean daily maximum VPD at our study site was between 0.3 and 0.6 kPa during most of the days. This VPD range was lower compared to a range of 0.5−2.2 kPa reported for the above studies and may account for the lower E_C measured at this study site.

In mixed forest stands, different species have different crown structures and characteristics that modify the crown environment. Different species and forest trees, therefore, have varying access to light above and within the canopy. The VPD below the canopy is modified since wind speed is reduced and air circulation lower compared to that above the canopy. Moreover, VPD below the canopy could be lower because of the transpiration of the understory and the lower canopy. Canopy trees, therefore, gain more access to direct solar radiation compared to suppressed ones, which grow below the canopy and have access only to diffuse light and light flecks (Köstner et al. 1992). Differences in crown exposure may, therefore, account for the differences in transpiration rates among the studied tree species. For example, *Q. mongolica*, *T. amurensis*, and *U. davidiana* were canopy trees, constituting more than 80% of the total canopy cover in the study plot and accounted for approximately 75% of the total stand transpiration.

2.4.2 Tree water use and functional convergence

Despite their phylogenetic diversities, the five deciduous species studied showed a convergence in their water use and water use functions (Figure 2.6b). These results support our hypothesis that trees of different species growing together in a common location tend to have converging water use strategies. This assumption was based on the fact that tree transpiration is regulated by the microclimate prevailing above the forest canopy and soil moisture condition (Hinckley et al. 1978). As long as soil water is not limiting, as was the case at our study site, tree transpiration will basically be influenced by the microclimate and the ability to transport water through the xylem (Oren and Pataki 2001). We established a strong relationship between the conducting surface area and TWU. It is, therefore, not surprising that water use by the different species is similar. Thus, water use by the different tree species in a mixed stand could be explained by the existing A_S as long as the trees are exposed to similar environments

Estimation of SA in forest trees is complex and destructive. Previous attempts have been made to identify easily measurable parameters that accurately describe sapwood area, and which can ultimately be employed as surrogates for A_S. For example, Vertessy et al. (1995) compared stem DBH, A_S and leaf area as a scaling factor in tree water use from individual tree level to stand level and all three methods gave similar results. Although leaf area may potentially be estimated from remotely sensed data (Wessman et al. 1988), which require less manpower in the filed, DBH is the more easily available and measurable scaling factor. Therefore, the revelation that DBH describes SA of this mixed forest could be a significant step towards quantifying forest water use in the species rich temperate forests, which occur in this complex mountainous terrain of S. Korea. In our study, a power function of the form $Y = \alpha \times X^{\beta}$ appeared to be an adequate model for estimating A_S and TWU from DBH. Thus, in mixed native temperate stands, water use traits of diverse species could be generalized with tree size characteristics. This relationship between water use traits and tree size was not influenced by the species under consideration. In our study, DBH accounted for 87% but SA accounted for 84% of the variation in total daily TWU among five different tree species. Köstner et al. (1992) suggested that TWU could be more closely related to tree circumference or diameter than A_S. We also found that the relationship between mean TWU (kg d^{-1}) and DBH was somewhat stronger than A_S. Both regressions were however, significant with P <0.0001. Our results resemble those of Zeppel and Eamus (2008), who observed that the relationship between daily total water use and DBH did not differ between broad-leaved and needle-leaved species, at any time in a native temperate stand in Australia.

The relationship between DBH and F_d was weak (R^2 = 0.21). We however established an increasing trend of F_d with increasing DBH (P = 0.036). Our results compared well with other previous studies conducted by Granier et al. (1996) and Oren et al. (1998). On the other hand, Meinzer et al. (2001) observed a negative correlation between maximum F_d and DBH from 23 species (R^2 = 0.85). Phillips et al. (1999) observed no relationship at all between DBH and F_d.

The relationship between A_S and DBH in temperate forests may be different from other forest ecosystems. For example, the degree of increasing A_S with DBH in tropical forest (Meinzer et al. 2001) is steeper than the result we found in this temperate forest. This is mainly because plants are differently adapted to different habitats and vary in their plant traits (Grime and Hunt 1975). The allometric model with tree transpiration rate reported here is not consistent with the predicted universal model suggested by Enquist et al. (1998), which considered 37 different species and growth forms, including herbaceous plants, shrubs, tree seedlings, and mature evergreen and deciduous trees. Even though the increasing pattern with DBH was same, the model we proposed here showed much less transpiration rates against DBH. We attribute these differences to the existing climate conditions, which regulate daily maximum transpiration rates. This result could be caused by different compositions of the samples and different DBH range of studied plants. Besides, their universal model covered a larger DBH range, from 0.2 to 100 cm, while in our study we considered DBH range from 13 to 38 cm only. If we consider habitat effects, calibrations should be done for each measurement site and the environmental conditions of the calibration should represent the measurement period (Sevanto et al. 2008).

Although we found that for these five deciduous species, variation in water use was governed largely by tree size, during the course of the day, however, this capacity may be regulated by stomatal response to light and VPD. During the morning hours, transpiration increased with increasing light intensities but saturated or decreased when PAR levels rose above 1,200 μmol m^{-2} s^{-1}. PAR above 1,200 μmol m^{-2} s^{-1} in most cases coincided with VPD greater than 0.2 kPa at which stomatal closure was observed. Stomatal conductance in *Nothofagus* trees located near the top of the canopy decreased by 50% as VPD increased from 0.5 to 1.2 kPa (Köstner et al. 1992). We observed stomatal closure from a VPD of 0.2 kPa but it was only from a VPD of 0.6 kPa that a significant reduction in transpiration was observed (not shown). Our study site was located at an elevation of 960 m a.s.l and is influenced by cool climatic conditions and high precipitation such that VPD remains below 0.2 kPa most of the time. It is likely that long-term adaptations make trees more sensitive to VPD changes, and trees growing in cool and moist environments experience stomatal closure at lower VPD compared to their counterparts in warmer and drier locations. For example, Luis et al. (2005) showed stomata closing in the range of VPD from 0.1 to 1.5 kPa at 1,650 m a.s.l. during the wet season. Kumagai et al (2008) working under similar low VPD conditions reported stomatal closure starting at 0.25 kPa. These are very interesting findings that require further investigations and an extension to more species in order to derive general principles that explain water use by highly mixed forest stands.

2.5 Conclusion

Tree water use in the five deciduous species was effectively explained by tree size (DBH) irrespective of species. Thus, whole tree water use could be effectively estimated using a simple general model that relates TWU with DBH, for these five different deciduous species. Although there is need to extend these investigations onto other forest species, results from these five species showed that DBH is a good scaling factor for estimating forest water use in the rugged terrain of S. Korea. The advantage of DBH is that it is easily obtainable and is also non-destructive compared to, for example, LAI and A_S, respectively. Our findings are a significant contribution to the ongoing efforts to build hydrology budgets of S. Korea.

2.6 Acknowledgements

This research was supported by the Complex Terrain and Ecological Heterogeneity (TERRECO) project and the "Sustainable Water Resources Research Center of 21st Century Frontier Research Program" (Grant code: 1-8-3), "Eco-technopia 21" projected from the Ministry of Environment, "BK21 program" from the Ministry of Education and Human Resource Management of Korea. We would like to acknowledge the input from Ms. Margarete Wartinger of Plant Ecology Department, University of Bayreuth and students of Seoul National University, Kangwon National University and University of Bayreuth for their support during filed work.

2.7 References

Alsheimer M, Köstner B, Falge E, Tenhunen JD (1998) Temporal and spatial variation in transpiration of Norway spruce stands within a forested catchment of the Fichtelgebirge, Germany. Ann Sci For 55:103−123

Bovard BD, Curtis PS, Vogel CS, Su H-B, Schmid HP (2005) Environmental controls on sap flow in a northern hardwood forest. Tree Physiol 25:31−38

Bucci SJ, Goldstein G, Meinzer FC, Scholz FG, Franco AC, Bustamante M (2004) Functional convergence in hydraulic architecture and water relations of tropical savanna trees: from leaf to whole plant. Tree Physiol 24:891−899

Dierick D, Hölscher D (2009) Species-specific tree water use characteristics in rainforestation stands in the Philippines. Agric For Meteorol 149:1317−1326

Enquist BJ, Brown JH, West GB (1998) Allometric scaling of plant energetics and population density. Nature 395:163−165

Granier A (1987) Evaluation of transpiration in a Douglas-fir stand by means of sap flow measurements. Tree Physiol 3:309−320

Granier A, Bréda N (1996) Modeling canopy conductance and stand transpiration of an oak forest from sap flow measurements. Ann Sci For 53:537−546

Granier A, Huc R, Barigah ST (1996) Transpiration of natural rain forest and its dependence on climate factors. Agric For Meteorol 78:19−29

Grime JP, Hunt R (1975) Relative growth-rate: Its range and adaptive significance in a local flora. J Ecol 63:393−422

Han SS, Kim SH (1996) Ecophysiological interpretations on the water relations' parameters of trees (IX)– Measurement of the transpiration rate by the heat pulse method in a *Quercus mongolica* stand. J Korean For Soc 85(2):288−299

Herbst M, Rosier PTW, Morecroft MD, Gowing DJ (2008) Comparative measurements of transpiration and canopy conductance in two mixed deciduous woodlands differing in structure and species composition. Tree Physiol 28:959−970

Hinckley TM, Lassoie JP, Running SW (1978) Temporal and spatial variations in water status of forest trees. For Sci 24(3):1−72

Hubbard RM, Ryan MG, Giardina CP, Barnard H (2004) The effect of fertilization on sap flux and canopy conductance in a *Eucalyptus saligna* experimental forest. Glob Change Biol 10:427−436

Kim C (2003) Mass loss rates and nutrient dynamics of oak and mixed-hardwood leaf litters in a Gyebang (Mt.) forest ecosystem. Korean J Ecol 26:335−340

Köstner BMM, Schulze ED, Kelliher FM, Hollinger DY, Byers JN, Hunt JE, McSevenz TM, Meserth R, Weir PL (1992) Transpiration and canopy conductance in a pristine broad-leaved forest of *Nothofagus*: an analysis of xylem sap flow and eddy correlation measurements. Oecologia 91:350−359

Köstner BMM, Tenhunen JD, Alsheimer M, Wedler M, Scharfenberg H-J, Zimmermann R, Falge E, Joss U (2001) Controls on evapotranspiration in a spruce forest catchment in the Fichtelgebirge. In: Temhunen JD, Lenz R, Hantschel R (eds) Ecosystem approaches to landscape management in Central Europe. Springer-Verlag, Berlin, Germany, pp378−415

Kumagai T, Tateishi M, Shimizu T, Otsuki K (2008) Transpiration and canopy conductance at two slope positions in a Japanese cedar watershed. Agric For Meteorol 148:1444–1455

Lee IK, Lim JH, Kim C, Kim YK (2006) Nutrient dynamics in decomposing leaf litter and litter production at the long-term ecological research site in Mt. Gyebangsan. J Ecol Field Biol 29:585–591

Lohammer T, Larsson S, Linder S, Falk SO (1980) FAST–simulation models of gaseous exchange in Scots pine. Ecol Bull 32:505–523

Luis VC, Jiménez MS, Morales D, Kucera J, Wieser G (2005) Canopy transpiration of a Canary islands pine forest. Agric For Meteorol 135:117–123

Meinzer FC (2003) Fuctional convergence in plant responses to the environment. Oecologia 134:1–11

Meinzer FC, Goldstein G, Andrade JL (2001) Regulation of water flux through tropical forest canopy trees: Do universal rules apply? Tree Physiol 21:19–26

Meinzer FC, Bond BJ, Warren JM, Woodruff DR (2005) Does water transport scale universally with tree size? Funct Ecol 19:558–565

O'Brien JJ, Oberbauer SF, Clark DB (2004) Whole tree xylem sap flow responses to multiple environmental variables in a wet tropical forest. Plant Cell Environ 27:551–567

O'Grady AP, Cook PG, Eamus D, Duguid A, Wischusen JDH, Fass T, Worldege D (2009) Convergence of tree water use within an arid-zone woodland. Oecologia 160:643–655

Oren R, Phillips N, Katul G, Ewers B, Pataki DE (1998) Scaling xylem sap flux and soil water flux in forests. Ann Sci For 55:191–216

Oren R, Pataki DE (2001) Transpiration in response to variation in microclimate and soil moisture in southeastern deciduous forests. Oecologia 127:549–559

Phillips N, Oren R (1998) A comparison of daily representations of canopy conductance based on two conditional time-averaging methods and the dependence of daily conductance on environmental factors. Ann Sci Forest 55:217–235

Phillips N, Oren R, Zimmermann R, Wright SJ (1999) Temporal patterns of water flux in trees and lianas in a Panamanian moist forest. Trees 14:116–123

R Development Core Team (2009) R: a language and environment for statistical computing. R Foundation for Statistical Computing, Vienna, Austria, ISBN 3-900051-07-0. Accessed 17 Nov 2009

Schmidt MWT (2007) Canopy transpiration of beech forests in Northern Bavaria−Structure and function in pure and mixed stands with oak at colline and montane sites. Dotoral dissertation, University of Bayreuth, Germany, 239 pp. URL: http://opus.ub.uni-bayreuth.de/volltexte/2008/428

Sevanto S, Nikinmaa E, Riikonen A, Daley M, Pettijohn C, Mikkelsen TN, Phillips N, Holbrook NM (2008) Linking xylem diameter variations with sap flow measurements. Plant Soil 305:77−90

Vertessy RA, Benyon RG, O'sullivan SK, Gribben PR (1995) Relationships between stem diameter, sapwood area, leaf area and transpiration in a young mountain ash forest. Tree Physiol 15:559−567

Walter H, Lieth H (1967) Klimadiagramm-Weltatlas. VEB Gustav Fischer Verlag, Jena

Wessman CA, Aber JD, Peterson DL, Melillo JM (1988) Remote sensing of canopy chemistry and nitrogen cycling in temperate forest ecosystems. Nature 335:154−156

Wilson KB, Hanson PJ, Mulholland PJ, Baldocchi DD, Wullschleger SD (2001) A comparison of methods for determining forest evaporation and its components: sap-flow, soil water budget, eddy covariance and catchment water balance. Agric For Meteorol 106:153−168

Wullschleger SD, Hanson PJ, Todd DE (2001) Transpiration from a multi-species deciduous forest as estimated by xylem sap flow techniques. For Ecol Manage 143:205−213

Zeppel M, Eamus D (2008) Coordination of leaf area, sapwood area and canopy conductance leads to species convergence of tree water use in a remnant evergreen woodland. Aust J Bot 56:97−108

Chapter 3

Water use by a warm-temperate deciduous forest under the influence of the Asian monsoon: Contributions of the overstory and understory to forest water use

Journal of Plant Research (2013) DOI 10.1007/s10265-013-0563-5

Eun-Young Jung[a*], Dennis Otieno[a], Hyojung Kwon[a,c], Bora Lee[a], Jong-Hwan Lim[b], Joon Kim[c], John Tenhunen[a]

[a]Department of Plant Ecology, University of Bayreuth, D-95440 Bayreuth, Germany

[b]Department of Forest Conservation, Korea Forest Research Institute, 130-712 Seoul, Republic of Korea

[c]Department of Landscape Architecture and Rural Systems Engineering, Seoul National University, 151-742 Seoul, Republic of Korea

Abstract

Understanding the dynamics of transpiration of the overstory (E_O) and understory (E_U) in forest stands under the influence of the Asian monsoon is needed to improve estimation of forest water budget and identify key factors controlling forest water use under climate change. In this study, E_O and E_U of a temperate deciduous forest stand located in South Korea were measured during the growing season of 2008 using sap flow methods. The objectives of this study were to (1) quantify the total transpiration of the forest stand, (2) determine their relative contribution to ecosystem evapotranspiration, and (3) identify factors controlling the transpiration of each layer. E_O and E_U were 174 and 22 mm, respectively. Total transpiration accounted for 55% of the total E_{eco}, revealing the importance of unaccounted contributions to E_{eco} (i.e., soil evaporation and wet canopy evaporation). During the monsoon period, there was a strong reduction in the total transpiration, likely because of reductions in photosynthetic active radiation (PAR), vapor pressure deficit (VPD) and plant area index (PAI). The ratio of E_U to E_O declined during the same period, indicating an effect of monsoon on the partitioning of E_{eco} in its two components. The seasonal pattern of E_O was synchronized with the overstory canopy development, while E_U varied in function of the understory canopy development as long as the overstory canopy remained open. Following the overstory canopy closure, environmental conditions of the understory controlled the variations in E_U.

Key-words: Asian monsoon, Canopy conductance, Transpiration of overstory, Understory, Warm-temperate deciduous forest

3.1 Introduction

Temperate deciduous forests in China and Korea composed of *Quercus*, *Carpinus*, *Ulmus*, and *Tilia* species have developed together with the establishment of warm-temperate summer conditions, a strong decrease in winter temperatures and an increase in monsoon-induced precipitations. These forests have been compared with other major deciduous forest types of the region and are described as warm-temperate deciduous forests (Nakashizuka and Iida 1995). In general, two to three times higher plant species diversity is found in the temperate forests of the Asian monsoon region than in North America (Latham and Ricklefs 1993; Qian and Ricklefs 1999). This difference in plant diversity appears to result from a greater physiographic heterogeneity in Asia, which allowed for an allopatric speciation in response to the sea level fluctuations after temperate forest zones became disjunct in the late Tertiary (Qian and Ricklefs 2000). Warm and humid summer conditions due to the monsoon also contribute to the great diversity of plant species in the eastern Asian forests (Röhrig and Ulrich 1991). Thus, the warm-temperate deciduous forests of Korea and other parts of Asia represent an important ecosystem type with multi-layered physiognomy (Kim 2002), where both the overstory and understory are well developed and display diverse species compositions. As a result, large differences are expected in the partitioning of water use between the overstory and understory, which may influence forest ecosystem functions. In particular, these differences can influence forest energy flows, nutrient cycling and niche partitioning within species (Jackson et al. 1995).

The species composition of understory vegetation is in part determined by canopy tree species and structure which modify microclimate, light availability, soil water content, and soil nutrients inputs below the canopy (Canham et al. 1994; Augusto et al. 2003; Barbier et al. 2008). Simultaneously, understory vegetation competes with overstory trees for resources and may influence tree growth (Riegel et al. 1992). In temperate deciduous forests, light availability at the understory is high in early spring before canopy closure, but decreases in early summer with the leaf emergence of overstory trees. Low radiation and wind speed below the canopy create an environment of relatively low vapor pressure gradient, resulting in low transpiration rates of the understory (Landsberg and Gower 1997). However, even in relatively closed canopies, there is enough light reaching the understory to allow the physiological functioning of the vegetation (Lieffers et al. 1999). Following precipitation events, as the forest canopy dries, the rate of transpiration of the understory is expected to increase with the increasing vapor pressure gradient (Black and Kelliher 1989). However, it will still remain below the canopy transpiration. Thus, although the understory may be composed of plant species different from those of the canopy, the transpiration of the former may still be tightly coupled to canopy processes given that the canopy can strongly influence the understory

microclimate. Trends and partitioning of transpiration at both levels, therefore, usually display strong seasonality according to the dynamics of canopy cover and leaf area index (Wullschleger et al. 2001).

Evapotranspiration (E_{eco}) in such forest stands consists of four main components, namely, overstory transpiration (E_O), understory transpiration (E_U), soil evaporation (E_g), and evaporation from wet canopy surface (E_w) (Barbour et al. 2005). Quantifying the relative contribution of each component to E_{eco} is essential in order to determine their importance and to identify key factors controlling forest water use. In turn, this allows for accurate assessment of water use by forest ecosystems, provides empirical data for the parameterization and calibration or validation of forest hydrological models, which requires all these components, as well as information for the sustainable management of forests (Hatton et al. 2003; Zeppel et al. 2006). To the best of our knowledge, there have been no attempts to partition E_{eco} into E_O and E_U in any warm-temperate forest stands under the influence of the Asian monsoon climate, although E_{eco} has been widely measured in several studies including those of the Asia Flux groups (Kosugi et al. 2007; Shi et al. 2008; Tanaka et al. 2008; Kang et al. 2012). The Asian monsoon, which is characterized by strong southwest surface winds and heavy rains (Lau and Li 1984), leads to forest canopy disturbance that affects canopy structure and function, including canopy plant area index (PAI). The monsoon is also generally characterized by hot and humid conditions, a reduction in vapor pressure deficit (VPD) and low photosynthetic active radiation (PAR). All these changes are likely to influence forest water use differently than that of the dry-summer deciduous temperate forests located in Europe and North America. According to the climate simulations for South Korea (Im et al. 2008), the frequency, intensity and duration of the Asian monsoon are likely to increase in the next 30 years. This will alter the structure and function of the warm-temperate deciduous forests of Asia and how they are managed. There is, therefore, an urgent need to fill the gaps in the knowledge on the influence of the Asian monsoon on forest water use and its dynamics.

In this study, we conducted transpiration measurements using sap flow methods at both the overstory and understory of a warm-temperate deciduous forest stand located in Pocheon-si, Gyeonggi-do, South Korea. Our objectives were to (1) quantify E_O and E_U over the growing season, (2) determine their relative contribution to E_{eco}, and (3) identify controlling factors on the total amount and rates of E_O and E_U. The specific questions addressed were: (1) How does overstory development influences understory microclimate? (2) How is the partitioning of E_{eco} into E_O and E_U influenced by overstory and understory development? and (3) How does the monsoon affect on the total amount and rates of E_O and E_U? We hypothesized that the contribution of both E_O and E_U to E_{eco} is strongly dependant on microclimatic factors, mainly PAR and VPD that control canopy transpiration and the status of the overstory and understory canopy development.

3.2 Materials and methods

3.2.1 Study sites

The study was conducted in a warm-temperate deciduous forest stand of the Gwangneung National Arboretum located in the central part of the Korean peninsula (37°45'25.37''N, 127°9'11.62''E) at an elevation of 340 m above sea level. The site is registered as a KoFlux Supersite (Kim et al. 2006) and long-term ecological monitoring station (Oh et al. 2000). Mean annual precipitation over the past 25 years was 1,436 mm and was mainly concentrated in the months of late June and late July due to the influence of the monsoon rainband. The Korean monsoon is characterized by persistent and intense rainfall and is known as *Changma*. In 2008, when the measurements were made, *Changma* started on June 17 and ended on July 26 (Figure 3.2; Korea Meteorological Administration 2011). For the last 30 years, mean annual temperature was 11.5°C and temperature ranged of −11.5 and 30.0°C (Kim et al. 2006). Soil depth ranges from 0.4 to 0.8 m and the soil texture is predominantly sandy loam. The bedrock primarily consists of granite gneiss and schist (MOST 1999). The site is located on a slope of 15°, facing southwest. The forest stand is at climax and is dominated by 80- to 200-year-old *Quercus serrata* Thunb. ex Murray and *Carpinus laxiflora* (Siebold & Zucc.) Blume var. *laxiflora* of an average height of 18 m (Cho et al. 2007). The understory is composed of a high diversity of species of saplings and shrubs and has an average height of 2 m (Lim et al. 2003).

3.2.2 Micrometeorological measurements

Air temperature (T_a), water vapor density, photosynthetically active radiation (PAR), net radiation (R_N), wind speed (U) and rainfall were measured at 40-m height tower. Below the canopy, T_a, water vapor density, R_N, and U were measured at a height of 4 m. T_a and U at both height were measured with a three-dimensional sonic anemometer (model: CSAT3, Campbell Scientific Inc., Logan, Utah, USA). PAR was measured by photodiode sensors (model: BPW21, Osram Semiconductor GmbH, Regensburg, Germany) at a height of 2 m at six random locations in the plot of sap flow measurements. Light transmittance was calculated as the ratio of PAR at the 40-m height (PAR_{40}) and PAR at the 2-m height (PAR_2). Vapor pressure deficit at the 40-m height (VPD_{40}) and at the 4-m height (VPD_4) were derived from air temperature and water vapor density measured at the respective heights (Murray 1967). Soil water content integrated over 0 to 30 cm depth was measured using soil moisture probes (model: CS616, Campbell Scientific Inc.). The data from the eddy covariance system were sampled at 10 Hz and the meteorological data were monitored every 30 seconds, and half-hourly means of both data were calculated. The data was stored on three types of data loggers (model: CR-5000 and CR-3000, Campbell Scientific Inc. and DL2e, Delta-T Devices, Cambridge, UK). The measurements of meteorological variables at the overstory and understory

were used to analyze the impacts of environmental conditions on E_O and E_U and to calculate canopy conductance (G_C) of both layers.

3.2.3 Biometric measurements

PAI, which includes understory and overstory trees, was measured every three weeks throughout the year using a plant canopy analyzer (model: LI-2000, LI-COR Inc., Lincoln, Nebraska, USA) under diffuse light conditions at 12 sampling points with 50 m x 50 m grid interval over the plot of sap flow measurements (Kwon et al. 2010). In order to measure maximum understory leaf area index (LAI_U), leaf samples of all the saplings in three plots measuring 2 m × 2 m were collected in early July, and the area of the leaf samples was measured with a leaf area meter (model: LI-3100, LI-COR Inc.). LAI_U reached its peak in May and did not decrease until early September. Therefore, we assumed that the leaf area measurement conducted in July reflected the maximum value of LAI_U.

In order to measure bark and sapwood depth of the sample trees of *Q. serrata* and *C. laxiflora*, an increment corer was used to extract cores from the stems at sap flow sensor installation height. Bark and sapwood were visually distinguishable for both species. Sapwood area (A_S) was calculated from the measurements of diameter at breast height (DBH) and depths of bark and sapwood. A non-linear regression was established between A_S and DBH for both species (Figure 3.1a). The regression was used to estimate total A_S of all trees of the study plot (A_{st}) (Vertessy et al. 1995; Meinzer et al. 2005).

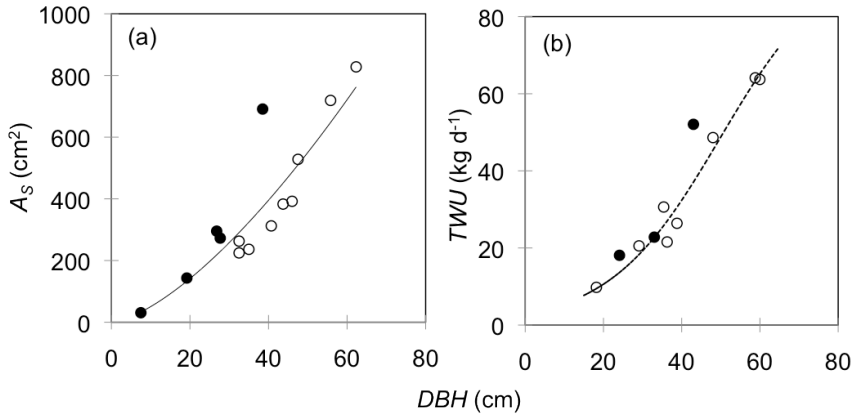

Figure 3.1 Climate diagram Relationships (a) between stem diameter at breast height (DBH) and sapwood area (A_S) in power function ($A_S = 1.664DBH^{1.483}$, n = 14, $R^2 = 0.90$, $P < 0.001$) and (b) between DBH and tree water use (TWU) in three-parameter sigmoidal function ($TWU = 97.07/(1 + e^{-[(DBH-49.85)/14.22]})$, n= 11, $R^2 = 0.97$, $P < 0.001$) for canopy tree species of *Quercus serrata* (Q.s.) and *Carpinus laxiflora* (C.l.) from the years 2007 and 2008.

In a 30 m x 30 m plot, the DBH of all stems larger than 5 cm in diameter (70 stems in total) was measured. Basal area was then calculated from the measured DBH. The total basal area of the plot was 38.5 m^2 ha^{-1}. The dominant tree species were *Q. serrata* and *C. laxiflora*, constituting for 71% and 22% of the total basal area, respectively. The average DBH of *Q. serrata* and *C. laxiflora* were 45.4 ± 13 and 33.8 ± 10 cm (hereafter standard deviation (SD) is indicated as ±), respectively. The understory was composed of saplings and shrubs of different species, such as *Euonymus oxyphyllus*, *Celtis jessoensis, Styrax obassia*, *Cornus kousa* and *Sorbus alnifolia*. The basal area of the understory saplings was about 7% of the total basal area.

3.2.4 Measurement of overstory and understory transpiration

Overstory (E_O) and understory (E_U) transpiration were measured from April 1 to September 27 in 2008, and total transpiration (E_O + E_U) during this period was considered as total annual transpiration since leaf senescence started at the end of September and no evergreen species existed in the study area.

E_O was estimated from sap flux density (F_d, g m^{-2} s^{-1}) measured using thermal dissipation probes (TDP), which were constructed at the technical laboratory of the Department of Plant Ecology, University of Bayreuth, based on the original design by Granier (1987). The TDP consisted of two probes (2 mm in diameter and 20 mm in length) aligned vertically 10 cm apart into the sapwood. Each probe contained a copper-constant thermocouple and was connected in parallel (Granier 1987). The temperature of the upper probe, constantly heated by a 0.2 W power supply, was influenced by the rate of convective heat transport away from the heat source, with the vertically flowing sap in the xylem. The lower probe, which was an unheated reference, reflected the ambient sap temperature. The probes were inserted in two depths between 0 and 20 mm of the outer ring and between 20 and 40 mm of the inner ring, at a height of 1.3 m above ground, on the north-facing side to minimize the effects of direct shortwave radiation (Wilson et al. 2001; Wullschleger et al. 2001). After installation, each probe was covered with Styrofoam sheaths and aluminum foil to avoid direct thermal load from radiation. Temperature differences (ΔT) between the upper and lower reference probes were measured every 30 seconds and half-hourly means were calculated. Data were recorded on data loggers (model DL2e, Delta-T Devices).

F_d was calculated as a function of ΔT according to standard calibration of the TDPs (e.g., Granier, 1987),

$$F_d = 119 \cdot [(\Delta T_{\max} - \Delta T) \cdot \Delta T^{-1}]^{1.231} \quad (1)$$

where ΔT_{max} is the maximum temperature difference between the two probes during a day when sap flow was null. F_d at different sapwood depths of the same individual was used to calculate the sapwood area weighted sap flow density (F_{dt}) with the following equation:

$$F_{dt} = (F_{do} \cdot A_{so} + F_{di} \cdot A_{si}) \cdot (A_{so} + A_{si})^{-1} \quad (2)$$

where F_{do} is the sap flux density of the outer ring, A_{so} is the area of the outer ring, F_{di} is the sap flux density of the inner ring and A_{si} is the area of the inner ring. We used a weighted average F_{dt} to estimate total forest transpiration because F_{di} was lower than F_{do} in *Q. serrata* and *C. laxiflora* by 0.2 and 0.8, respectively. F_d in the sapwood deeper than 40 mm sapwood depth, i.e., outside the heating probe, was estimated by applying an empirical function described by Poyatos et al. (2007) for *Quercus* spp. and Gebauer et al. (2008) for *Carpinus* spp.

E_O (mm h^{-1}) was calculated as:

$$E_O = \overline{F_{dt}} \cdot A_{st} \cdot A_{plot}^{-1} \quad (3)$$

where $\overline{F_{dt}}$ is the mean F_{dt} of the sample trees, A_{st} is the total sapwood area of all trees in the plot, and A_{plot} is the plot area. In order to determine circumferential differences in sap flow, we installed multiple sap flow probes, i.e., three per species, within the outer 20 mm sapwood on the south- and north-facing side of the stem from July to October. The two sets of the probes (on each tree) were placed at relatively similar heights, but carefully positioned apart so that heating from one sensor on the southern azimuth did not interfere with the other on the north-side. However, we observed no circumferential variation in F_d between the south and north sides of the overstory tree stems (P <0.0001), hence we did not perform any further corrections on E_O.

In order to measure E_O, we selected three individuals of *Q. serrata* (dominant species) and three individuals of *C. laxiflora* (sub-dominant species) with DBH between 24 and 59 cm and heights between 12 and 18 m. For the measurement of E_U, three individuals of *E. oxyphyllus*, one individual of *C. jessoensis* and one individual of *S. alnifolia* saplings with stem diameters ranging from 1.7 to 3.0 cm (at 1 m above the ground) and heights ranging from 1.8 to 2.5 m were selected (Table 3.1). The choice of a species was based on the health status and its dominance within the plot.

The number of individuals used for the measurements was severely restricted by the National Arboratum management policy since the Gwangneung forest is one of the only natural forests at climax whithin Korea. These forests have been placed under strict protection. Any destruction of trees of this forest is, therefore, strongly prohibited. However, the scaling of sap flow measurements from plot-scale to stand-scale requires that a sample be representative of the spatial distribution of species and size classes within a stand (Köstner et al. 1998; Oren et al. 1998; Kumagai 2005). Therefore, we used the results of previous measurements for comparison. In the previous year (2007), sap flow measurements were comducted on five individuals of *Q. serrata* trees (dominant species), with DBH distribution within the classes of 10−20, 20−30, 30−40, 40−50 and 50−60 cm which are representative of the DBH classes in this forest stand (*unpublished data*). We examined the relationship between DBH and rates of sap flow after combining data from the years 2007 and 2008. DBH explained 97% of the variations in water use among trees in a sigmoidal function relationship described by Meinzer et al. (2005) (Figure 3.1b), which agrees with the findings of previous studies in

similar forest types (Vertessy et al. 1995; Meinzer 2003; Meinzer et al. 2005; Jung et al. 2011). Thus, despite the limited sample size used in subsequent analyses, we are convinced that the data are well representative of the forest stand and that the type II error is within acceptable limits.

Table 3.1 Characteristics of the sample trees for sap flow measurements. DBH, A_S, and A_L indicate diameter at breast height, sap wood area of the overstory trees, and leaf area of the understory trees, respectively.

Sample trees	Tree species	Tree height [m]	DBH [cm]	A_S/A_L [m^2]
Q1	*Quercus serrata*	15	35.4	0.03
Q2		17	58.8	0.07
Q3		17	38.8	0.03
C1	*Carpinus laxiflora*	18	43.0	0.07
C2		16	33.0	0.04
C3		12	24.1	0.02
SHB1	*Euonymus oxyphyllus*	1.8	1.9	0.83
SHB2		2.0	2.1	0.98
SHB3		1.9	1.7	0.90
SHB4	*Celtis jessoensis*	2.5	2.0	1.08
SHB5	*Sorbus alnifolia*	2.5	3.0	1.39

E_U was estimated from sap flow (F, g h^{-1}), which was measured by the stem heat balance (SHB) technique (Sakuratani 1981). This technique has been successfully applied to accurately estimate sap flow of herbaceous stems (Baker and van Bavel 1987), saplings (Lei et al. 2010), and branches of large trees (Otieno et al. 2007) with diameters ranging from 2 to 125 mm. The SHB sensors used for the measurements were manufactured at the electronic workshop, University of Bayreuth, according to the original design by Sakuratani (1981), improved by Weibel and de Vos (1994) for stems or branches with diameter ranging

between 9 and 13 mm. Each sensor consisted of a heating tape (Heater Designs, Inc., Bloomington, CA, USA) mounted on a flexible cork sheet enclosing the entire stem. Copper-constantan thermocouples were positioned within the cork insulation to monitor temperature gradients. The heater was supplied with a constant voltage of 3.8 V. Heat flows in the vertical direction, the radial direction and by convection through sap flow were estimated from temperature differences between thermocouple junctions placed on the mounting cork. The sensors were installed on well-exposed branches of five tree saplings in the understory so as to avoid possible shading and, hence, estimate the maximum rates of transpiration within the understory. Installed sensors were insulated with thick closed Styrofoam jackets and aluminum foil to prevent direct heating from radiation. The signals from the thermocouple junctions and heating voltage were recorded every 30 seconds and half-hourly means were calculated. Data were recorded on a data logger (DL2e, Delta-T Devices).

E_U (mm h^{-1}) was calculated as:

$$E_U = \overline{F} \cdot A_L^{-1} \cdot LAI_U \qquad (4)$$

where $\overline{F}$ is the mean F of the sample branches, A_L is total leaf area of the sample branches and LAI_U is the understory leaf area index of the study plot. A_L of branches was measured with a LI-3100C area meter (LI-COR Inc.) at the end of the sap flow measurement. E_U was estimated by multiplying mean sap flux densities per unit leaf area by LAI_U of the plot (Ham et al. 1990).

The measurement of branch sap flow with the SHB technique is not influenced by circumferential variations in sap flow since the heater and thermocouples are wrapped around the branch (Grime and Sinclair 1999). Due to the small cross-section of the heated branches, heat storage was assumed to be null (Weibel and de Vos 1994; Smith and Allen 1996; Grime and Sinclair 1999). Once fully developed, the understory formed a relatively flat layer of leaves. Hence, it was assumed that no variation in transpiration rates induced by differences in exposure existed among the different tree branches measured.

3.2.5 Calculation of canopy conductance

Canopy conductance (G_C) of the overstory and understory were calculated using E_O and E_U by rearranging Penman-Monteith equation (Monteith 1965; Herbst et al. 2008) as:

$$G_C = \frac{\lambda \cdot E \cdot \gamma \cdot G_A}{\Delta \cdot R_N + \rho \cdot c_p \cdot VPD \cdot G_A - \lambda \cdot E \cdot (\Delta + \gamma)} \qquad (5)$$

where λ is the latent heat of vaporization of water (J kg^{-1}), E is the transpiration rate (kg m^{-2} s^{-1}), γ is the psychrometric constant (Pa K^{-1}), G_A is the canopy aerodynamic conductance (m s^{-1}), Δ is the rate of change of saturation water vapor pressure with temperature (Pa K^{-1}), ρ is the density of dry air (kg m^{-3}) and c_p is the

specific heat of air at constant pressure (J kg^{-1} K^{-1}). G_A of the overstory and understory were estimated using the boundary layer conductance (g_b) and the turbulent conductance (g_t) according to Thom (1972), Köstner et al. (1992), Magnani et al. (1998) and Tateishi et al. (2010) as:

$$G_A^{-1} = g_b^{-1} + g_t^{-1} \quad (6)$$

$$g_b = b \cdot \sqrt{\frac{U \cdot [1 - \exp(-\alpha/2)]}{d_m \cdot \alpha}} \quad (7)$$

$$g_t = \frac{\kappa^2 \cdot U}{LAI \cdot \{\ln[(z-d)/z_0]\}^2} \quad (8)$$

where b is the proportionality coefficient (3.62 x 10^{-3}; see Campbell and Norman 1998), U is the wind speed above the vegetation layers (m s^{-1}), α is the attenuation coefficient for wind speed inside the canopy (3.0), d_m is the characteristic dimension (m) calculated as the square root of a leaf area, κ is the von Karman constant (0.4), z is the canopy height (m), d is the zero-plane displacement (m), set as two thirds of the vegetation layer height, and z_0 is the roughness length (m), set as one tenth of the vegetation layer height. We used daytime (11:00h to 17:00h) data to calculate daily mean G_C, as was done for daily mean VPD_{40} and VPD_4.

To assess stomatal sensitivity of the overstory and understory G_C to VPD, a modified Lohammar's function was applied.

$$G_C(VPD) = G_{Cref} - m \cdot \ln(VPD) \quad (9)$$

where, G_{Cref} is the canopy conductance at VPD = 1 kPa and $-m$ is the sensitivity of G_C response to VPD (Oren et al. 1999). This analysis was limited to the conditions in which VPD ≥0.6 kPa in order to minimize the uncertainties of G_C estimates (Ewers and Oren 2000).

3.2.6 Eddy covariance flux measurements

Hourly evapotranspiration (E_{eco}, mm h^{-1}) was measured with an eddy covariance system installed at the same study site on a 40-m high tower. The quality of data was controlled following the standardized KoFlux protocol (Hong et al 2009). The protocol includes planar fit rotation, Webb-Pearman-Leuning correction, spike detection, and gap filling. Following the quality control, 85% of the data gathered during the study period was available for analysis. Data gaps were filled using a modified lookup table (MLT) following the gap-filling method proposed by FLUXNET (Reichstein et al. 2005). In the MLT, values of E_{eco} were binned by environmental conditions (i.e., R_N, T_a, and VPD) for 28 days and binned values filled missing values with similar meteorological conditions (Kang et al. 2009a; Kang et al. 2012). According to Kang et al. (2012), gap-filled E_{eco} by the MLT was biased during wet canopy conditions because the MLT used

environmental conditions collected during dry or partially wet canopy conditions, Kang et al. (2012) stated that, as a result, the MLT did not properly consider the controlling mechanisms (e.g., aerodynamic coupling, advection of sensible heat, and heat storage) of E_W. In this study, therefore, we used the gap-filled values that were estimated by a new gap-filling strategy suggested by Kang et al. (2012). Since the new gap-filling method includes E_W, which can significantly contribute to E_{eco} but is uncounted for the existing gap-filling method, we believe that this improved the reliability of the gap-filled E_{eco} particularly during wet canopy conditions.

3.2.7 Statistical analyses

Non-linear regression analyses were conducted to assess the relationships between DBH vs. A_S, monthly rainfalls vs. $((E_O + E_U)/E_{eco})$, environmental parameters (PAR and VPD) vs. transpiration (E_O and E_U), VPD vs. G_C. One-way ANOVA was used to compare sap flow rates among species after conducting a Breusch-Pagan test to confirm the homoscedasticity of the residuals. To investigate seasonal variations of dependencies of E_O and E_U on PAR and VPD, non-linear regression analysis was conducted. To test for significant differences between the groups before and after *Changma*, t-tests were performed. The level of significance was set to $P < 0.05$. All analyses were conducted with the R software (R development Core Team, 2010).

3.3 Results

3.3.1 Environmental parameters

PAI increased from 1.2 before bud break to 3.3 on April 25 following leaf-out, and reached a peak value of 5.2 by the end of June (Figure 3.2a). PAI, however, dropped to 3.5 in September after heavy rainfall associated with the Asian monsoon in July and strong winds associated with a typhoon in August. This value remained almost constant until October, after which there was a strong decline due to leaf senescence. Leaf-out of the understory occurred in early April, two weeks earlier than that of the overstory. LAI_U reached a maximum of 0.9 in mid May, which was about 20% of the maximum PAI.

Annual mean air temperature (T_a) above (at 40-m height) and below (at 4-m height) the canopy was 13.5 ± 11.5 and 10.7 ± 9.9°C, respectively (Figure 3.2b). Before the leaf-out of the overstory, T_a at 4-m height was on average about 1.2°C lower than that at 40-m height. The difference increased to 5.1 ± 0.8°C after canopy development. Daily mean VPD at 40-m height (VPD_{40}) and at 4-m height (VPD_4) were 0.9 ± 0.6 and 0.4 ± 0.3 kPa, respectively (Figure 3.2c). Daily mean VPD_{40} increased from 0.9 to 1.4 kPa, while daily mean VPD_4 declined from 0.78 to 0.38 kPa after canopy development. As the overstory canopy developed, the

difference between VPD_{40} and VPD_4 increased from 0.05 to 1.0 kPa. Maximum VPD_{40} was 3.1 kPa in August, whereas maximum VPD_4 was 2.0 kPa in April.

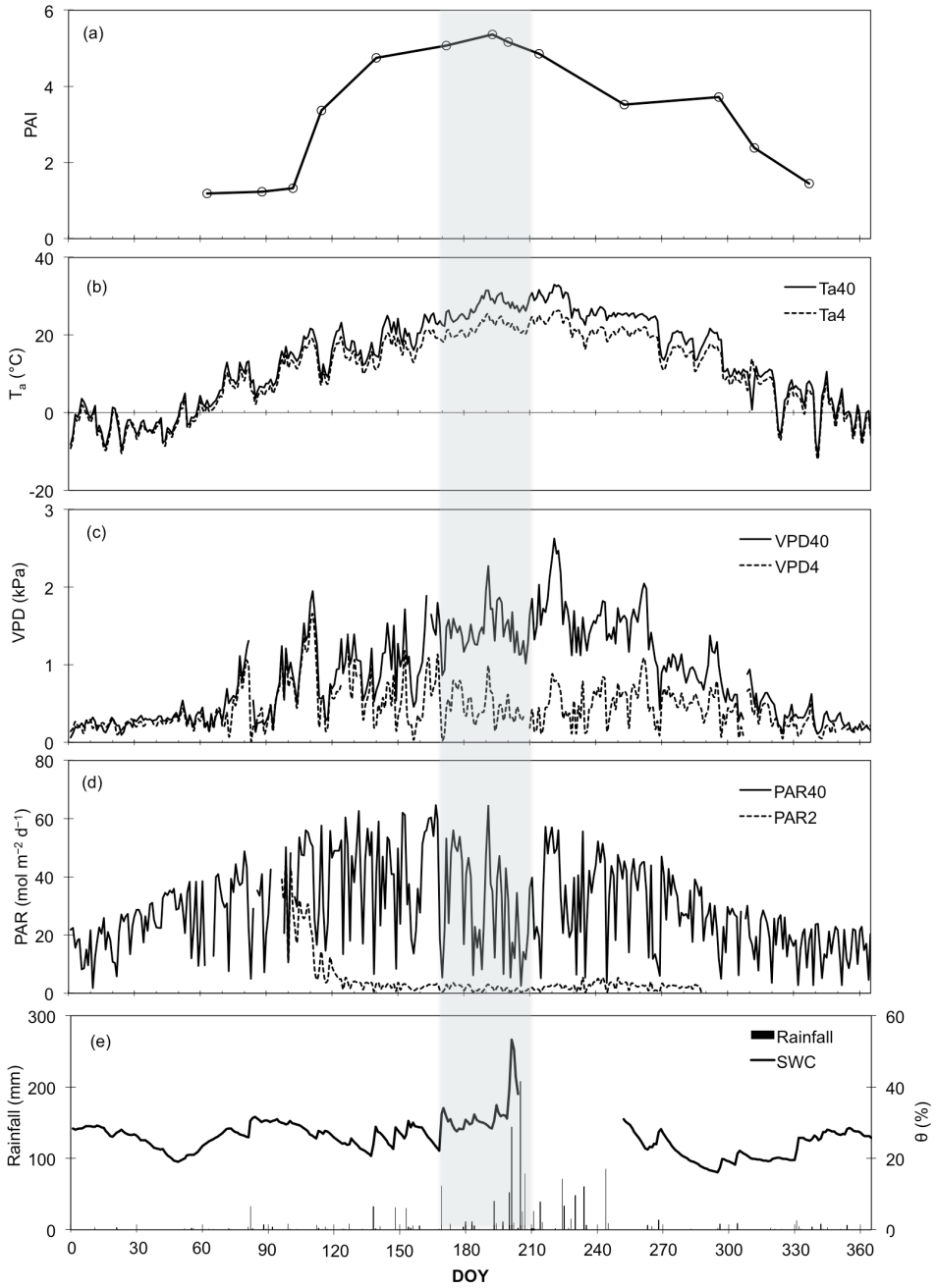

Figure 3.2 Seasonal patterns of (a) plant area index (PAI), (b) daily mean air temperature (T_a), (c) daily mean vapor pressure deficit (VPD), (d) daily sum photosynthetically active radiation (PAR), and (e) daily rainfall and soil water content (θ) in 2008. The shaded area indicates the period of *Changma*. Numbers of 40, 4, and 3 indicate 40-m, 4-m, and 2-m heights, respectively.

Mean daily sum of PAR was 35.3 ± 17.0 mol m^{-2} d^{-1} at 40-m height (PAR_{40}) and 2.3 ± 1.2 mol m^{-2} d^{-1} at 2-m height (PAR_2), and, on average, 6.8% of PAR_{40} reached the understory (Figure 3.2d). Mean light transmittance varied from 8.5% before full understory canopy development to 5.3% following the development. It increased to 7.7% in September during the period when a significant decline in PAI was observed.

Annual precipitation was 1,421 mm of which 44% occurred in July, associated with *Changma* (Figure 3.2e). Mean soil water content (θ) over the year was 25.8 ± 4.7%, with lower values (<20%) in February and October and higher values (>40%) in July, coinciding with heavy rainfalls during *Changma* (Figure 3.2e).

3.3.2 Overstory and understory transpiration

Mean daily maximum F_d of the overstory was 16.3 ± 1.6 g m^{-2} s^{-1} and there were no significant differences among sample trees (one-way ANOVA, P >0.05). Mean daily maximum F per unit of A_L of the understory was 0.05 ± 0.003 g m^{-2} s^{-1} with no significant variation among the sample trees (one-way ANOVA, P >0.05). Mean daily E_O was 1.0 ± 0.5 mm d^{-1}, with a range in daily E_O of 0.1 to 1.9 mm d^{-1}. Mean daily E_U was 0.1 ± 0.1 mm d^{-1}, with a range in daily E_U of 0.01 to 0.3 mm d^{-1} (Figure 3.3a). Maximum E_O coincided with maximum PAI in June. Unlike E_O, E_U reached its peak in late April and the largest variations in magnitude of E_U occurred in June. Both E_O and E_U declined substantially in July, in response to lower mean daily PAR and VPD (down to around 50% of its value June). Following *Changma*, both E_O and E_U increased to around 65% of their value in June. The ratio of E_U to E_O was largest (0.22) at the beginning of the growing season and declined to 0.14 in May and 0.10 in June. These low values persisted until the end of the growing season (Table 3.2).

3.3.3 Ecosystem evapotranspiration

Annual stand transpiration (E_O + E_U) was 195.8 mm, with E_O and E_U accounting for 89% and 11%, respectively. Annual E_{eco} was 355.2 mm, which was 15% of the annual rainfall. Mean daily E_{eco} was 1.97 ± 0.92 mm d^{-1}, with a maximum of 3.85 mm d^{-1} during the period of sap flow measurements (Figure 3.3b). Monthly mean E_{eco} gradually increased until June along with canopy development and favorable environmental conditions, but declined sharply during the monsoon and reached its lowest value in July. The monthly maximum E_{eco} occurred in August. During this period, the rates of both E_O and E_U were relatively lower than the rates recorded before *Changma*. The contribution of monthly mean total transpiration to monthly mean E_{eco} was 89% in April, > 80% in May, > 74% in September, > 68% in June, >

58% in July and > 42% in August (Table 3.2). The proportion of total transpiration to E_{eco} showed a non-linear decrease with increasing rainfall (Figure 3.4).

3.3.4 Regulation of transpiration

Responses of daily E_O and E_U to PAR and VPD were examined using monthly dataset in order to isolate differences that may arise due to leaf phenology (Figure 3.5). Except in April, when leaves were still in the developing stage, the relationships were curvilinear and significant (P <0.0001). Throughout the growing season, PAR_{40} explained 75 to 88% of the variations in E_O. Also, PAR_2 explained 20 to 79% of the variation in E_U. In most instances, E_O saturated at PAR_{40} of between 45 and 50 mol m^{-2} d^{-1}.

Both E_O and E_U were non-linearly correlated with VPD. VPD_{40} explained 62 to 83% of the variation in E_O, while VPD_4 explained more than 78% of the variation in E_U, except in July for both. E_O increased with increasing VPD_{40} until VPD_{40} reached 2.0 kPa, but declined afterwards in response to VPD_{40} >2.0 kPa. As expected, VPD_4 was always lower than VPD_{40} and never exceeded 1.5 kPa during the measurements.

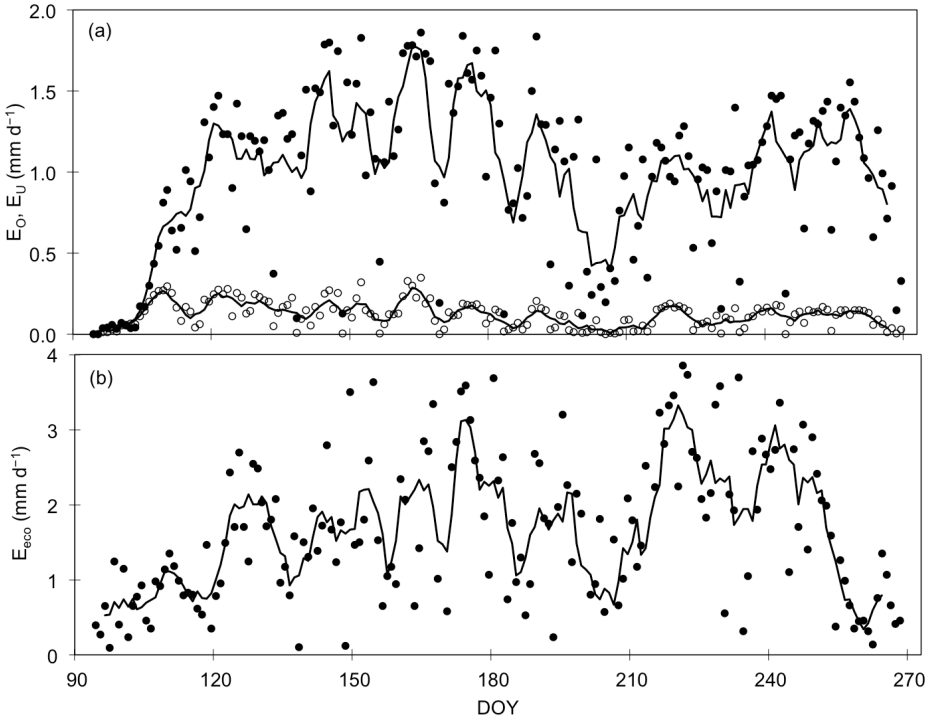

Figure 3.3 Seasonal patterns of (a) daily transpiration from the overstory (E_O, closed circles), the understory (E_U, open circles) and (b) ecosystem evapotranspiration (E_{eco}). Solid lines were five days running mean of daily E_O, E_U, and E_{eco}.

Table 3.2 Monthly mean overstory transpiration (E_O), understory transpiration (E_U), evapotranspiration (E_{eco}) and monthly accumulated rainfall during the growing season of 2008. Numbers in parenthesis indicate standard deviation.

Month	E_O [mm d^{-1}]	E_U [mm d^{-1}]	E_{eco} [mm d^{-1}]	E_U/E_O	$(E_O + E_U)/E_{eco}$	Rainfall [mm mon^{-1}]
Apr	0.64 (± 0.4)	0.14 (± 0.1)	0.87 (± 0.3)	0.22	0.89	24.0
May	1.20 (± 0.4)	0.17 (± 0.1)	1.71 (± 0.7)	0.14	0.80	82.0
June	1.39 (± 0.4)	0.16 (± 0.1)	2.27 (± 1.1)	0.11	0.68	136.5
July	0.80 (± 0.5)	0.07 (± 0.1)	1.50 (± 0.8)	0.09	0.58	630.0
Aug	0.99 (± 0.3)	0.11 (± 0.1)	2.60 (± 1.0)	0.11	0.42	291.5
Sept	0.98 (± 0.4)	0.10 (± 0.1)	1.45 (± 0.9)	0.10	0.74	121.0

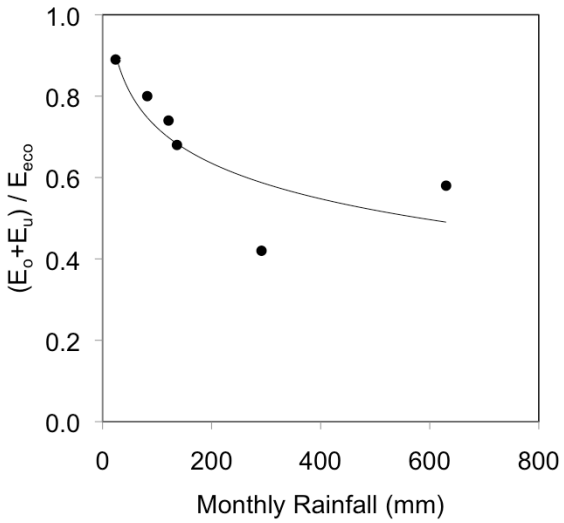

Figure 3.4 Relationship between monthly cumulative rainfall and the ratio of monthly averaged stand transpiration (= E_O + E_U) to monthly averaged ecosystem evapotranspiration (E_{eco}). The relationship was significant ($R^2 = 0.71$, $P < 0.01$, $y = -0.131\ln(x) + 1.3247$).

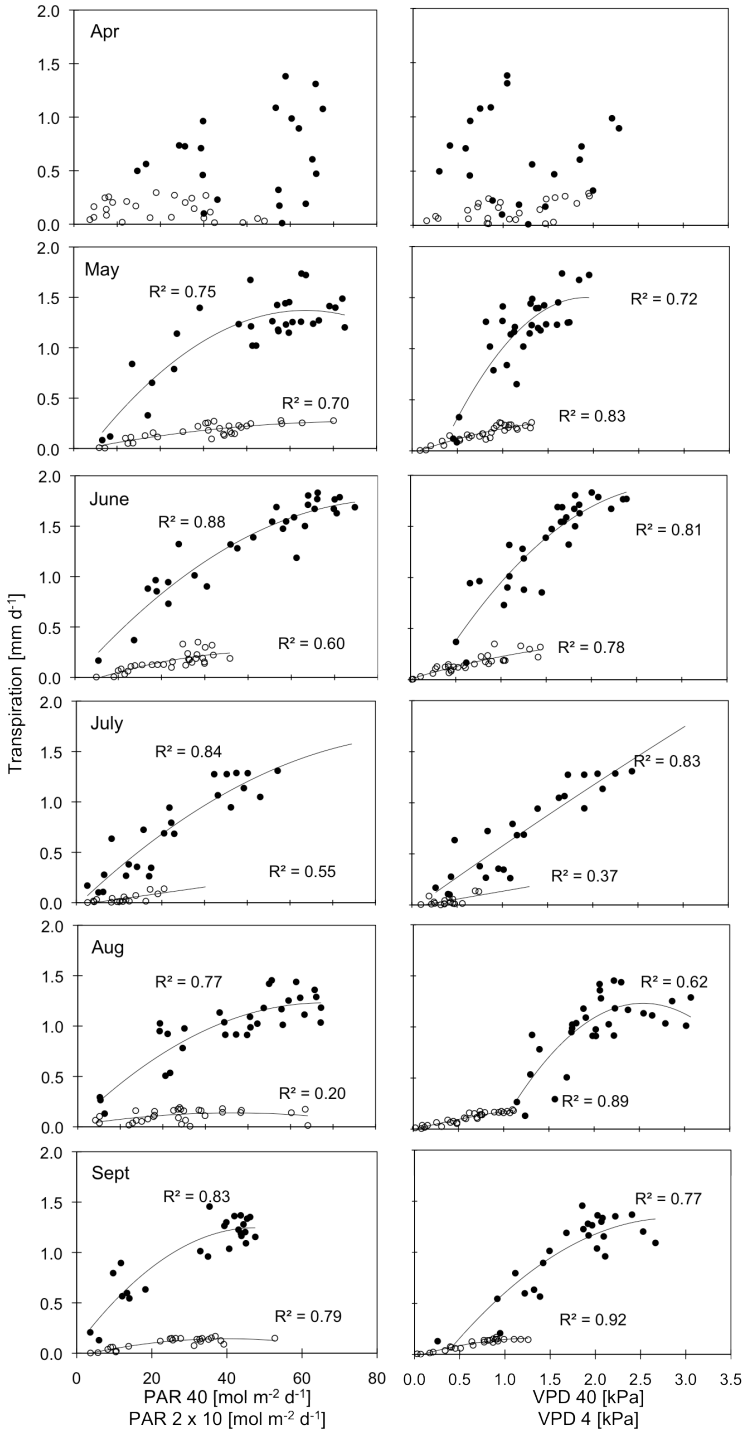

Figure 3.5 Relationships between transpiration and photosynthetic active radiation (PAR) and between transpiration and vapor pressure deficit (VPD). Numbers of 40, 4, and 2 indicate 40-m, 4-m, and 2-m heights, respectively. Note that PAR_2 was multiplied by a factor 10 for the convenience of plotting with PAR_{40} except for April. Closed and open circles indicate overstory and understory, respectively. All the regressions are in polynomial functions.

3.3.5 Canopy conductance

Mean daytime G_C of the overstory was significantly higher before *Changma* than after (t-test, df = 42, t = 5.02, P <0.0001). Thus, mean daytime G_C of the overstory was 8.5 ± 4.5 mm s^{-1} before (May 24 to June 16) *Changma* compared to 4.5 ± 1.4 mm s^{-1} after (August) *Changma* (Table 3). Similarly, mean daytime G_C of the understory decreased from 2.6 ± 1.0 mm s^{-1} to 1.9 ± 1.2 mm s^{-1} after *Changma*. The difference was, however, not statistically significant. Declining trend of G_{Cref} was also found after *Changma*, showing G_{Cref} of the overstory at 12.8 mm s^{-1} before *Changma* compared to 11.9 mm s^{-1} after *Changma* and G_{Cref} of the understory at 2.2 mm s^{-1} and 1.0 mm s^{-1} (Table 3.3).

Daytime G_C of the overstory exponentially and significantly declined with increasing daytime VPD, (R^2 = 0.46, P = 0.0012 before *Changma*; R^2 = 0.66, P <0.0001 after *Changma*), while the relationship between G_C of the understory and VPD_4 was not significant (Figure 3.6). The ratio of $-m/G_{Cref}$, which indicates the variations of $-m$ (the sensitivity of G_C response to VPD; see Eq. 9) to G_{Cref}, for the overstory was 0.66 and 0.68 before and after *Changma*, respectively, and that for the understory was 0.81 and 0.91. The observed $-m/G_{Cref}$ ratio for the overstory was close to the theoretical ratio of 0.6 (Oren et al. 1999), while that for the understory was higher than the theoretical ratio (Table 3.3).

Table 3.3 Mean values of daytime vapor pressure deficit (VPD, kPa), daily sum of photosynthetic active radiation (PAR, mol m^{-2} d^{-1}), canopy conductance (G_C, mm s^{-1}), canopy conductance at VPD = 1 kPa (G_{Cref}, mm s^{-1}) and the ratio of the sensitivity of G_C response to VPD to G_{Cref} ($-m/G_{Cref}$) at the overstory and understory for the period before and after *Changma*. Numbers in paranthesis indicate standard deviation.

	Before *Changma* (May 24−June 16)		After *Changma* (August 1−31)	
	Over	Under	Over	Under
VPD	1.4 (± 0.5)	0.7 (± 0.4)	2.1 (± 0.5)	0.7 (± 0.3)
PAR	42.4 (± 15.4)	2.3 (± 0.8)	39.9 (± 12.7)	2.7 (± 1.2)
G_C	8.5 (± 4.5)	2.6 (± 1.0)	4.5 (± 1.5)	1.9 (± 1.2)
G_{Cref}	12.8	2.2	11.9	1.0
$-m/G_{Cref}$	0.66	0.68	0.81	0.91

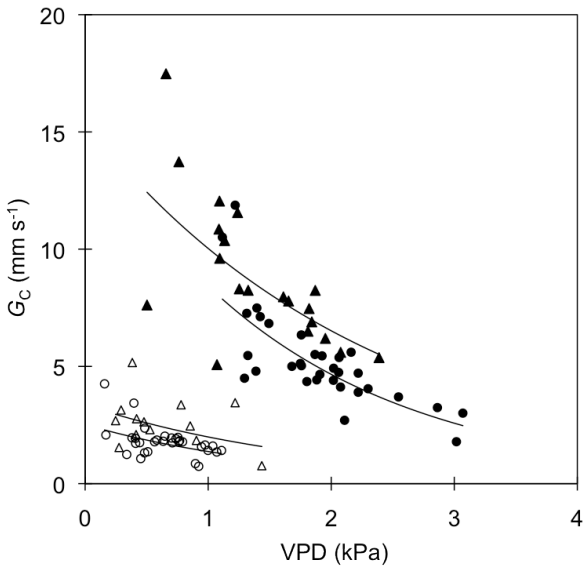

Figure 3.6 Relationships between daytime canopy conductance (G_C) and daytime vapor pressure deficit (VPD) for the overstory (closed) and the understory (opened) before *Changma* (June 1−June 16) (triangles) and after *Changma* (August 1 to August 30) (circles).

3.4 Discussion

3.4.1 Regulation of the overstory and understory transpiration

The seasonal pattern of E_O was synchronized to the seasonal development of leaf area until July, at the onset of the monsoon period. Similarly, patterns of E_U early in the season reflected the pattern of LAI_U development. However, this relationship became distorted with increasing development and closure of the overstory canopy. After full overstory canopy development, E_U was mainly influenced by the prevailing environmental conditions in the understory. The understory canopy had an earlier bud break than the overstory canopy and the former attained its maximum leaf area earlier than the latter. As a result, maximum E_U occurred in late April, coinciding with the highest leaf area, highest PAR and VPD in the understory, at a time when the overstory canopy was not yet fully developed. Maximum E_O occurred in early June, coinciding with the peak overstory leaf area. Differences in timing of the canopy development of the understory and overstory have been reported for a similar forest type in Japan (Nasahara et al. 2008). In this temperate forest stand, the understory, therefore, accounts for most of the total leaf area early in the growing season, since overstory leaf development is delayed. These phenological differences between the two layers result into temporal shifts in functionalities, in terms of forest transpiration. Similar observations have been

made by Unsworth et al. (2004), who reported shifts in the E_O to E_U ratio during the growing season due to the temporal differentiation in phenology and canopy development of the dominant species of the two layers.

Responses of E_O and E_U to the corresponding PAR and VPD were similar throughout the vegetative period, except in April when the leaves in both layers were in their developing stages. The behavior observed in April is likely due to premature leaves and less developed stomata at this stage (Hiyama et al. 2005). Throughout most of the growing season, except in July, E_O saturated on the days when PAR reached 40 to 60 mol m^{-2} d^{-1}, which at most times corresponded to a daily VPD_{max} of 1.8 to 2.0 kPa. E_U, however, never reached saturation likely due to the low light and VPD environment in the understory. Although PAR at the understory was slightly higher in August and September, due to canopy opening (decreased PAI) caused by the monsoon and typhoons, this change in PAR did not influence the magnitude of E_U since this period was characterized by low VPD, low stomatal conductance and aging leaves.

According to Kang et al. (2009b; 2010), decoupling coefficient (Ω), defined as a degree of decoupling between vegetation and the atmosphere, was, on average, equal to 0.39 for the overstory and 0.15 for the understory during the growing season at Gwangneung. This was comparable with Ω of 0.35 for the overstory and 0.23 for the understory in the temperate deciduous oak forest in Tennessee whose total contribution of transpiration to E_{eco} was similar with that of Gwangneung. Low Ω at both layers demonstrated a greater dependence of E_O and E_U on VPD than PAR.

Another notable observation was the significant drop in the magnitudes of E_O and E_U during and after *Changma*. This was attributed to the strong decline in PAR and VPD (Figure 3.2), the decrease in PAI and the advanced leaf age. A decrease in stomatal conductance with increasing leaf age has been reported in other studies (Field and Mooney 1983; Radoglou 1996; Rey and Jarvis 1998). Consistent with this, after *Changma* decreased G_C and G_{Cref} for both the overstoy and understory were observed in our study. Moreover, the ratio of $-m/G_{Cref}$ of both layers was slightly increased after *Changma*, which suggests an increased stomatal sensitivity to VPD due to aging leaves. Greater $-m/G_{Cref}$ of the understory, compared to the overstory and the theoretical ratio of 0.6 (Oren et al. 1999) might be because of smaller VPD range in the understory (0.6–1.5 kPa) (Herbst et al. 2008). Herbst et al. (2008) reported that there is a tendency of increasing the value of $-m/G_{Cref}$ for low ranges of VPD. These changes in G_C and stomatal sensitivity together with the altered environmental factors after *Changma*, may explain the decline in E_O and E_U after *Changma*.

3.4.2 Partitioning of ecosystem water use

The maximum rate of E_O observed in this forest stand was 1.9 mm d^{-1} (Figure 3.4). This value is within the range of maximum E_O rates reported for similar forest types located within the same latitudinal range. For

example, the maximum E_O reported for a temperate deciduous forest stand in Duke, North Carolina, with PAI of 5.4, was 2.0 mm d^{-1} (Oren and Pataki 2001). Wullschleger et al. (2001) reported a value of E_O of 2.2 mm d^{-1} in a temperate deciduous oak forest stand in Tennessee with a PAI of 6.2. On the other hand, the average E_U was 0.1 ± 0.1 mm d^{-1}, which contributed approximately 13% of the total stand transpiration amounting to 196 mm p.a. This proportion of E_U to total stand transpiration is similar to those reported for other temperate forest stands. E_U of a similar temperate oak forest stand accounted for 17% of total stand transpiration (Wullschleger et al. 2001). Baldocchi and Vogel (1996) reported 5 to 25% contribution of the understory to the total stand transpiration of a similar deciduous forest stand in North America. Our total stand transpiration was, however, approximately 30% lower compared to values measured in the temperate deciduous forests of North America (i.e., Wullschleger et al. 2001). Despite similarities in magnitudes of the annual mean R_N and T_a and annual precipitation between the two sites, total stand transpiration is lower, in comparison, at our Asian study site because of differences in distribution patterns of these environmental drivers.

In total, E_O and E_U contributed 47% and 8% of the annual E_{eco}, respectively. Consequently, the remaining 45% of E_{eco} originated from E_g and E_w. Previous studies conducted at the same forest stand estimated 16% contribution from E_g (Kang et al. 2009b) and 13~32% from E_w to annual E_{eco} (Kang et al. 2012). Kang et al. (2009b) reported that E_g was high in March and November when light availability at the forest floor was high, but was negligible during the growing season when light availability at the forest floor and VPD were low. Even though E_w reported by Kang et al. (2012) was highly variable, its relatively high contribution to E_{eco} reveals that E_w is a major component of the partitioning of ecosystem water use, especially during the growing season.

The contribution of stand transpiration ($E_O + E_U$) to E_{eco} varied seasonally. Between April and May, stand transpiration accounted for 80 to 89% of the total water loss from the forest. This value declined to 58% in July and 42% in August (Table 3.2). The decline in July was primarily due to the decrease in E_O in response to the declining PAR and VPD associated with *Changma* and PAI reduction due to heavy rainfall and strong winds. However, the reduced contribution of transpiration to E_{eco} in July and August may be due to the unaccounted amount of E_w, which was found to be highest in these months, corresponding with intensified rainfall (Kang et al. 2012). In September, the proportion increased to 74% as transpiration became the dominant contributor to E_{eco}. The partitioned components of E_{eco} in our study indicate the importance of the unaccounted contributions of E_w to E_{eco} of Gwangneung forest stand during the growing season.

3.5 Conclusions

The understory contributes significantly to the total annual forest water budget. Since bud break in the understory occurs almost one month earlier than the overstory canopy, the understory becomes the dominant source of transpiration water loss early in the season. Its dominance is, however, subdued with the development and closure of the overstory canopy, even though it still accounts for a significant proportion of the total forest PAI most of the year. The seasonal pattern and contribution of E_O to E_{eco}, however, are strongly synchronized to the overstory canopy development. Despite the understory comprising of different plant species, its role in total forest water budget seems to be governed by processes of the overstory.

Considering the daily maximum and mean rates of E_O and E_U and their contributions to E_{eco}, the warm Asian temperate deciduous forest is functionally (in terms of water use) similar to the temperate oak forests in North America. Total stand transpiration in the temperate forests in Asia, however, is lower in comparison, likely due to the depression in transpiration during the monsoon as a result of decline in canopy PAI, PAR and VPD, suggesting that ecosystem process (i.e., E_O and E_U) is decoupled from rainfall input. Independent estimates of E_O and E_U and their partitioning to E_{eco} in this study can improve our understanding of the seasonal dynamics of forest water use, with a holistic assessment and enhancement of the performance of forest hydrology models, by highlighting the need of incorporating separate canopy development stage of the overstory and understory, in the case, regions under the influence of monsoon climates.

3.6 Acknowledgements

This study was carried out as part of the International Research Training Group TERRECO (GRK 1565/1) funded by the Deutsche Forschungsgemeinschaft (DFG) in cooperation with the University of Bayreuth, Germany and the Korean Research Foundation (KRF) at Kangwon National University, Chuncheon, S. Korea and a grant (code: 1-8-3) from Sustainable Water Resources Research Center of 21st Century Frontier Research Program. We would like to acknowledge the input from Ms. Margarete Wartinger of Plant Ecology Department, University of Bayreuth and students of Seoul National University and Kangwon National University for their support during fieldwork.

3.7 References

Augusto L, Dupouey JL, Ranger J (2003) Effects of tree species on understory vegetation and environmental conditions in temperate forests. Ann For Sci 60:823−831

Baldocchi DD, Vogel C (1996) A comparative study of water vapor, energy and CO_2 flux densities above and below a temperate broadleaf and a boreal pine forest, Tree Physiol 16:5−16

Barbier S, Gosselin F, Balandier P (2008) Influence of tree species on understory vegetation diversity and mechanisms involved–A critical review for temperate and boreal forests. For Ecol Manage 254:1−15

Barbour MM, Hunt JE, Walcroft AS, Rogers GND, McSeveny TM, Whitehead D (2005) Components of ecosystem evaporation in a temperate coniferous rainforest, with canopy transpiration scaled using sapwood density. New Phytol 165:549−558

Black TA, Kelliher FM (1989) Processes controlling understorey evapotranspiration. Philos. Trans R Soc London B 324:207−229

Campbell GS, Norman JM (1998) An introduction to environmental biophysics. Springer, New York

Canham DC, Finzi AC, Pacala SW, Burbank DH (1994) Causes and consequences of resource heterogeneity in forests: interspecific variation in light transmission by canopy trees. Can J For Res 24:337−349

Cho YC, Shin HC, Kim SS, Lee CS (2007) Dynamics and Conservation of the Gwangneung National Forest in Central Korea: A National Model for Forest Restoration. J Plant Biol 50:615−625

Ewers BE, Oren R (2000) Analyses of assumptions and errors in the calculation of stomatal conductance from sap flux measurements. Tree Physiol 20:579−589

Field C, Mooney HA (1983) Leaf age and seasonal effects on light, water and nitrogen use efficiency in a California shrub. Oecologia 56:348−355

Granier A (1987) Evaluation of transpiration in a Douglas-fir stand by means of sap flow measurements. Tree Physiol 3:309−320

Grime VL, Sinclair FL (1999) Sources of error in stem heat balance sap flow measurements. Agric For Meteorol 94:103−121

Ham JM, Heilman JL, Lascano RJ (1990) Determination of sol water evaporation and transpiration from energy balance and stem flow measurements. Agric For Meteorol 52:287−301

Hatton TJ, Ruprecht J, George RJ (2003) Preclearing hydrology of the Western Australia wheatbelt: Target for the future. Plant Soil 257:341–356

Herbst M, Rosier PTW, Morecroft MD, Gowing DJ (2008) Comparative measurements of transpiration and canopy conductance in two mixed deciduous woodland differing in structure and species composition. Tree Physiol 28:959−970

Hiyama T, Kochi K, Kobayashi N, Sirisampan S (2005) Seasonal variation in stomatal conductance and physiological factors observed in a secondary warm-temperate forest. Ecol Res 20:333−346

Hong J, Kwon H, Lim JH, Byun YH, Lee J, Kim J (2009) Standardization of KoFlux eddy-covariance data processing. Kor J Agric For Meteorol 2:12−26

Im ES, Ahn JB, Kwon WT, Giorgi F (2008) Multi-decadal scenario simulation over Korea using a on-way doubled-nested regional climate model system. Part 2: future climate projection (2021-2050). Clim Dyn 30:239−254

Jackson PC, Cavelier J, Goldstein G, Meinzer FC, Holbrook NM (1995) Partitioning of water resources among plants of a lowland tropical forest. Oecologia 101:197−203

Jung EY, Otieno D, Lee B, Lim JH, Kang SK, Schmidt MWT, Tenhunen J (2011) Up-scaling to stand transpiration of an Asian temperate mixed-deciduous forest from sing tree sapflow measurements. Plant Ecol 212:383−395

Kang M, Park S, Kwon H, Choi HT, Choi YJ, Kim J (2009a) Evapotranspiration from a deciduous forest in a complex terrain and a heterogeneous farmland under monsoon climate. Asia-Pacific J Atmos Sci 45:175−191

Kang M, Kwon H, Lim JH, Kim J (2009b) Understory evapotranspiration measured by Eddy-Covariance in Gwangneung deciduous and coniferous forests. Kor J Agric For Meteorol 11:233−246

Kang M, Kwon H, Cheon JH, Kim J (2012) On estimating wet canopy evaporation from deciduous and coniferous forests from Asian monsoon climate, J Hydrometeorl 13:950−965

Kim J, Lee D, Hong JY (2006) HydroKorea and CarboKorea: cross-scale studies of ecohydrology and biogeochemistry in a heterogeneous and complex forest catchment of Korea. Ecol Res 21:881−889

Kim JH (2002) Community ecological view of the natural deciduous forest in Korea. In: Ecology of Korea, Bumwoo, Seoul

Korea Meteorological Administration (2011) A white paper on *Changma*.

Kosugi Y, Takanashi S, Tanaka H, Ohkubo S, Tani M, Yano M, Katayama T (2007) Evapotranspiration over a Japanese cypress forest. I. Eddy covariance fluxes and surface conductance characteristics for 3 years. J Hydrol 337:269−283

Köstner BMM, Schulze ED, Kelliher FM, Hollinger DY, Byers JN, Hunt JE, McSeveny TM, Meserth R, Weir PL (1992) Transpiration and canopy conductance in a pristine broad-leaved forest of *Nothofagus*: an analysis of xylem sap flow and eddy correlation measurements. Oecologia 91:350−359

Köstner B, Granier A, Cermák J (1998) Sapflow measurements in forest stands: methods and uncertainties. Ann Sci For 55:13−27

Kumagai T, Aoki S, Nagasawa H, Mabuchi T, Kubota K, Inoue S, Utsumi Y, Otsuki K (2005) Effects of tree-to-tree and radial variations on sap flow estimates of transpiration in Japanese cedar. Agric For Meteorol 135:110−116

Kwon H, Kim J, Hong J, Lim JH (2010) Influence of the Asian monsoon on net ecosystem carbon exchange in two major ecosystems in Korea. Biogeoscience 7:1493−1504

Landsberg JJ, Gower ST (1997) Applications of Physiological Ecology to Forest Management. Academic Press, San Diego

Latham RE, Ricklefs RE (1993) Global patterns of tree species richness in moist forests: energy-diversity theory does not account for variation in species richness. Oikos 67:325−333

Lau K-M, Li M-T (1984) The monsoon of E. Asia and its global associations−A survey. Amer Met Soc 65:112−125

Lei H, Zhang ZS, Li XR (2010) Sap flow of *Artemisia ordosica* and the influence of environmental factors in a revegetated desert area: Tengger Desert, China. Hydrol Proc 24:1248−1253

Lieffers VJ, Messier C, Stadt KJ, Gendron F, Comeau PG (1999) Predicting and managing light in the understory of boreal forests. Can J For Res 29:796−811

Lim JH, Shin JH, Jin GJ, Chun JH, Oh JS (2003) Forest stand structure, site characteristics and carbon budget of the Kwangneung natural forest in Korea. Kor J Agric For Meteorol 5:101−109

Magnani F, Leonardi S, Tognetti R, Grace J, Borghetti M (1998) Modeling the surface conductance of a broad-leaf canopy: effects of partial decoupling from the atmosphere. Plant Cell Environ 21:867−879

Meinzer FC (2003) Functional convergence in plant responses to the environment. Oecologia 134:1−11

Meinzer FC, Bond BJ, Warren JM, Woodruff DR (2005) Does water transport scale universally with tree size? Funct Ecol 19:558−565

Monteith JL (1965) Evaporation and environment. Symp Soc Expt Biol 19:205–234

MOST (1999) Geologic map of Seoul-Namchon report. Ministry of Science and Technology, Korea

Murray FW (1967) On the computation of saturation vapor pressure. J Appl Meteor 6:203−204

Nakashizuka T, Iida S (1995) Composition, dynamics and disturbance regime of temperate deciduous forests in Monsoon Asia. Vegetatio 121:23−30

Nasahara KN, Muraoka H, Nagai S, Mikami H (2008) Vertical integration of leaf area index in Japanese deciduous broad-leaved forest. Agric For Meteorol 148:1136−1146

Oh JS, Shin JH, Lim JH (2000) Long-term ecological research programme in Korea Forest Institute. Kor J Ecol 23:131−134

Oren R, Phillips N, Katul G, Ewers B, Pataki E (1998) Scaling xylem sap flux and soil water balance and calculating variance: A method for partitioning water flux in forests. Ann Sci For 55:191−216

Oren R, Sperry JS, Katul GG, Pataki DE, Ewers BE, Phillips N, Schäfer KVR (1999) Survey and synthesis of intra- and interspecific variation in stomatal sensitivity to vapour pressure deficit. Plant Cell Environ 22:1515−1526

Oren R, Pataki DE (2001) Transpiration in response to variation in microclimate and soil moisture in southeastern deciduous forests. Oecologia 127:549−559

Otieno DO, Schmidt MWT, Kurz-Besson C, Lobo Do Vale R, Pereira JS, Tenhunen JD (2007) Regulation of transpirational water loss in *Quercus suber* trees in a Metiterranean-type ecosystem. Tree Physiol 27:1179−1187

Pyatos R, Čermák J, Llorens P (2007) Variation in the radial patterns of sap flux density in pubescent oak (*Quercus pubescens*) and its implications for tree and stand transpiration measurements. Tree Physiol 27:537−548

Qian H, Ricklefs RE (1999) A comparison of the taxonomic richness of vascular plants in China and the United States. Am Nat 154:160−181

Qian H, Ricklefs RE (2000) Large-scale processes and the Asian bias in species diversity of temperate plants. Nature 407:180−182

Radoglou K (1996) Environmental control of CO_2 assimilation rates and stomatal conductance in five oak species growing under field conditions in Greece. Ann Sci For 53:269–278

Reichstein M and Coauthors (2005) On the seperation of net ecosystem exchange into assimilation and ecosystem respiration: Review and improved algorithm. Global Change Biol 11:1424−1439

Rey A, Jarvis PG (1998) Long-term photosynthetic acclimation to increased atmospheric CO_2 concentration in young birch (*Betula pendula*) trees. Tree Physiol 18:441–450

Riegel GM, Miller RF, Krueger WC (1992) Competition for resources between understory vegetation and overstory *Pinus ponderosa* in Northeastern Oregon. Ecol Appl 2:71−85

Röhrig E, Ulrich B (1991) Ecosystems of the world 7. Temperate Deciduous Forests. Elsevier, Amsterdam

Sakuratani T (1981) Heat balance method for measuring water flux in the stem of intact plants. J Agric Meteorol 1:9−17

Shi TT, Guan DX, Wu JB, Wang AZ, Jin CJ, Han SJ (2008) Comparison of methods for estimating evapotranspiration rate of dry forest canopy: Eddy covariance, Bowen ratio energy balance, and Penman-Montheith equation. J Geophys Res 113:D19116, doi:10.1029/2008JD010174.

Smith DM, Allen SJ (1996) Measurement of sap flow in plant stems. J Expt Bot 47:1833−18

Tateishi M, Kumagai T, Suyama Y, Hiura T (2010) Differences in transpiration characteristics of Japanese beech trees, *Fagus crenata*, in Japan. Tree Physiol 30:748−760

Tanaka N, Kume T, Yoshifuji N, Tanaka K, Takizawa H, Shiraki K, Tantasirin C, Tangtham N, Suzuki M (2008) A review of evapotranspiration estimates from tropical forests in Thailand and adjacent regions. Agric For Meteorol 148:807−819

Thom AS (1972) Momentum, mass, and heat exchange of vegetation. Quart J Roy Met Soc 98:124−134

Unsworth MH, Philips N, Link T, Bond BJ, Falk M, Harmon ME, Hinckley TM, Marks D, Paw UK-T (2004) Component and controls of water flux in an old-growth Douglas-fir-western hemlock ecosystem. Ecosystems 7:468−481

Vertessy RA, Benyon RG, O'sullivan SK, Gribben PR (1995) Relationships between stem diameter, sapwood area, leaf area and transpiration in a young mountain ash forest. Tree Physiol 15:559−567

Weibel FP, de Vos JA (1994) Transpiration measurements on apple tree s with an improved stem heat balance method. Plant Soil 166:203−219

Wilson KB, Hanson PJ, Mulholland PK, Baldocchi DD, Wullschleger SD (2001) A comparison of methods for determining forest evaporation and its components: sap flow, soil water budget, eddy covariance and catchment water balance. Agric For Meteorol 106:153−168

Wullschleger SD, Hanson PJ, Todd DE (2001) Transpiration from a multi-species deciduous forest as estimated by xylem sap flow techniques. For Ecol Manage 143:205−213

Zeppel MJB, Yunusa IAM, Eamus D (2006) Daily, seasonal and annual patterns of transpiration from a stand of remnant vegetation dominated by a coniferous *Callitris* species and a broad-leaved *Eucalyptus* species. Physiol Plantarum 127:413–422

Chapter 4

Influence of elevation on canopy transpiration of temperate deciduous forests in a complex mountainous terrain of South Korea

Submitted to *Plant and Soil*

Eun-Young Jung[a*], Dennis Otieno[a], Hyojung Kwon[a], Sina Berger[b], Melanie Hauer[a], John Tenhunen[a]

[a]Department of Plant Ecology, University of Bayreuth, 95440 Bayreuth, Germany

[b]BayCEER − Laboratory of Isotope Biogeochemistry, University of Bayreuth, 95440 Bayreuth, Germany

Abstract

• Background and Aims: Variations in microclimate and soil characteristics on mountain slopes influence forest structure and function. Precipitation, incoming solar radiation and relative humidity change along a mountain slope. Equally, soil depth and the amount of stored soil moisture vary. The objective of this study was to examine the impacts of these factors on forest water use in mountainous terrains.

• Methods: Transpiration of four temperate deciduous forest stands located at different elevations in South Korea was monitored with a sap flow technique throughout the growing season 2010. The study sites were located on the north slope at 450 m (450N), 650 m (650N), and 950 m (950N). To examine the effect of aspect, an additional site with a southern aspect was studied at 650 m (650S). All the sites were dominated by *Quercus* species, with leaf area index (LAI) ranging between 5−6 m^2 m^{-2}.

• Results: Rainfall increased, while air temperature (T_a) and daytime vapour pressure deficit (VPD) decreased with increasing elevation. We did not observe any gradients in solar radiation (R_S), soil moisture and sap flux density of the individual trees (J_{st}) with an elevational gradient. Sapwood area (A_S), i.e., hydro-active xylem area, and daily maximum tree water use (max TWU) increased non-linearly with increasing diameter at breast height (DBH). Neither A_S or max TWU varied across tree species or elevation. The annual canopy transpiration (E_C) was 175, 115, 110, and 90 mm for 450N, 650N, 650S, and 950N, respectively. E_C declined with increasing elevation as a result of decreasing length of the growing season, VPD, and T_a along the elevation. Significantly higher stomatal sensitivity to changes in VPD was found at 950N, leading to lower annual E_C and lower water use efficiency (WUE) at this elevation.

• Conclusions: We conclude that differences in E_C exist along the mountain slope studied, corresponding to changing T_a, VPD, length of the growing season, and stomatal sensitivity to VPD, which should be considered when establishing forest catchment water balances.

Keywords: Elevational gradient; Tree water use; Canopy transpiration; Asian temperate deciduous forest; Stomatal sensitivity

4.1 Introduction

About 70% of South Korea is covered with forests, most of which are found in the mountain regions since mountains receive more rainfall and are difficult terrains not suitable for agriculture (Korea Forest Service 2009). Because mountains are important water sources for cities and human population downstream, establishing water balances for forest catchments has become a research priority. Complexity and inter-dependency of abiotic and biotic environmental processes in mountain landscapes, however, pose significant challenges for such studies (Beniston 2003) due to rapidly changing microclimate, especially temperature and precipitation, systematic variation in radiation and wind speeds (Körner 2003). These variations in microclimate enhance differences in runoff and soil erosion, soil types and plant species; factors that have direct influence on water availability and forest water use. Typically, relatively shallow soils are found at higher elevations due to high precipitation and runoff at higher elevations, which move and deposit the soil down slope (Hirobe et al. 1998; Tateno et al. 2004; Tromp-van Meerveld and McDonnell 2006). Gradients in rainfall (Körner 2007) and soil depth experienced along a mountain slope, therefore, interact to determine the soil water storage. Thus, despite higher precipitation amounts at high elevations, soils here are shallow hence, much of the rain-water drains into down slope. At lower elevations, soils are deep, but precipitation is low hence, the soils remain relatively dry. The mid slope experiences the most favorable soil moisture conditions as a result of moderate precipitation amounts, drainage from upslope and relatively large capacitance due to moderate soil depth. These spatial gradients in soil moisture along a mountain slope must, therefore, result in spatial variability in the total amount of water available to forest trees.

Microclimatic conditions above forest stands in mountain terrains are also temporally and spatially variable. Generally, air temperature drops with increasing elevation, and in temperate zones, the temperature gradients are steeper during spring and summer than in winter (Körner 2003). Solar radiation, on the other hand, does not show definite trend and in many cases, may even decline at higher elevations (Yoshino 1975; Barry 1981), while wind velocities are related to the topographical characteristics and exposure, rather than elevations (Barry 1981). Higher, exposed elevations on the windward side, therefore, tend to experience higher wind speeds compared to the sheltered, leeward azimuths. The interaction between temperature,

precipitation (humidity), radiation and wind determines the trend of vapor pressure deficit (VPD) along the elevation. Climatic variables and hydrology determine ecosystem functioning (Running and Nemani 1987). For example, forest canopy transpiration is regulated by canopy conductance changing in short-term in response to variations in light, temperature, soil water availability, and VPD (Schulze 1994; McDowell et al. 2008). Stomatal conductance decreases in response to higher VPD at lower soil moisture availability (Schulze et al. 1994; Schulze et al. 2005). Additionally, availability of soil nutrients has significant effects on the maximum stomatal conductance (Schulze et al. 1994). Thus, spatial variability in microclimate and soil properties at different elevations will likely to generate heterogeneous transpiration rates defined by the complex interactions along a mountain slope. At higher elevations, the tendency to have higher VPD, lower soil moisture and low soil nutrient availability is likely to lead to low transpiration rates compared to down slope.

Tree transpiration also depends on water transport from the soil, determined by the nature and amount of the conducting vessels, i.e., sapwood area (Wullschleger et al. 2001; Bucci et al. 2004; Meinzer et al. 2005; Jung et al. 2011). Sapwood area in tree stems tends to decrease with increasing elevation due to reduced tree growth rates at cooler temperatures, reduced length of the growing season at higher elevations as in the temperate climate (Dittermar and Elling 2006; Vitasse et al. 2009) and lower soil nutrient availability (Vitousek and Howarth 1991; Tateno et al. 2004; Hoch and Körner 2005; Miyajima and Takahashi 2007).

Several studies have examined the relations between microclimate and vegetation processes in mountainous regions (Granier et al. 1996; Kelliher et al. 1997; Köstner 2001; Meinzer et al. 2001; Wullschleger et al. 2001; Clausnitzer et al. 2011), but there is knowledge gap on how spatial patterns of microclimate and soil moisture along mountain slopes simultaneously influence transpiration patterns and the regulation of forest water use. In temperate mountains, most of these parameters show declining trends at higher elevation, potentially lowering the transpiration rates at higher elevations (Matyssek et al. 2009). Kumagai et al. (2008) observed higher sap flux densities at lower elevations in a Japanese cedar forest and attributed this to the difference in the response of canopy conductance to VPD between high and low elevations. On the other hand, Kubota et al. (2005) observed no differences in sap flux densities among three Japanese beech forest stands at 550, 900, and 1500 m above sea level. McDowell et al. (2008) reported decreasing daily canopy transpiration with increasing elevation in different forest types in northern New Mexico. Matyssek et al. (2009), however, found no trend in daily canopy transpiration among different forest stands in the Bavarian Alps.

These contradicting results among studies point to the complexity in the interactions among factors involved in the regulation of tree transpiration in mountain landscapes and likely contribute to the lack of widely accepted approaches for estimating forest water us. In most cases, models describing forest water use at local and regional scales are generally too crude to adequately represent the orographic detail of most

mountain landscapes. Complexity in interactions, however, can be reduced by performing transpiration estimates with fine spatial definition and by limiting the choice to one tree species or same genera that has a wide distribution range across the mountain slope.

In this study, we conducted high spatial resolution measurements of sap flow, soil moisture and micrometeorology along a mountain slope to define controls of water use by deciduous forests in the complex terrain of the Haean basin, South Korea. We examined how soil characteristics and microclimate change along the elevation and also in two different slope aspects. We quantified the impact of changing soil and microclimatic environments on tree growth characteristics, forest canopy transpiration, and canopy conductance. We hypothesized that: 1. Soil characteristics and microclimate change rapidly along a vertical gradient of mountain slope; 2. Plant growth and size of the conducting sapwood decline with increasing elevation; 3. Therefore, water use by trees on a mountain slope decreases along an elevation due to the decline in soil moisture, D, sapwood area, and day of growing season.

4.2 Materials and methods

4.2.1 Study sites

The study was conducted in the rugged mountain terrain of the Haean basin, northeast of South Korea (128°05'−128°11'E, 38°13'−38°20'N). The average annual air temperature and rainfall (2001−2011) were 8.7 ± 0.4°C and 1,620 ± 400 mm, respectively. Rainfall is mainly concentrated in the month of July, during the summer monsoon.

We measured sap flow in selected forest trees at four locations (sites) situated at three different elevations. The sites were identified as (1) 450N, located at 450 m a.s.l. on a north aspect, (2) 650N, located at 650 m on a north aspect, and (3) 950N, located at 950 m on a north aspect. To examine how the aspect may influence our results, a third site was established at 650 m elevation, on the opposite, south aspect (650S). Site characteristics have been summarized in Table 1. Tree basal area (BA) was 26 m^2 ha^{-1} at the 650S whereas BA at the three other sites ranged between 21−22 m^2 ha^{-1}. Stand sapwood area (A_S) ranged between 17 m^2 ha^{-1} at 650S and 13 m^2 ha^{-1} at 650N. The 950N had the highest tree density (1.4 Tree m^{-2}) and the smallest mean DBH (4 cm), while 650N had the lowest stem density (0.2 Tree m^{-2}) and the largest mean DBH (9 cm) (Table 4.1). 450N and 650S had similar tree densities (0.4−0.5 Tree m^{-2}) and mean DBH (6−7 cm). The contributions of *Quercus* spp. to the total BA were 65%, 80%, 65%, and 80% at 450N, 650N, 650S, and 950N, respectively. The contributions of sub-dominant species to total BA were 20% for *Alnus sibirica* at 450N, 17% for *Betula davurica* at 650N, 23% for *Tilia mandshurica* at 650S, and 10% for *Euonymus hamiltonianus* at 950N. *Quercus mongolica* was common among the study sites, providing us with the opportunity to compare the same species growing at different elevations.

Table 4.1 Locations, sizes, geological traits, soil characteristics and structural characteristics of the study sites. Trees with diameter at breast height (DBH) ≥1.0 cm were considered for calculating basal area (BA), tree density, mean DBH, and stand sapwood area (A_S). ± indicates standard deviation (SD).

	450N	650N	650S	950N
Coordinates	128°7’50.09’’E 38°17’18.64’’N	128°8’26.07’’E 38°18’56.83’’N	128°8’27.13’’E 38°18’57.07’’N	128°6’0.86’’E 38°14’43.37’’N
Elevation [m a.s.l.]	450	650	650	950
Plot area [m^2]	575	750	325	200
Inclination [°]	20	23	15	21
Exposure	Southeast	Southeast	Northwest	Southeast
Bedrock	Granite	Granite	Granite	Granitic gneiss
Soil texture	Loam	Sandy-loam	Sandy-loam	Sandy (surface) Loam
Soil depth [cm]	8–100	18–68	19–65	22–100
Soil N contents [mg g^{-1}]	1.6 ± 0.9	5.0 ± 2.3	5.0 ± 2.3	1.7 ± 0.7
Stand age [yrs]	ca. 30	ca. 30	ca. 30	ca. 20
BA [m^2 ha^{-1}]	21.2	20.7	25.9	22.3
Tree density [Tree m^{-2}]	0.4	0.2	0.5	1.4
Mean DBH [cm]	5.6 ± 5.8	9.4 ± 5.3	6.6 ± 4.4	4.2 ± 1.6
Stand A_S [m^2 ha^{-1}]	13.7	13.3	17	15.4
Canopy height [m]	10	12	10	5
Species composition (BA cover [%])	*Quercus mongolica* (24) *Alnus sibirica* (18) *Q. aliena* (15) *Q. serrata* (15) *Ulmus laciniata* (10) *Q. dentate* (8) *Tilia mandshurica* (6)	*Q. dentate* (65) *Betula davurica* (19) *Q. mongolica* (14)	*Q. mongolica* (50) *T. mandshurica* (25) *Q. dentate* (14) *Fraxinus rhynchophylla* (4) *Q. serrata* (4)	*Q. mongolica* (72) *F. rhynchophylla* (13) *Euonymus hamiltonianus* (9)

4.2.2 Measurement of abiotic factors

4.2.2.1 Micrometeorology

Solar radiation (R_S), air temperature (T_a), rainfall, relative humidity, and wind speed were measured every 30 seconds, averaged and logged every 30 minutes by automatic weather stations (AWS; WS-GP1, Delta-T Devices, Cambridge, UK) installed at 2 m above the ground. AWS at 450 m (450 AWS) and 950 m (950 AWS) were installed in the open space next to the respective. AWS at 650 m (650 AWS) was located in an open space between 650N and 650S. Additional air humidity and temperature sensors (Funky Clima, ESYS GMBH, Berlin, Germany) were installed within the crowns at each site and half-hourly averages of five-minute data recorded. Vapor pressure deficit (D) of each site was derived from measured T_A and relative humidity (Murray 1967).

4.2.2.2 Soil water content and soil water retention

Soil water content (θ) in 30 cm depth was measured at each site using soil moisture sensors (5TE, Decagon Devices, Washington, USA) and data logged every 30 minutes (EM50 Data logger, Decagon Devices) over the period of sap flow measurements. Relative θ was determined at each site as daily mean θ divided by maximum value of daily mean θ, allowing for a better comparison of soils with different textures. To analyze soil texture and bulk density, three soil samples were collected from each study site using a soil corer and a bulk density sampler, respecttively. A and B horizons of the soils were separately analyzed. Humus was eliminated by H_2O_2. Sand, silt and clay contents were determined by wet sieving for sand and laser particle analyzer (Mastersizer S MAM5004, Malvern Instruments, Herrenberg, Germany) for silt and clay in the Soil Physics laboratory, University of Bayreuth. Based on the bulk density and soil texture data, soil hydraulic parameters for each site, such as residual water content (θ_r), saturated water content (θ_s) and empirical shape parameters (α and n) were estimated using a computer program RETC−Retention Curve Program (PC−Progress, Prague, Czech Republic) and then soil water retention curves were determined following van Genuchten function (van Genuchten 1980, Schaap et al. 2001). From these retention curves soil water retention levels, corresponding to measured daily mean θ, was read out and also wilting point (θ_w) and field capacity (θ_c) for each site determined, and then applied to gap−filling of canopy transpiration (E_C; see the section 4.2.4).

4.2.3 Measurement of biotic factors

4.2.3.1 Biometric data

Monthly leaf area index (LAI) at each site was measured once a month with a plant canopy analyzer (LAI-2000, LI-COR Inc., Lincoln, USA) under diffuse light conditions at fixed 9 sampling points with 10 m × 10 m grid interval in order to determine the seasonal changes of LAI. The maximum leaf area index (LAI_{max}) was estimated from leaf litter collected with 0.5 m × 0.5 m litter traps (five in each site) randomly placed at ca. 1 m height above the forest floor in order to calibrate the values of LAI measured by LAI-2000. Leaf litter was collected monthly, transferred to the laboratory and sorted according to species. A sub-sample of leaf litter was measured for leaf area (LI-3100, LI-COR Inc.), dried for 48 hours at 75°C and weighed. Specific leaf area was determined from the ratio of leaf area/dry mass ($cm^2\ g^{-1}$). L of each species (A_L) from each site was computed from dry leaf weight multiplied by specific leaf area, summed over the season and divided by the area of the litter trap.

In July 2010, a survey of all stems larger than 2 cm in diameter at 1 m height was carried out on 25 m x 25 m grids. Based on this survey, mean DBH, basal area (BA, $m^2\ ha^{-1}$) and tree density (Tree m^{-2}) were calculated for each plot. Sapwood area (A_S, m^2) of sample trees was calculated from the sapwood depths at sap flow sensor heights, determined from tree cores extracted at the end of the sap flow measurements. Sapwood was identified by dying the core samples, using bromocresol green (Sigma Chemicals, Germany) (Burrows 1980). Data from the sample trees were used to build an allometric function from which A_S of all the trees in the stand were estimated (Vertessy et al. 1995, Meinzer et al. 2005):

$$A_S = \alpha DBH^{\beta} \quad (1)$$

where α is a constant and β is the allometric scaling exponent. Using this empirical relationship of each site, stand A_S ($m^2\ ha^{-1}$), i.e., total A_S of all trees in the plot (A_{st}) per ground area (A_G), was estimated on the basis of the stem survey.

Allometric relationships for the studied species (*Querucs* spp., *A. sibirica*, *B. davurica*, and *T. mandshurica*) are shown in Figure 4.1. Three respective regressions in the form of power function were built separately for *Quercus* spp. alone (ring porous; $A_S = 0.7642DBH^{1.8057}$, n = 31, $R^2 = 0.89$, $P < 0.0001$), for the rest of the species without *Quercus* spp. (diffuse porous; $A_s = 0.8838DBH^{1.8905}$, n = 13, $R^2 = 0.98$, $P < 0.0001$), and for all the species together ($A_S = 0.5974DBH^{1.9374}$, n = 44, $R^2 = 0.84$, $P < 0.0001$). Total stand A_S estimated from separate regressions (*Quercus* spp. alone vs. the rest of the species) were similar or slightly larger than estimates from a combined species regression (i.e., the difference was less than 1% at 450N and 650N, 5% at 650S, and 10% at 950N). We, therefore, chose the general regression for further analyses related to A_S.

After determination of total A_L and total A_S of each species from each site, species-specific $A_L A_S^{-1}$ was calculated for all studied species from each site.

The tree cores extracted for the determination of the A_S were brought to the lab and ring widths were visually measured using a stereo microscope.

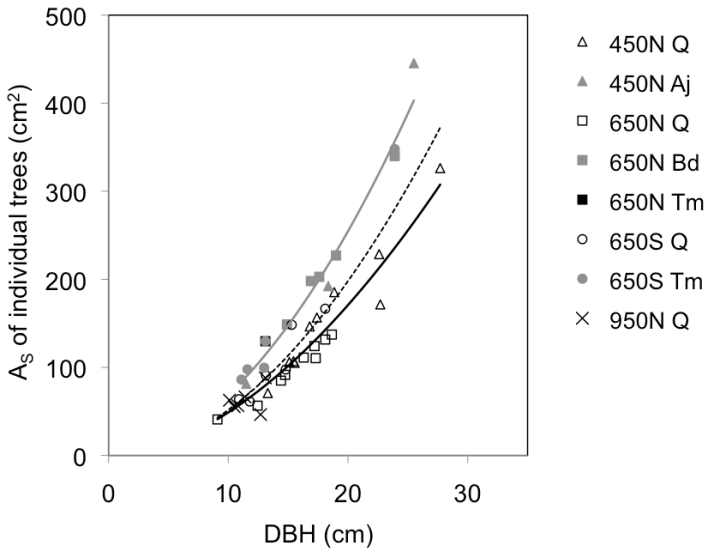

Figure 4.1 Relationship between stem diameter at breast height (DBH, cm) and sapwood area (A_S, cm^2) for *Quercus* species (open symbols) and for the rest of the studied species (close symbols) from all study sites. Black solid line is the regression for *Quercus* spp.: $A_S = 0.7642DBH^{1.8057}$ (n = 31, $R^2 = 0.89$, $P < 0.0001$), gray solid line is the regression for the rest of the species: $A_S = 0.8838DBH^{1.8905}$ (n = 13, $R^2 = 0.98$, $P < 0.0001$), and broken line is a regression of all species: $A_S = 0.5974DBH^{1.9374}$ (n = 44, $R^2 = 0.84$, $P < 0.0001$). Letters of Q, As, Bd, Tm indicate *Quercus* spp., *Alnus sibirica*, *Betula davurica*, *Tilia mandshurica*, respectively.

4.2.3.2 Sap flux density and transpiration

To estimate canopy transpiration (E_C), dominant and sub-dominant tree species covering more than 80% of BA at each plot were selected as sample trees of sap flow measurements. Sample size per species was decided based on the species dominance in each plot. Trees with larger than 7 cm diameter at breast height (DBH), were chosen in order to apply sap flow probes. Detailed information of sample trees including species and number of individuals are indicated in Table 4.2.

Sap flux density was monitored with 20 mm long thermal dissipation probes heated at constant power supply. The probes were constructed at the technical laboratory, Department of Plant Ecology, University of Bayreuth, based on the original design of Granier (1987). The probes were inserted into 0−20 mm of the sapwood in all the sample trees. Depending on the determined sapwood depth (d), additional sensors were installed deeper into 20−40 mm or 40−60 mm of the sapwood in order to cover the most of the sapwood. Sensors were installed at ca. 1.3 m height above the ground and on the north-facing side (azimuth) of the trees to minimize direct solar heating (Wilson et al. 2001; Wullschleger et al. 2001). Further, each probe was covered with Styrofoam sheaths and aluminum foil to minimize direct thermal load from the sun. The temperature differences (ΔT) between the heated and reference probes aligned vertically 10 cm apart in the sapwood was recorded, and by comparing ΔT to the maximum temperature difference (ΔT_{max}) occurring at predawn when there is no sap flow, sap flow density (F_d, g m^{-2} s^{-1}) was calculated according to Granier (1987):

$$F_d = 119\left[\frac{(\Delta T_{\max} - \Delta T)}{\Delta T}\right]^{1.231} \qquad (2)$$

Natural ΔT without heating was negligible since all measurements in the present study were carried out in forest stands with relatively closed canopies. The Clearwater-correction (Clearwater et al. 1999) was applied to J_s of ring-porous *Quercus* with less than 20 mm sapwood depth. Azimuth variation in J_s was not considered during E_C estimates, based on the findings of our previous study (Jung et al. 2011), which showed no significant differences in J_s in different azimuths of the tree trunk.

Tree water use (TWU, kg h^{-1}) of the individual trees was computed as:

$$TWU = F_{dt} A_s \qquad (3)$$

$$F_{dt} = \frac{\sum (F_{di} A_{si})}{\sum A_{si}} \qquad (4)$$

where F_{dt} is sapwood area weighted sap flow density, F_{di} is sap flow density of annulus *i*, and A_{si} is sapwood area of annulus *i*.

Canopy transpiration (E_C, mm h^{-1}) was calculated as:

$$E_C = \overline{F_{dt}} A_{st} A_G^{-1} \quad (5)$$

where $\overline{F_{dt}}$ is the mean F_{dt} of the sample trees.

Measurements were conducted between May and October 2010, during the vegetation period. F_d data were sampled every 30 seconds, averaged and recorded every 30 minutes (DL2, Delta-T Devices, Cambridge, UK). The period with active transpiration was regarded as the vegetative/growth period.

4.2.3.3 Canopy conductance

Canopy conductance (G_C, mm s^{-1}) is estimated from transpiration per unit leaf area (E_L, mm s^{-1}) scaled from F_{dt} (Monteith and Unsworth 1990) as:

$$G_C = \frac{K_G E_L}{VPD} \quad (6)$$

where K_G is the conductance coefficient as a function of T_a ($115.8 + 0.4236T_a$, kPa m^3 kg^{-1}) accounting for temperature effects on the psychrometric constant, latent heat of vaporization, specific heat of air at constant pressure and the density of air (Phillips and Oren 1998). E_L (mm s^{-1}) is transpiration per unit leaf area determined by:

$$E_L = F_{dt} \frac{A_S}{A_L} \quad (7)$$

This simplification of the Penman-Monteith equation is based on the assumption that forests are well coupled aerodynamically, when leaves are exposed to sufficiently high wind speeds. Thus, VPD can be used as an approximation of the total driving force for transpiration. We tested the assumption of strong coupling in all the studied sites by comparing aerodynamic conductance (G_A) and G_C for 8 days from 1–8 June. G_C reached ca. 1% of G_A, agreeing with the assumption of Eq. 6.

To assess stomatal sensitivity to VPD at each site, a modified Lohammar's function was applied.

$$G_C(VPD) = G_{Cref} - m \ln VPD \quad (8)$$

where G_{Cref} is canopy conductance at VPD = 1 kPa and $-m$ (i.e., $-\Delta G_C/\Delta \ln VPD$) is the sensitivity of G_C response to VPD (Oren et al. 1999). Stomatal sensitivity analysis was limited to G_C under conditions in which VPD ≥0.6 kPa in order to minimize the uncertainties of G_C estimates (Ewers and Oren 2000).

Table 4.2 Species, number (n), ranges of diameter at breast height (DBH, cm), sapwood depth (d, mm), maximum sap flow density weighted by sapwood area of each tree (max F_{dt}, g m^{-2} s^{-1}) and maximum tree water use (max TWU, kg d^{-1}) of all the sample trees with sap flow sensors at each site.

		Quercus mongolica	*Q. dentata*	*Q. serrata*	*Q. aliena*	*Alnus sibirica*	*Betula davurica*	*Tilia mandshurica*
450N	n	5	3	1	1	3	-	-
	DBH	14.7–25.3	13.6–16.3	12.0	26.0	11.5–25.5	-	-
	d	22–40	23–33	20	36	40–70		
	max F_{dt}	14.7–28.5	13.3–22.0	48.3	45.2	40.7–88.2	-	-
	max TWU	8.6–40.9	6.6–8.5	13.3	34.5	18.1–59.1	-	-
650N	n	4	5	-	-	-	5	1
	DBH	8.9–14.4	15.8–18.2	-	-	-	14.0–22.9	23.0
	d	16–24	18–25				42–60	58
	max F_{dt}	15.2–21.8	11.2–15.7	-	-	-	33.1–64.2	36.1
	max TWU	2.7–6.6	3.9–5.5	-	-	-	17.6–42.6	10.4
650S	n	5	1	-	-	-	-	4
	DBH	9.9–17.8	14.3	-	-	-	-	10.4–22.7
	d	20–37	20					40–60
	max F_{dt}	19.4–26.5	13.6	-	-	-	-	20.4–55.6
	max TWU	2.8–9.1	3.3	-	-	-	-	4.3–58.6
950N	n	6	-	-	-	-	-	-
	DBH	7.3–9.8	-	-	-	-	-	-
	d	15–23						
	max F_{dt}	15.7–41.2	-	-	-	-	-	-
	max TWU	2.4–8.2	-	-	-	-	-	-

4.2.3.4 Gap-filling

A modified Jarvis-Stewart model as defined by Whitley et al. (2009) was used to estimate E_C for the period when data gap occurred. Whitley et al. (2008) and Whitley et al. (2009) expressed E_C in the same way as G_C, as defined by Jarvis (1976) and Stewart (1988).

$$E_C = E_{C\max} f_1(R_S) f_2(VPD) f_3(\theta) f_4(LAI) \qquad (9)$$

The functions f_i, which take on values between 0 and 1, are a set of scaling terms reducing a maximum stand transpiration (E_{Cmax}, mm d^{-1}) in response to changes in R_S, VPD and θ. Daily estimates of E_C were determined by the functions f_i using the optimal estimates of parameters. The functions of R_S, VPD and θ were taken from Whitley et al. (2008) based on those of Stewart (1988), Wright et al. (1995) and Harris et al. (2004). A function describing a radiation response is:

$$f_1(R_S) = \left(\frac{R_S}{30}\right)\left(\frac{30 + k_1}{R_S + k_1}\right) \qquad (10)$$

where k_1 is an empirical coefficient describing the curvature of the relationship. It shows an asymptotic function saturating at approximately 30 MJ m^{-2} d^{-1}.

A functional response of E_C to VPD was expressed as:

$$f_2(VPD) = k_2 VPD \exp(-k_3 VPD) \qquad (11)$$

where k_2 and k_3 are the parameters describing the rate of change at low and high VPD. This function of VPD for Ec follows Boltzmann distribution.

A function of soil moisture response was described to be a three-phase relationship as:

$$f_3(\theta) = \begin{cases} 0, & \theta < \theta_w \\ \dfrac{\theta - \theta_w}{\theta_c - \theta_w}, & \theta_w < \theta < \theta_c \\ 1, & \theta > \theta_c \end{cases} \qquad (12)$$

where θ_w and θ_c are wilting point and field capacity of each site, respectively.

A function of LAI response to E_C was described as:

$$f_4(LAI) = \frac{LAI}{LAI_{\max}} \qquad (13)$$

A model parameterization was performed using measured data on daily basis via nonlinear least squares analysis. To avoid errors of division by zero and conditions of wet canopy, only the data between 8:00h and 18:00h were included, and the data on the rainy days were excluded. The data from each study site were partitioned into two separate sets of random days in order not to use same data for both parameterizations and validation of the model. Root-mean-square-error (RMSE) and an agreement index (d), developed by Willmott (1984) were used to evaluate the agreement between the predicted E_C and the observed E_C. The

ideal model would give RMSE = 0 and d = 1. Total gap-filled period of each site was 27 days for 450N, 54 days for 650N, 68 days for 650S, and 8 days for 950N. The gap-filled data were only used for quantification of annual E_C.

Annual E_C was estimated by summing up the measured and simulated E_C as Eq. 9–Eq. 13. Table 3 contains the best estimates of parameters (k1, k2, and k3) along with their respective standard errors. Parameters of k2 and k3 were found to be statistically significant (P <0.001), but k1 was not significant (P >0.1), with large standard errors. RMSE was less than 0.2 and d was larger than 0.9 for all study sites (Table 4.3).

Table 4.3 Optimal estimates of Jarvis-Stewart model parameters (k_1, k_2, k_3) and statistical parameters for error assessment such as root-mean square-error (RMSE) and index of agreement (d) for all sites. Standard errors are given brackets next to each value.

	450N	650N	650S	950N
k_1	0.57 (1.63)	2.08 (3.81)	0.56 (1.24)	0.92 (3.92)
k_2	1.92 (0.21)	3.75 (0.65)	2.43 (0.24)	2.75 (0.45)
k_3	0.68 (0.07)	0.94 (0.12)	0.79 (0.08)	0.99 (0.14)
RMSE	0.16	0.21	0.12	0.18
d	0.96	0.91	0.97	0.96

4.2.3.5 Water use efficiency and leaf nitrogen contents

From each site, five sun- and five shade-leaves each from five *Q. mongolica* canopy trees were collected on 24 June 2010, during mid season. The samples were oven-dried at 75°C for 48 hours and then ball-milled before subjected to $^{13}C/^{12}C$ isotopic ratio analysis at BayCEER – Laboratory of Isotope Biogeochemistry, Germany. Analyses were conducted with an elemental analyzer NA 1108 (CE Instruments, Milan, Italy) coupled to an isotope ratio mass spectrometer delta S (Finnigan MAT, Bremen, Germany) via an open split interface ConFlo III (Finnigan MAT, Brement, Germany) as described by Bidartondo et al. (2004). Standard CO_2 gas was calibrated with respect to international standard (CO_2 in Pee Dee Belemnite) by use of the reference substance NBS 16 to 20 for carbon isotopic ratio provided by the international Atomic Energy

Agency IAEA, Vienna, Austria. The $^{13}C/^{12}C$ isotopic ratios, denoted as delta values were calculated according to the equation

$$\delta^{13}C = \left[\frac{R_{sample}}{R_{std}} - 1 \right] \times 1000 \qquad (14)$$

where $\delta^{13}C$ is the isotope ratio of carbon in delta units relative to the PDB standard. R_{sample} and R_{std} are the $^{13}C/^{12}C$ of the samples and the PDB standard, respectively. $\delta^{13}C$ was used as an index of seasonally integrated water use efficiency (WUE) (Tieszman and Archer 1990).

4.2.3.6 Statistical analysis

Statistical analyses including linear regression, ANOVA, and Tukey HSD, as well as model parameterizations were conducted with R (R development Core Team, 2010). Nonlinear curve fits were performed using Sigma Plot (Version 11, SPSS, San Rafael, CA).

4.3 Results

4.3.1 Elevation effects on microclimate

Annual mean solar radiation (R_S), daily air temperature (T_A), air humidity and rainfall differed among sites (Table 4). The annual mean R_S was higher (ANOVA, P <0.0001) at 450 m > 950 m > 650 m. The annual mean T_A and the mean annual daytime D were higher at 450 m > 650 m > 950 m. Thus, T_A and daytime D decreased with increasing elevation. Differences in T_A and daytime D among the sites were significant (ANOVA, P <0.001). Increasing annual rainfall was observed with increasing elevation. In other words, 950m received higher amount of rainfall than lower elevations, corresponding to higher rainfall intensities and frequencies through the year. Mean wind speed at 950 m was ca. 4.5 m s^{-1}, which was about twice as high as at 450 m (2.6 m s^{-1}).

Although absolute values of R_S, T_a, VPD, and rainfall were different among sites, their seasonal trends were similar across the sites (Figure 4.2). R_S increased during spring and reached its maximum in June. A strong decline in R_S occurred in July and August, during with the monsoon period. A second peak in R_S occurred in September, after the monsoon, but this peak was lower than the pre-monsoon value. R_S significantly dropped during fall and winter. The minimum and maximum T_a were recorded in January and August, respectively. VPD increased steadily during spring and reached its maximum in June, but declined to 20% of its maximum between July and August, during the monsoon. A slight increase in VPD occurred in

September, after the monsoon, but did not reach the pre-monsoon maxima. A significant decline was recorded after October. Most rains occurred in July and August, associated with the monsoon and typhoons.

The mean soil water content (θ) during the growing season was 30, 29, 19 and 18% at 950N, 450N, 650N and 650S, respectively. Relative θ were higher than 0.6 at all sites for the whole measuring period and soil water retention levels never reached θ_w and mostly in the range of θ_c, indicating lack of water stress at all the sites during the measurement period.

Diurnal courses of VPD at the 950N showed different patterns than at the other sites (Fig. 4.4b), while diurnal patterns of R_S were similar at all the sites (Fig. 4.4a). Thus, D at the 950N was relatively higher at the nighttime through most of the measured period associated with strong wind speed (around 4 m s^{-1}) at this site.

Table 4.4 Annually averaged microclimates (daily sum radiation (R_S), mean air temperature (T_a), mean daytime vapor pressure deficit (VPD), annual rainfall and wind speed) and soil water content (θ) during growing season of the study sites in Haean catchment, South Korea in 2010. ± are standard deviation (SD).

Site	450AWS	650AWS	950AWS
Annual R_S [MJ m^{-2} d^{-1}]	13.4 ± 6.8	11.6 ± 6.4	12.3 ± 8.0
Annual T_a [°C]	8.5 ± 11.1	7.3 ± 10.8	5.7 ± 11.3
Annual mean *daytime VPD [kPa]	0.5 ± 0.4	0.4 ± 0.4	0.2 ± 0.3
Annual rainfall [mm]	1,260	1,620	1,950
Wind speed [m s^{-1}]	2.6 ± 1.4	1.0 ± 0.6	4.5 ± 2.3
Soil water content [%]	28.6 ± 2.4	19.2 ± 1.1 (650N) 18.3 ± 2.5 (650S)	30.1 ± 1.5

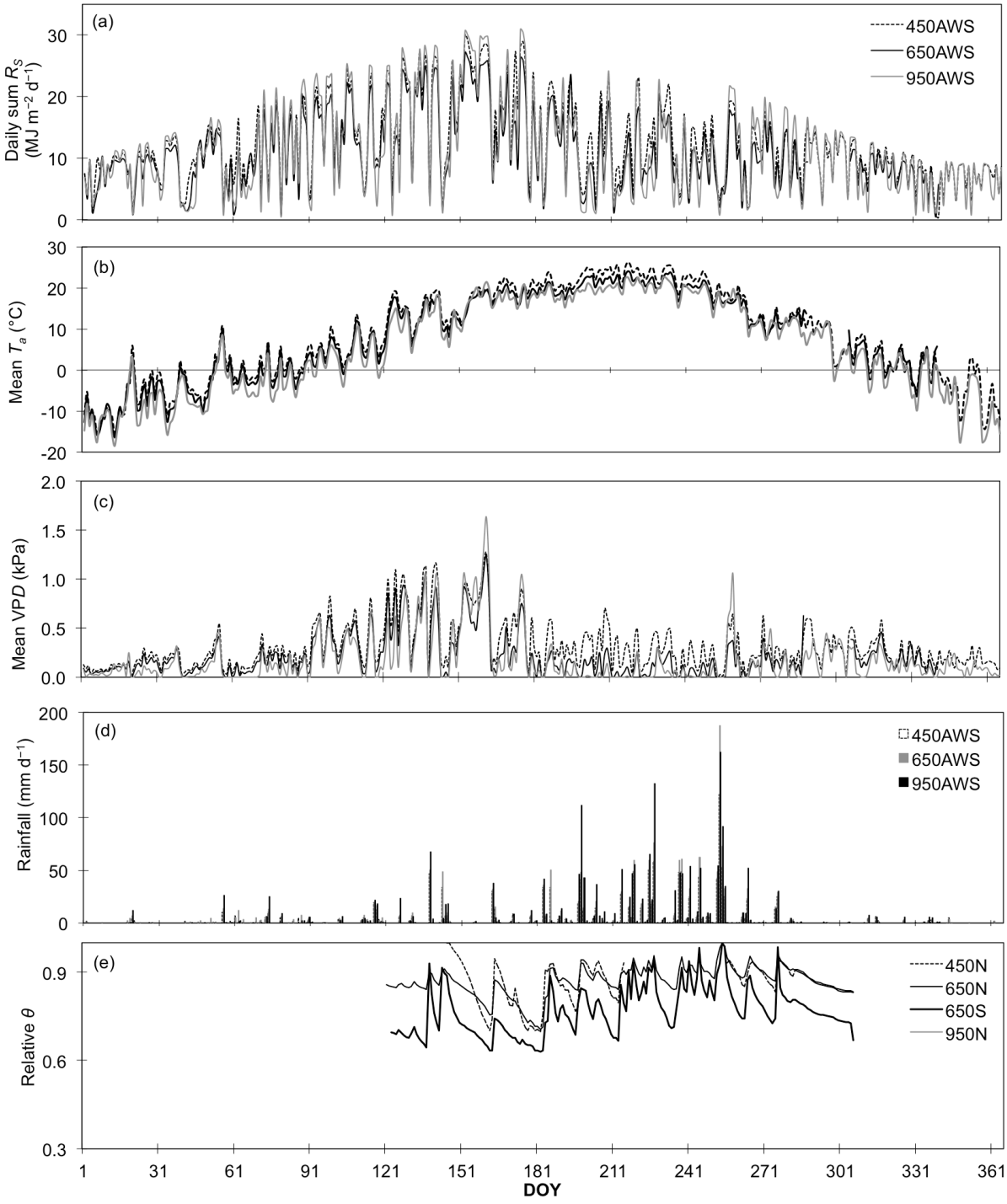

Figure 4.2 Seasonal patterns of meteorological variables at each study site. (a) Daily sum solar radiation (R_S, MJ m^{-2} d^{-1}), (b) mean air temperature (T_a, °C), (c) mean vapor pressure deficit (VPD, kPa), and (d) rainfall (mm d^{-1}) at 450, 650 and 950 m elevation. (e) Relative soil water content (θ) measured at 30 cm deep in the soil at each site where sap flow measurements were conducted.

4.3.2 Elevation effects on biotic factors

In all the sites, LAI increased gradually during spring to maximum of 5−6 in July. There were no significant differences among the sites (Table 4.5). During the monsoon and typhoon season (July−August), LAI declined to about 15−20%. Leaf senescence and shedding occurred from mid September leading to a strong declined in LAI. Although seasonal trends of LAI development and the maximum LAI were similar for the sites, the lengths of the growing season (period of active transpiration) were different among the sites due to varied timing of leaf flush and leaf-senescence. Leaf flush (starting of active transpiration) at 450N occurred about two weeks earlier than at the 950N and three days earlier than at the 650N. The timing was similar at 650N and 650S. Onset of leaf fall (ending of active transpiration) at the 450N was about a week later than at 950N and four days later than at 650N. In general, bud break in spring occurred when the mean daytime (06:00h−18:00h) temperature rose above 10°C. Similarly, leaf senescence in fall were recorded when mean daily temperature fell bellow 10°C, which occurred at different times across the study sites. Consequently, the growing season was longer at the 450N (176 days) and shorter at 950N (154 days) (Table 4.5). The length of the growing season decreased with increasing elevation and decreasing air temperature as 3.4 ± 0.2 days 100 m^{-1} (n = 4, R^2 = 0.68, P <0.01) and 6.2 ± 0.3 days $°C^{-1}$ (n = 4, R^2 = 0.72, P <0.001). Corresponding to this difference in length of the growing season at different elevations, varying mean ring widths (growth rate) in *Q. mongolica* stem cores were observed. Largest ring width of 4.4 ± 1.0 mm $year^{-1}$ was found at 450N and smallest ring width of 2.1 ± 0.3 mm $year^{-1}$ was found at 950N (Table 4.5).

The maximum F_{dt} measured during the days with R_S >20 MJ m^{-2} d^{-1} and VPD >0.5 kPa ranged between 16 and 64 g m^{-2} s^{-1} (Table 2). *Quercus* spp. at 450N and 950N showed higher maximum F_{dt} (26 ± 11 and 25 ± 12 g m^{-2} s^{-1}) than at 650N and 650S (16 ± 4 and 19 ± 5 g m^{-2} s^{-1}). The differences were, however, not significant (ANOVA, F = 2.31, P = 0.1; TukeyHSD, P_{adj} >0.1 for all) (Figure 4.3a). Diffuse porous species (*A. sibirica*, *B. davurica* and *T. mandshurica*) demonstrated higher F_{dt} than the ring porous, *Quercus* species, i.e., 60 ± 25, 49 ± 12, 34 ± 13, and 21 ± 10 g m^{-2} s^{-1} for *A. sibirica*, *B. davurica*, *T. mandshurica* and *Quercus* species, for all the sites, respectively. Even though F_{dt} differed among species, relations of DBH to A_S (Figure 4.2) and to maximum TWU (Figure 4.3b) for the combined data of all species were revealed significant (for both; P <0.0001). Both A_S and maximum TWU nonlinearly increased with increasing DBH regardless of tree species. Maximum TWU of individual trees was in the range of 2−59 kg d^{-1} and its relation to DBH was well described by a sigmoid function, $TWU = \frac{72.6}{1+\exp\left(-\frac{(DBH-23.1)}{4.39}\right)}$ (n = 44, R^2 = 0.62, P <0.0001).

Table 4.5 Maximum leaf area index (LAI_{max}), length of the growing season, total canopy transpiration (E_C, mm) during the growing season and mean ring width for *Quercus mongolica* at each study site. ± are standard deviation (SD).

	450N	650N	650S	950N
LAI_{max}	4.9 ± 1.3	5.3 ± 1.2	6.3 ± 1.4	5.7 ± 1.1
Length of the growing season [days]	176	171	168	154
E_C [mm]	175	115	110	90
Ring width [mm $year^{-1}$]	4.4 ± 1.0	2.5 ± 0.2	2.8 ± 0.5	2.1 ± 0.3

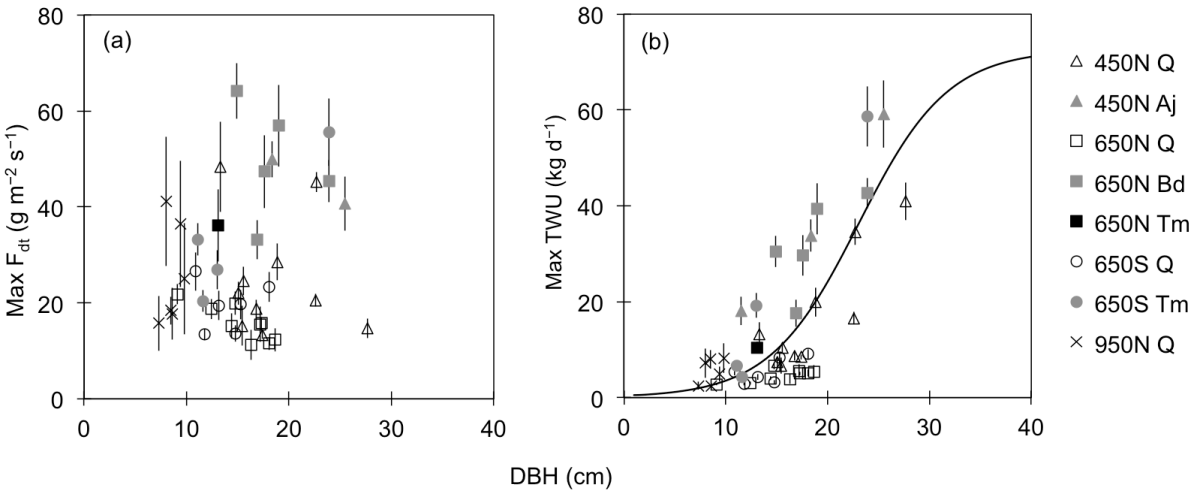

Figure 4.3 Relationship (a) between diameter at breast height (DBH, cm) and maximum sap flow density of the sample trees (Max F_{dt}, g m^{-2} s^{-1}) and (b) between DBH and maximum tree water use (Max TWU, kg d^{-1}) for the sample trees from all study sites. Sigmoid function for the relation of DBH to TWU was $TWU = \frac{72.6}{1+\exp\left(-\frac{(DBH-23.1)}{4.39}\right)}$ (n = 44, R^2 = 0.62, P <0.0001). Max F_{dt} and TWU was selected for the days with R_S >20 MJ m^{-2} d^{-1} and VPD >0.5 kPa. Letters of Q, As, Bd, Tm indicate *Quercus* spp., *Alnus sibirica*, *Betula davurica*, *Tilia mandshurica*, respectively. Bars indicate standard deviation from different days.

4.3.3 Elevation effects on canopy transpiration

Daily patterns of canopy transpiration (E_C) at all the sites, except the 950N, were similar. E_C increased in response to increasing R_S and D during the early hours of the day, attaining maximum just before noon (Figure 4.4). A gradual decrease in E_C occurred later in the day corresponding with the declining R_S and D. 450N displayed the highest E_C rates most of the day and showed an extended activity of E_C, i.e., stem refilling in the evening, after sunset. E_C at the 650S showed approximately one-hour lag compared to 650N due to differences in aspect, associated with delayed (one hour) exposure to light. At 950N, however, a bimodal peak was observed, first between 7:00h and 9:00h and then between 14:00h and 16:00h, with a depressed E_C between 10:00h and 13:00h, on clear, sunny days (Figure 4.4c). Nighttime E_C was not observed at all the sites including 950N where experienced relatively higher nighttime D than the other sites.

Maximum daily E_C were 1.9, 1.5, 1.7, and 1.9 mm d^{-1} at the 450N, 650N, 650S, and 950N, respectively, in June when the forest canopy was fully developed and the highest R_S and VPD prevailed. Daily maximum E_C declined to rates below 0.5 mm d^{-1} between July and August during the monsoon and typhoon (Figure 4.1 and Figure 4.5). A second peak occurred in September, after the monsoon, but this was lower than the peak E_C values before monsoon. E_C decreased to near zero between September and October, a period when significant leaf yellowing occurred. Such trends were similar at all the studied sites. Total E_C during the growing season (i.e., annual E_C in this study) was larger at 450N > 650N > 650S > 950N (175 >115 >110 >90 mm $year^{-1}$, respectively) (Table 4.5).

Fluctuations in E_C on bright sunny days between June and September (mature canopy) were explained by changes in VPD, for all the sites (Figure 4.6) following Eq. 11. All the estimated parameters of each regression were statistically significant (P <0.0001). E_C nonlinearly increased with increasing VPD and saturated at VPD >1.2 kPa. In this respect, the 950N was different, with E_C saturating at VPD = 0.8 kPa, approximately.

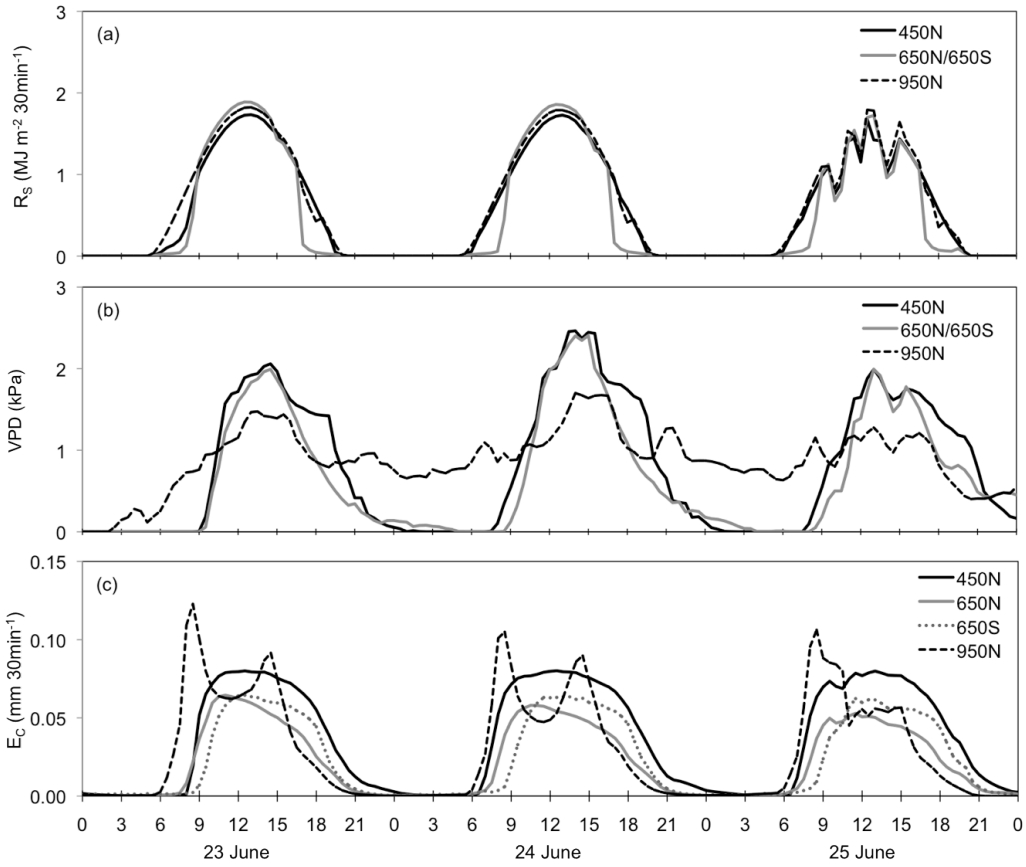

Figure 4.4 Diurnal patterns of (a) radiation (R_S, MJ m^{-2} $30min^{-1}$), (b) vapor pressure deficit (VPD, kPa), and, (c) canopy transpiration (E_C, mm $30min^{-1}$) at each site from 23 to 25 June.

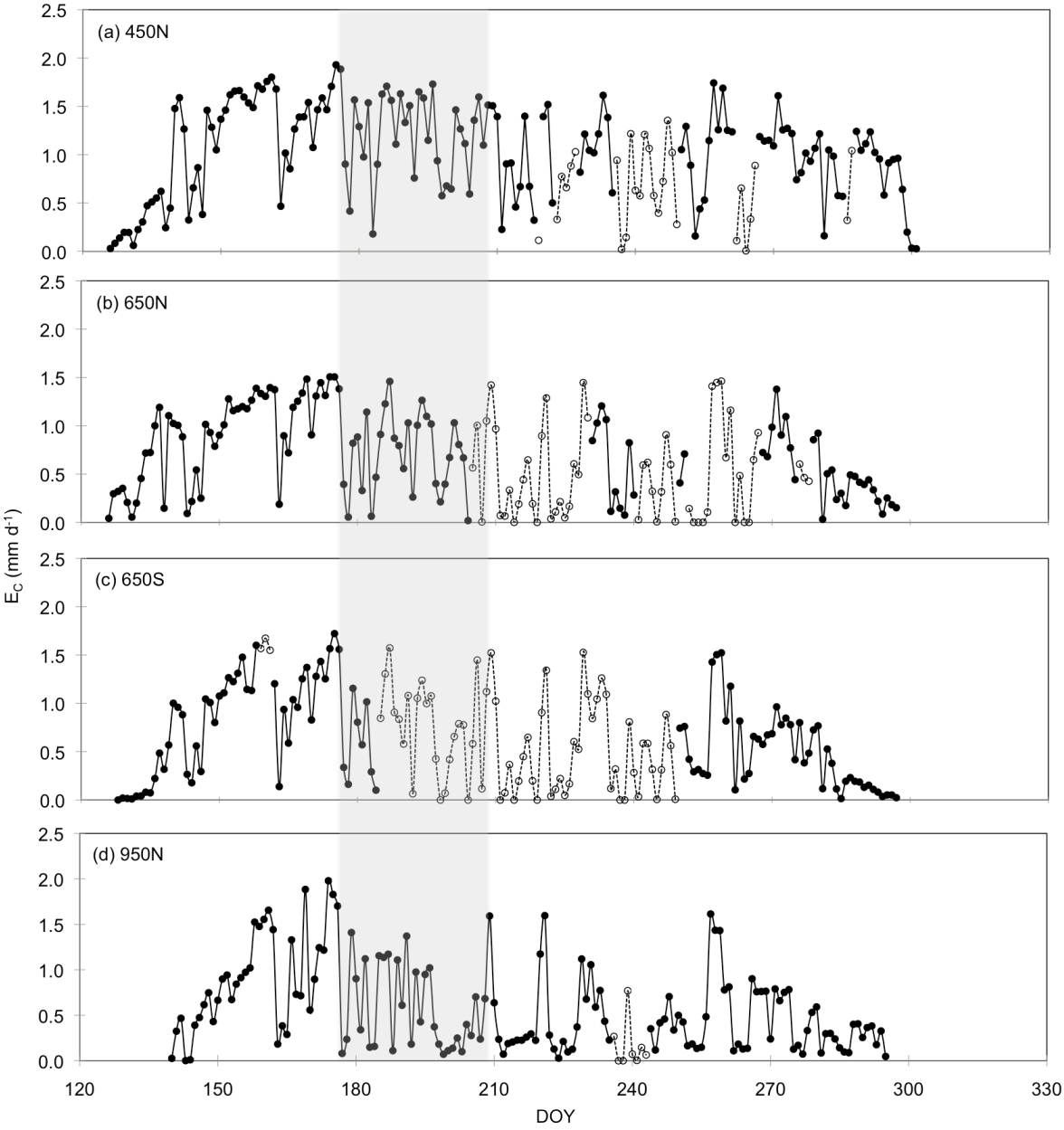

Figure 4.5 Seasonal patterns of daily canopy transpiration (E_C, mm d^{-1}) at each study site in 2010. Closed circles are measured and open circles are simulated values using Jarvis-Stewart model (Eq. 11). The shaded area indicates the period of the monsoon in Korea, 2010.

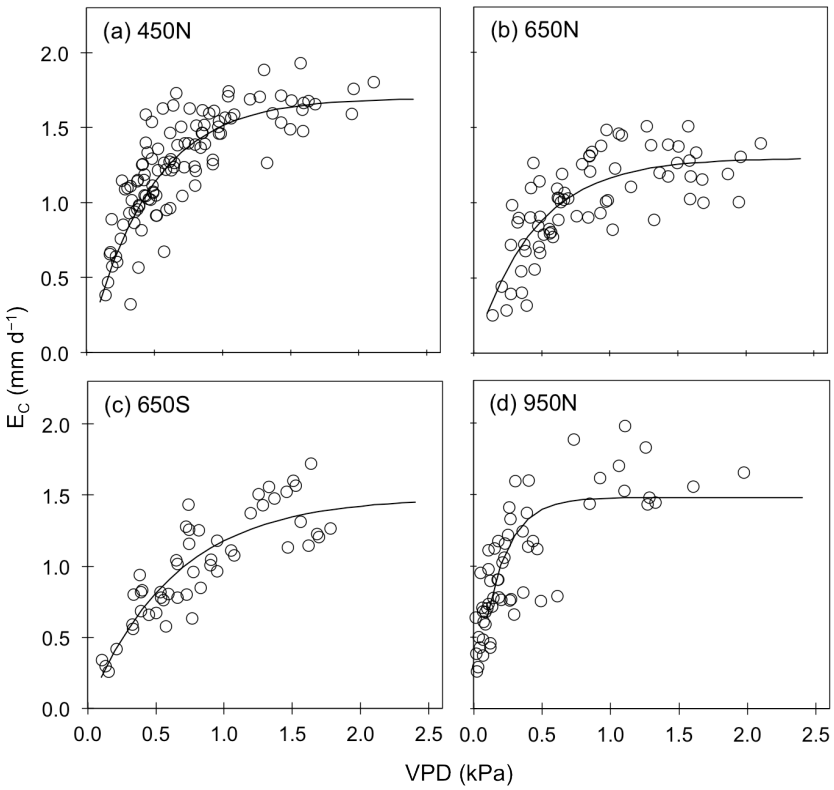

Figure 4.6 Relationship between vapor pressure deficit (VPD, kPa) and daily canopy transpiration (E_C, mm d^{-1}) at each site from June to September 2010. Fitted functions were (a) $E_C = 1.70VPD(1-e^{(-2.21VPD)})$ for 450N, (b) $E_C = 1.30VPD(1-e^{(-2.28VPD)})$ for 650N, (c) $E_C = 1.48VPD(1-e^{(-1.58VPD)})$ for 650S, (d) $E_C = 1.48VPD(1-e^{(-5.71VPD)})$ for 950N. All the estimated parameters of each regression were statistically significant (P <0.0001).

4.3.4 Elevation effects on canopy conductance

Canopy conductance (G_C) is a measure of the intensity of E_C regulation among forests. Mean daytime G_C on clear, sunny days between June (mature canopy) was similar at lower sites, i.e., 450N, 650N, and 650S, which was about 4 mm s^{-1} (TukeyHSD, P_{adj} >0.8), while G_C at the 950N was significantly higher than the other sites (ANOVA, F = 4.568, P = 0.003; Table 4.6). G_{Cref}, which denotes G_C at VPD = 1 kPa, was 5.4 ± 0.8 mm s^{-1} at 450N, 3.6 ± 0.4 mm s^{-1} at 650N, 3.7 ± 0.5 mm s^{-1} at 650S, and 4.5 ± 1.5 mm s^{-1} at 950N. G_{Cref} differed significantly (ANOVA, F = 24.52, P <0.0001) among the sites except between 650N and 650S (TukeyHSD, P_{adj} = 0.71). Thus, at the same range of VPD, G_C was higher at 450 > 950 > 650 m elevations. The response of G_C to VPD under saturating R_S (>400 W m^{-2}) at each site is plotted in Figure 4.7. The

gradient of the exponential regression curve relating G_C to VPD was significantly steeper for the 950N compared to the other sites.

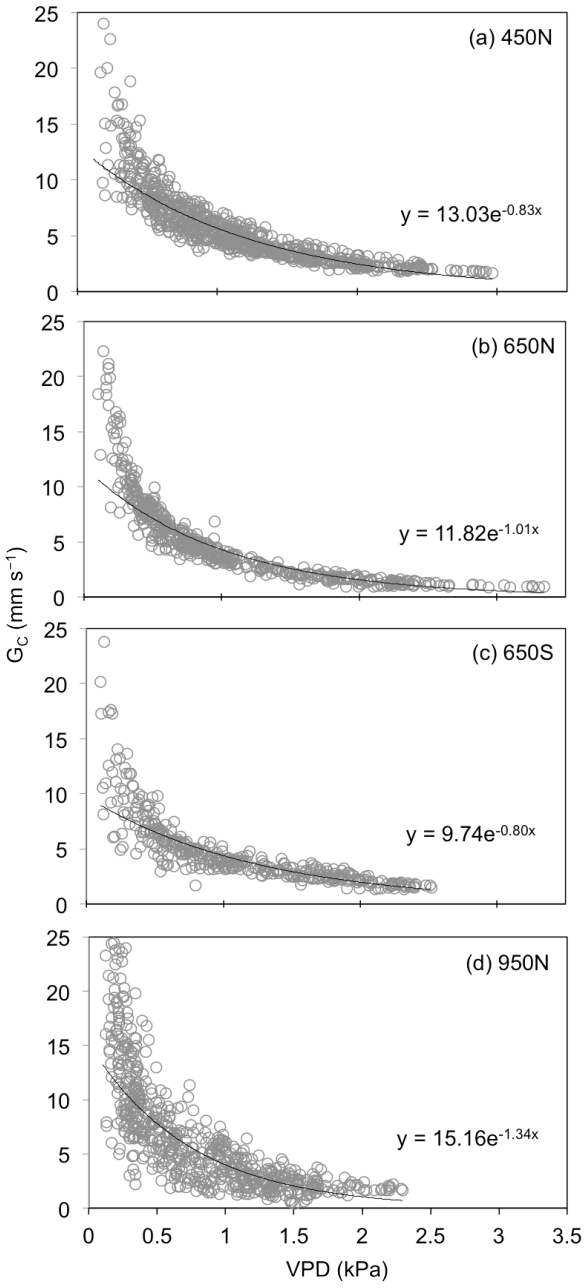

Figure 4.7 Relationships between canopy conductance (G_C, mm s^{-1}) and vapor pressure deficit (VPD, kPa) under saturating global radiation (R_S >400 W m^{-2}) at each study site. All the estimated parameters of each regression were statistically significant (P <0.0001).

Table 4.6 Canopy conductance (G_C, mm s^{-1}) on clear days in June, its respective vapor pressure deficit (VPD, kPa) for daytime (from 8:00h to 18:00h) and G_{Cref} (G_C at VPD = 1 kPa) at each site. ± are standard deviation (SD).

	450N	650N	650S	950N
G_C	4.4 ± 3.0	4.1 ± 4.1	4.3 ± 3.1	5.3 ± 6.2
VPD	1.4 ± 0.7	1.4 ± 0.8	1.3 ± 0.7	1.1 ± 0.5
G_{Cref}	5.4 ± 0.8	3.6 ± 0.4	3.7 ± 0.5	4.5 ± 1.5

In Figure 4.8, the values of sensitivity of G_C response to VPD ($-m = -\Delta G_C/\Delta \ln VPD$, see Eq. 8) were plotted against G_{Cref} at each site. The average of the empirical slopes (G_{Cref} to $-\Delta G_C/\Delta \ln VPD$) to for all the sample trees at 450N, 650N, 650S, and 950N were 0.64, 0.65, 0.67, and 0.84, respectively. The slope for the 950N site was significantly higher than those at the other sites (ANOVA, F = 24.33, P <0.0001; TukeyHSD, P_{adj} <0.0001). Thus, the slopes for the 450N, 650N, and 650S were close to the universal slope of 0.6 (Oren et al. 1999), while it was 25% higher at the 950N, which indicates higher stomatal sensitivity to VPD at this site/elevation.

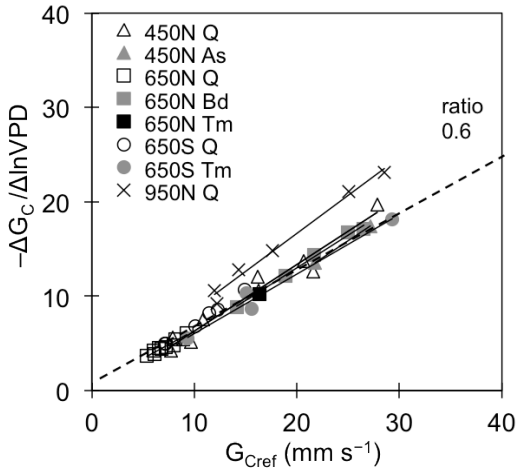

Figure 4.8 The response of canopy conductance to vapor pressure deficit ($-\Delta G_C/\Delta \ln VPD$, see Eq. 10) plotted against the reference conductance (G_{Cref}) for all studied trees at each site, i.e., *Quercus* spp. (Q), *Alnus sibirica* (As), *Betula davurica* (Bd), and *Tilia mandshurica* (Tm). The universal ratio of 0.6 suggested by Oren et al. (1999) is indicated by a broken line.

4.4 Discussion

4.4.1 Interactions among elevation, abiotic factors and tree growth parameters

A gradient along the elevation was found for T_a, rainfall, and VPD, while R_S, wind speed and relative θ showed no tendency. Low elevations are likely to have higher T_a and less rainfall (low humidity), which result in higher VPD (Tromp-van Meerveld and McDonnell 2006). Kubota et al. (2005) reported a decreasing VPD at higher elevations due to height-dependant decrease in T_a. In our study, the annual mean daytime VPD at the 450N was 0.5 kPa >0.4 kPa at 650N >0.2 kPa at 950N, corresponding to higher annual mean T_a and lower annual rainfall at lower elevations. We observed significant and negative linear relationships between elevation and annual daytime mean D, annual mean T_a, and annual rainfall (R^2 = 0.98 for VPD, 0.99 for elevation, and T_a, and 0.95 for rainfall; P <0.0001).

The amount of rainfall, soil characteristics (mainly infiltration rates), and soil depths interact to determine the amount of water available for plants (Chapin et al. 2002). Studies in rugged mountainous terrains report contrasting patterns of soil moisture availability along the elevational gradient. For example, Kumagai et al. (2008) observed that the upper slope soils were constantly drier than soils down slope in a Japanese cedar forest. On the other hand, Kubota et al. (2005) reported increasing soil water content with increasing elevation as a result of increasing rainfall at higher elevations. In our study, despite differences in soil depths and precipitation amounts at the three different elevations, there were no significant differences in soil water retention among the sites. In most cases, soil moisture was close to field capacity at all sites (Figure 4.1), as a result of high rainfall amounts in Haean region. The forests studied, therefore, never experienced water stress during the study period and any differences in water use among the forest sites cannot be attributed to soil moisture availability.

A correlation between TWU and DBH (Figure 4.3) and that between A_S and DBH (Figure 4.2) among tree species and across sites in different elevations provides a link between tree allometry and tree water use (Vertassy et al. 1995; Bucchi et al. 2004; Meinzer et al. 2001; Meinzer et al. 2005; Gebauer et al. 2008; Jung et al. 2011), demonstrating the deterministic role of xylem water transport on overall forest water use as well as the dependence of both parameters on tree size. We observed a nonlinear increase in A_S with increasing DBH, which was detached from elevation since DBH sizes were not defined by elevation. Similar universal functional relationships between DBH and A_S have been reported for 24 co-occurring canopy tree species in tropical forests (Meinzer et al. 2001; Meinzer et al. 2005) and for five tree species growing in an Asian temperate forest (Jung et al. 2011). However, Gebauer et al. (2008) reported considerably higher A_S (about 80% of stem cross-sectional area) in diffuse porous trees compared to 20% in ring porous trees. In our case, although ring and diffuse porous trees were distinguishable according to DBH:A_S ratios, a universal regression comparing all the trees together was statistically significant (Figure 4.1), suggesting that the

species basically function in a similar manner in terms of water use (see Figure 4.3). Our results compare favorably with those of Meinzer et al. (2005), who compared 18 angiosperm species. Based on these results, it was clear that comparisons of water use and its regulation among the respective forest stands at different elevations could be performed without considering species composition. This was a departure from our initial hypothesis that differences in species composition may mask differences arising from elevation.

In temperate forests, the time during which active leaf transpiration occurs corresponds to the productive period of the forest (Körner 2007) and has a strong influence on the total water use by forest ecosystems. The total period of transpiration decreased with increasing elevation and decreasing T_a, i.e., 4 days 100 m^{-1} and 6 days $°C^{-1}$, which was comparable with the results from the similar type of temperate deciduous forests in Europe and North America (3–5 days 100 m^{-1} and 7–13 days $°C^{-1}$) (Rotzer and Chmielewski 2001; Dittermar and Elling 2006; Richardson et al. 2006; Vitasse et al. 2009), even though the range of elevational gradient was relatively narrow (450 m to 950 m) in our case. This gradient in duration of active tree transpiration resulted from differences in timing of leaf onset and senescence at the different elevations, which is likely as a result of T_a variations among the sites. The vegetation at higher elevations experienced delayed leaf flush due to extended low winter temperatures and an earlier onset of leaf senescence as a result of rapid cooling in autumn, at higher elevations. These temperature changes along the elevational gradient also influence tree productivity and growth, as demonstrated by the relationship between annual tree ring width and mean annual temperature of the respective forest sites. This qualifies T_a as an important determinant of tree growth and functioning on mountain slopes.

4.4.2 Elevation effects on canopy transpiration and its regulation

The annual E_C declined from 175 mm $year^{-1}$ at 450N to 90 mm $year^{-1}$ at 950N. This trend of forest canopy transpiration is consistent with previous findings of McDowell et al. (2008) who reported a decline in E_C with increasing elevation in forests dominated by different coniferous species in the southern Rocky Mountains. Matyssek et al. (2009), however, found no relationship between the magnitude of E_C and elevation in mixed or coniferous forest stands at the collinear, mountainous, and subalpine elevations. Both McDowell et al. (2008) and Matyssek et al. (2009) compared E_C from different forest types or forest stands dominated by different species, which makes it difficult to separate the impact of elevation. Our study addressed similar forest types dominated by oaks. This made it possible to compare E_C from the different forest stands and key out elevation effects on forest water use. Although Kubota et al. (2005) studied elevation effects on J_S of mountainous beech forests in Japan, to the best of our knowledge, no such study in annual E_C regarding to elevational gradients has been conducted in similar forest types in Asia.

We established a functional relationship between E_C and T_a as $E_C = 29.56T_a - 85.19$ with $R^2 = 0.90$ and $P < 0.0001$ for the annual mean T_a and $E_C = 35.67T_a - 462.7$ with $R^2 = 0.97$ and $P < 0.0001$ for the growing season T_a. Based on these regressions, transpiration is zero when the annual mean T_a and a growing season's mean T_a drop down to ~3°C and ~13°C, respectively. Körner (2003; 2007) suggested that a strong relationship between growing season length and mean T_a contributes to the reduction in annual E_C at high elevations especially in humid, temperate forests where soil moisture is not limiting. Pfautsch et al. (2010) reported a strong linear relationship between daily mean F_{dt} and daily T_a, indicating a temperature-dependence of water use in *Eucalyptus regnans* forests in southeastern Australia. In our study, however, we did not observe any direct temperature-dependence of E_C on a daily scale, but on an annual scale. On a daily basis, VPD was the dominant determinant of transpiration (Figure 4.6). Similar observation was reported by Jung et al. (2011) for the deciduous forest in Korea. Our daily T_a and VPD were not correlated, likely due to the rapidly changing humidity at our study sites. This may explain the lack of a relationship between T_a and E_C on a daily basis, since T_a lags behind. On an annual basis, however, a significant linear relationship between T_a and VPD ($R^2 = 0.99$, $P < 0.0001$) was found.

Water transpired by forests is determined by the stomata. Stomatal functioning is influenced by VPD (Kelliher et al. 1997; Saugier et al. 1997), wind speeds (Campbell-Clause 1998; Schulze et al. 2005) and soil moisture (Sala and Tenhunen 1996; Kelliher et al. 1997; Tognetti et al. 2009). In our study, VPD was the dominant determinant of G_C and also E_C at all the sites. The similarities in the responses of daily E_C to VPD (Figure 4.6) as well as G_C to VPD (Figure 4.7) among the 450N, 650N, and 650S suggest similarities in stomatal functioning among the sites. Differences in E_C at 950N can be attributed to differences in the response of G_C to prevailing VPD at the highest elevation (Figure 4.7). A departure from this trend observed for trees at the 950N, which was characterized by a conspicuous depression in E_C between 10:00h and 13:00h (Figure 4.4). An early drop of E_C at relatively low VPD (Figure 4.6) and a steeper slope of the curve between VPD and G_C (Figure 4.7) were likely due to high wind speeds, since this site was more exposed. Campbell-Clause (1998) reported decreasing transpiration rates at wind speeds more than 4 m s^{-1}. Moreover, significant differences in the response of G_C to VPD occurred among sites at different elevations with the 950N showing higher (0.83) stomatal sensitivity to changes in VPD compared to the other study sites (0.63–0.65) (Figure 4.8). The greater sensitivity caused the higher G_C at 950N around VPD = 0.6–1.0 kPa, resulting in higher F_{dt} and hence higher E_C (in 30min), but the lower G_C at 950N at VPD >1.0 kPa, driving a drop in F_{dt} and E_C, consequently. Such adjustments to local conditions may have implications for the overall forest stand water use.

Furthermore, several studies reported that the intensity of exponentially decreasing G_C in relation to increasing VPD might vary among species (McNaughton and Jarvis 1991; Oren et al. 1999; Oren and Pataki 2001; Herbst et al. 2008), masking differences arising from elevation. For example, higher stomatal

sensitivity to VPD has been reported for diffuse porous (*Acer rubrum*) compared to ring porous species (*Quercus alba*) (Oren and Pataki 2001). A dissimilar result was found by Herbst et al. (2008) that the forest with higher proportion of ring-porous trees showed higher stomatal sensitivity. In this study, we did not find any significant difference in stomatal sensitivity to changing VPD between diffuse and ring porous tree species growing together at the same elevation (Figure 4.8).

Carbon isotope composition has been used as an indirect measure of stomatal conductance and water use efficiency (WUE) of leaves (Hubick et al. 1986; Körner et al. 1988, 1991) and can be employed to describe the variations in plant water use strategies (Marshall and Zhang 1994; Sun et al. 1996; Osorio et al. 1998; Li et al. 2006). $\delta^{13}C$ concentration in plants provides an integrated measure of WUE during plant growth since the $\delta^{13}C$ concentration of newly fixed carbon increases under conditions of low internal CO_2 concentration (Ehleringer 1993). In our study, $\delta^{13}C$ of *Q. mongolica* increased with elevation (Figure 4.9), and the difference between 950N and the other sites was significant (P_{adj} <0.01, TukeyHSD). Higher $\delta^{13}C$ at higher elevations suggests that WUE decreased with increasing elevation as observed by Körner et al. (1988; 1991), Sparks and Ehleringer (1997), and Cordell et al. (1998).

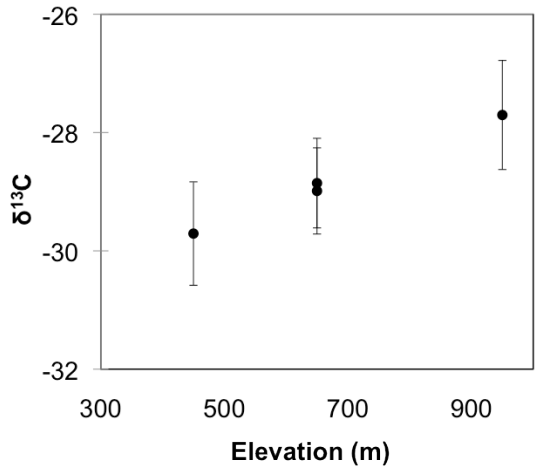

Figure 4.9 Stable carbon isotope (^{13}C) compositions in the leaves of *Quercus mongolica* distributed along an elevation gradient in the Haean catchment. Error bars indicate standard deviation from the means of individual trees along this gradient.

Although our study considered a relatively narrow elevational gradient (i.e., 450−950 m), significant reduction in total E_C occurred. This was attributed to changes in T_a, VPD, and the length of growing season along the elevation, which influence tree transpiration. We demonstrated that the maximum daily water use of individual trees was universally defined by tree size regardless of species and elevation. Stem diameter is, therefore, a good indicator of TWU irrespective of species and elevation. Differences in species composition, therefore, do not influence water use by forest stands in these temperate mountain forests. Differences in stomatal sensitivity as observed along the elevational gradient, however, impacted E_C and should be considered when conducting forest water budget in the mountain regions.

4.5 Acknowledgements

This study was carried out as part of the International Research Training Group, TERRain and ECOlogical Heterogeneity (TERRECO; GRK 1565/1) funded by the Deutsche Forschungsgemeinschaft (DFG) at University of Bayreuth, Germany and the Korean Research Foundation (KRF) at Kangwon National University, Chuncheon, Korea. The isotope abundance analyses by the BayCEER – Laboratory of Isotope Biogeochemistry are kindly acknowledged.

4.6 References

Barry RG (1981) Mountain weather and climate. Methuen, London

Beniston M (2003) Climatic change in mountain regions: a review of possible impacts. Climatic Change 59: 5–31

Bidartondo MI, Burghardt B, Gebauer G, Bruns TD, Read DJ (2004) Changing partners in the dark: isotopic and molecular evidence of ectomycorrhizal liaisons between forest orchids and trees. Proc R Soc Lond B 271:1799−1806

Bucci SJ, Goldstein G, Meinzer FC, Scholz FG, Franco AC, Bustamante M (2004) Functional convergence in hydraulic architecture and water relations of tropical savanna trees: from leaf to whole plant. Tree Physiol 24:891−899

Burrows LE (1980) Differentiating sapwood, heartwood and pathological wood in live mountain beech. New Zealand Forest Service, Forest Research Institute, Protection Forestry Report 172

Campbell-Clause M (1998) Stomatal response of grapevines to wind. Aust J Exp Agr 38:77−82

Chapin FS III, Matson PA, Mooney HA (2002) Principles of Terrestrial Ecosystem Ecology. Springer, New York

Clearwater MJ, Meinzer FC, Andrade JL, Goldstein G, Holbrook NM (1999) Potential errors in

measurement of nonuniform sap flow using heat dissipation probes. Tree Physiol 19:681–687

Dittmar C, Elling W (2006) Phenological phases of common beech (*Fagus sylvatica* L.) and their dependence on region and altitude in Southern Germany. Eur J For Res 125:181−188

Ehleringer JR (1993) Carbon and water relations in desert plants: an isotopic perspective. In Ehleringer JR, Hall AE, Farquhar GD (Eds.), Stable isotopes and plant carbon-water relations, Academic Press, San Diego, California, USA

Engelhardt S, Matyssek R, Huwe B (2009) Complexity and information propagation in hydrological time series of mountain forest catchments. Eur J For Res 128:621−631

Ewers BE, Oren R (2000) Analyses of assumptions and errors in the calculation of stomatal conductance from sap flux measurements. Tree Physiol 20:579−589

Gebauer T, Horna V, Leuschner C (2008) Variability in radial sap flux density patterns and sapwood area among seven co-occurring temperate broad-leaved tree species. Tree Physiol 28:1821−1830

Granier A (1987) Evaluation of transpiration in a Douglas-fir stand by means of sap flow measurements. Tree Physiol 3:309−320

Granier A, Biron P, Bréda N, Pontailler JY, Saugier B (1996) Transpiration of trees and forest stands: short and long-term monitoring using sapflow methods. Global Change Biol 2:265−274

Harris PP, Huntingford C, Coxb PM, Gasha JHC, Malhi Y (2004) Effect of soil moisture on canopy conductance of Amazonian rainforest. Agric For Meteorol 122:215−227

Hirobe M, Tokuchi N, Iwatsubo G (1998) Spatial variability of soil nitrogen transformation patterns along a forest slope in a *Cryptomeria japonica* D. Don plantation. Eur J Soil Biol 34:123−131

Hoch G, Körner C (2005) Growth, demography and carbon relations of *Polylepis* trees at the world's highest tree line. Funct Ecol 19:941−951

Hubick KT, Farquhar GD, Shorter R (1986) Correlation between water-use efficiency and carbon isotope discrimination in diverse peanut (Arachis) germplasm. Australian J Plant Physiol 13:803−816

Jarvis PG (1976) The interpretation of the variations in leaf water potential and stomatal conductance found in canopies in the field. Phil Trans Roy Soc Lond B 273:593−610

Jung EY, Otieno D, Lee B, Lim JH, Kang SK, Schmidt MWT, Tenhunen J (2011) Up-scaling to stand transpiration of an Asian temperate mixed-deciduous forest from sing tree sapflow measurements. Plant Ecol 212:383−395

Kelliher FM, Hollinger DY, Schulze ED, Vygodskaya NN, Beyers JN, Hunt JE, McSeveny TM, Milukova I, Sogatchev A, Varlargin A, Ziegler W, Arneth A, Bauer G (1997) Evaporation for an eastern Siberian larch forest. Agric For Meteorol 85:135−147

Korea Forest Service (2009) National Report on Sustainable Forest Management in Korea 2009

Korea Meteorological Administration (2011) A white paper on *Changma*.

Körner C, Farquhar GD, Roksandik Z (1988) A global survey of carbon isotope discrimination in plants from high altitude. Oecologia 74:623−632

Körner C, Farquhar GD, Wong SC (1991) Carbon isotope discrimination by plants follows latitudinal and altitudinal trends. Oecologia 88:30−40

Körner C (2003) Alpine Plant Life (2nd ed.), Springer-Verlag Berlin Heidelberg New York

Körner C (2007) The use of 'altitude' in ecological research. Trends Ecol Evol 22:569−574

Köstner B (2001) Evaporation and transpiration from forests in Central Europe–relevance of patch-level studies for spatial scaling. Meteorol Atmos Phys 76:69−82

Kubota M, Tenhunen J, Zimmermann R, Schmid M, Adiku S, Kakubari Y (2005) Influences of environmental factors on the radial profile of sap flux density in *Fagus crenata* growing at different elevations in the Naeba Mountains, Japan. Tree Physiol 25:545−556

Kumagai T, Tateishi M, Shimizu T, Otsuki K (2008) Transpiration and canopy conductance at two slope positions in a Japanese cedar forest watershed. Agric For Meteorol 148:1444−1455

Lauscher F (1976) Weltweite Typen der Höhenabhängigkeit des Hiederschlags. Wetter und Leben 28:80−90

Li C, Zhang X, Liu X, Luukkanen O, Berninger F (2006) Leaf morphological and physiological responses of *Quercus aquifolioides* along an altitudinal gradient. Silva Fenn 40:5−13

Marshall and Zhang (1994) Carbon isotope discrimination and water use efficiency of native plants of the north-central Rockies. Ecology 75:1887−1895

McDowell NG, White S, Pockman WT (2008) Transpiration and stomatal conductance across a steep climate gradient in the southern Rocky Mountains. Ecohydrol 1:193−204

McNaughton KG, Jarvis PG (1991) Effects of spatial scale on stomatal control of transpiration. Agric For Meteorol 54:279−301

Matyssek R, Wieser G, Patzner K, Blaschke H, Häberle K-H (2009) Transpiration of forest trees and stands at different altitude: consistencies rather than contrasts? Eur J Forest Res 128:579−596

Meinzer FC, Goldstein G, Andrade JL (2001) Regulation of water flux through tropical forest canopy trees: do universal rules apply? Tree Physiol 21:19−26

Meinzer FC, Bond BJ, Warren JM, Woodruff DR (2005) Does water transport scale universally with tree size? Funct Ecol 19:558−565

Miyajima Y, Takahashi K (2007) Changes with altitude of the stand structure of temperate forests on Mount Norikura, central Japan. J For Res 12:187−192

Murray FW (1967) On the computation of saturation vapor pressure. J Appl Meteorol 6:203–204

Oren R, Sperry JS, Katul GG, Pataki DE, Ewers BE, Phillips N, Schäfer KVR (1999) Survey and synthesis of intra- and interspecific variation in stomatal sensitivity to vapour pressure deficit. Plant Cell

Environ 22:1515−1526

Oren R, Pataki DE (2001) Transpiration in response to variation in microclimate and soil moisture in southeastern deciduous forests. Oecologia 127, 549-559

Osorio J, Osorio ML, Chaves MM, Pereira JS (1998) Water deficits are more important in delaying growth than in changing patterns of carbon allocation in *Eucalyptus globulus*. Tree Physiol 18:363−373

Phillips N, Oren R (1998) A comparison of daily representations of canopy conductance based on two conditional time-averaging methods and the dependence of daily conductance on environmental factors. Ann Sci For 55:217−235

Priestley CHB, Taylor RJ (1972) On the assessment of surface heat flux and evaporation using large scale parameters. Monthly Weather Rev 100:81−92

Richardson AD, Bailey AS, Denny EG, Martin CW, O'Keefe J (2006) Phenology of a northern hardwood forest canopy. Global Chang Biol 12:1174−1188

Rotzer T, Chmielewski FM (2001) Phenological maps of Europe. Clim Res 18:249−257

Running SW, Nemani RR, Hungerford RD (1987) Extrapolation of synoptic meteorological data in mountainous terrain and its use for simulating forest evapotranspiration and photosynthesis. Canadian J For Res 17:472−483

Sala A, Tenhunen J (1996) Simulations of canopy net photosynthesis and transpiration of *Quercus ilex* L. under the influence of seasonal drought. Agric For Meteorol 78:203–222

Saugier B, Granier A, Pontailler JY (1997) Transpiration of a boreal pine forest measured by branch bag, sap flow and micrometeorological methods. Tree Physiol 17:511–519

Schaap MG, Feike JL, van Genuchten MT (2001) ROSETTA: a computer program for estimating soil hydraulic parameters with hierarchical pedotransfer functions, J Hydrol 251:163−176

Schulze ED, Chapin FS III (1987) Plant specialization to environments of different resource availability. Ecological Studies 61. Springer, Berlin Heidelberg New York, pp 120−148

Schulze ED, Kelliher FM, Körner C, Lloyd J, Leuning R (1994) Relationships among maximum stomatal conductance, carbon assimilation rate, and plant nitrogen nutrition: a global ecology scaling exercise. Annu Rev Ecol Syst 25:629−660

Schulze ED, Beck E, Müller-Hohenstein (2005) Plant Ecology. Springer Berlin Heidelberg

Stewart JB (1988) Modelling surface conductance of pine forest. Agric For Meteor 43:19−35

Sun ZJ, Livingston NJ, Guy RD, Ethier GJ (1996) Stable carbon isotopes as indicators of increased water use efficiency and productivity in white spruce [*Picea glauca* (Moench) Voss] seedlings. Plant Cell Environ 19:887−894

Tateno R, Hishi T, Takeda H (2004) Above- and belowground biomass and net primary production in a cool-temperate deciduous forest in relation to topographical changes in soil nitrogen. For Ecol

Manage 193:297−306

Tenhunen JD, Valentini R, Köstner B, Zimmermann R, Granier A (1998) Variation in forest gas exchange at landscape to continental scales. Ann Sci For 55:1−12

Tieszman LL, Archer S (1990) Isotope assessment of vegetation changes. In: Osmond CB, Pitelka LF, Hidy GM (Eds.), Plant Biology of the Basin and Range, vol. 80. Ecological Studies, pp. 144–178

Tilman D (1988) Plant Strategies and the Dynamics and Structure of Plant Communities. Princeton University Press, Princeton

Tognetti R, Giovannelli A, Lavini A, Morelli G, Fragnito F, d'Andria R (2009) Assessing environmental controls over conductances through the soil–plant-atmosphere continuum in an experimental olive tree plantation of southern Italy. Agric For Meteorol 149:1229–1243

Tromp-van M, McDonnell JJ (2006) On the interrelations between topography, soil depth, soil moisture, transpiration rates and species distribution at the hillslope scale. Adv Water Resour 29:293−310

van Genuchten MTh (1980) A closed-form equation for predicting the hydraulic conductivity of unsaturated soils. Soil Sci Am J 44:892−898

Vertessy RA, Benyon RG, O'Sullivan SK, Gribben PR (1995) Relationships between stem diameter, sapwood area, leaf area and transpiration in a young mountain ash forest. Tree Physiol 15:559−567

Vitasse Y, Porté AJ, Kremer A, Michalet R, Delzon S (2009) Responses of canopy duration to temperature changes in four temperate tree species: relative contributions of spring and autumn leaf phenology. Oecologia 161:187−198

Vitousek PM, Howarth RW (1991) Nitrogen limitation on land and in the sea: how can it occur? Biogeochemistry 13:87−115

Wiens JA (2000) Ecological heterogeneity: an ontogeny of concepts and approaches. In: Stewart AJA, John EA, Hutchings MJ (Eds.) The Ecological Consequences of Environmental Heterogeneity. Blackwell, Oxford, pp 9−31

Willmott CJ (1984) On the validation of models. Phys Geogr 2:184−194

Whitley R, Zeppel M, Armstrong N, Macinnis-Ng C, Yunsa IAM, Eamus D (2008) A modified JS model for predicting stand-scale transpiration of an Australian native forest. Plant Soil 305:35−47

Whitley R, Medlyn B, Zeppel M, Macinnis-Ng C, Eamus D (2009) Comparing the Penman-Monteith equation and a modified Jarvis-Stewart model with an artificial neural network to estimate stand-scale transpiration and canopy conductance. J Hydrol 373:256−266

Wright IR, Manzi AO, Da Rocha HR (1995) Surface conductance of Amazonian pasture: model application and calibration for canopy climate. Agric For Meteorol 75:51−70

Wullschleger SD, Hanson PJ, Todd DE (2001) Transpiration from a multi-species deciduous forest as estimated by xylem sap flow techniques. For Ecol Manage 143:205−213

Yoshino MM (1975) Climate in a small area. University of Tokyo Press, Tokyo

Appendix

List of other publications

Kallarackal J, Otieno DO, Reineking B, Jung E, Schmidt MWT, Granier A, Tenhunen JD (2013) Functional convergence in water use of trees from different geographical regions: a meta-analysis. Trees 27:787−799

Berger S, Jung E, Köpp J, Kang H, Gebauer G (2013) Monsoon rains, drought periods and soil texture as drivers of soil N_2O fluxes – soil drought turns East Asian temperate deciduous forest soils into temporary and unexpectedly persistent N_2O sinks. Soil Biol Biochem 57: 273−281

Erklärung

Hiermit erkläre ich, dass ich die Arbeit selbständig verfasst und keine anderen als die von mir angegeben Quellen und Hilfsmittel benutzt habe.

Bayreuth, 04.06.2013 ——————————————————

Eunyoung Jung

Ferner erkläre ich, dass ich anderweitig mit oder ohne Erfolg nicht versucht habe, diese Dissertation einzureichen. Ich habe keine gleichartige Doktorprüfung an einer anderen Hochschule endgültig nicht bestanden.

Bayreuth, 04.06.2013 ——————————————————

Eunyoung Jung